Ultrastructural Changes in Diabetic Retinal Capillaries

Loubna ElSaboni

School of Medicine

September 2021

Acknowledgements

Diabetic/SPHINX-31 Experiment:

Claire Allen: *in vivo* physiology and perfusion fixation

Zubair Nizamudeen: EM Processing and dissection training.

EXT1 Experiment

Penny Lohrer: *in vivo* physiology and perfusion fixation

Julie Watts: Transmission electron microscopy (FEI Tecnai T12 BioTwin 120 keV) training

Denise Mclean: TEM Retina sectioning (EM UC6, Leica)

TABLE OF CONTENTS

List of Figures

List of Tables

ABSTRACT

Background

Diabetic vascular retinopathy is the most common microvascular complication of diabetes. While it is clinically reported and understood that diabetes increases vascular permeability, understanding of the structural molecular pathogenesis of diabetic vascular complications remains incomplete. Increase in vascular basement membrane thickness is recognised as hallmark signs of diabetic microangiopathy. While the endothelial glycocalyx plays a role in maintaining vascular permeability. The effect of hyperglycaemic states in diabetes has been shown to decrease the ability of the eGLX to perform this role. The eGLX and basement membrane are both disrupted by production of angiogenic isoforms of vascular endothelial growth factor (VEGFAxxxa) and reversed by its anti-angiogenic isoforms1, under control of splicing by SRPK12.

Furthermore, endothelial specific EXT1 inducible knockout phenotype mice will be used to demonstrate the effect of defective endothelial glycocalyx has on permeability due to loss of the heparan sulphate elongation gene.

Hypothesis & Aims

Hypothesis: Hyperglycaemic states cause structural change in the endothelial glycocalyx, which leads to the increased permeability observed in diabetic vasculature. The increased basement membrane thickness observed in diabetes is due to impairment in the function of the eGLX as a ultrafiltrating barrier.

Aims: Quantify diabetic changes in the eGLX coverage, Basement Membrane thickness and associate it with the known increased retinal permeability.

Measure changes in permeability, basement membrane thickness and eGLX parameters in diabetic and control mice.

Determine whether SRPK1 inhibition reverses increased basement membrane thickness.

Methods:

Diabetes was induced in DBA2J female mice using STZ (40mg/kg, x5 consecutive daily doses). Fundus fluorescein angiography (FFA) was performed 21 days after diabetic induction to measure retinal microcirculation permeability. One group of diabetic mice were treated systemically with Sphinx314 (0.8mg/kg i.p. twice per week) for three weeks before tissue removal for electron microscopy. Fiji software was used to measure the mean basement membrane thickness and eGLX coverage. EXT1 knockout was established through induction by tamoxifen on days 5 & 9 followed by weekly urine measurement of albumin levels and urine creatinine ratio. FFA was performed on day 1, day 21 and Day 35. After 42 days mice were anesthetized using ketamine 75mg/kg (Ketaset) and medetomidine 1mg/kg (Sedastart) and an eye was removed. The mice were then euthanised by perfusion fixing using the LaDy GAGa buffer. Retinal resin blocks were 80nm sectioned and transmission electron micrographs collected.

Results:

Diabetic Albumin Creatinine Ratio is increased after inducing Diabetes and reversed after Sphinx31 Treatment. Retinal Permeability is increased in early STZ-induced Diabetes. Basement Membrane thickness increased in Diabetes and reversed after Sphinx31 treatment. Endothelial Glycocalyx has less coverage in Diabetic Retinal microcirculation.

EXT1 knockout mice display a change in eGLX coverage and basement membrane thickness similar to that observed in diabetic mice.

Conclusion:

As predicted, there was an increase in basement membrane thickness and decreased eGLX coverage in STZ model correlated to an increase retinal vascular permeability. A pilot diabetic group treated with systemic SRPK1 inhibition showed a normal basement membrane thickness. These data are consistent with the hypothesis, yet to be confirmed, that the initial basement membrane thickening in diabetes could be increased hydration rather than remodelling due to increase permeability at least in part due to eGlx. The inferred

reversal by treatment with an SRPK1 inhibitor indicates that basement membrane thickness is relatively rapidly reversed either by remodelling or reducing hydration.

The increase in basement membrane thickness observed in EXT1 knockout mice supports the rationale that attributes this change to an increase in oncotic pressure that leads to a build-up of water within the basement membrane thickness. All of which occurring due to impairment in eGLX function in both sets of experiments.

CHAPTER 1 INTRODUCTION:

1.1 DIABETES

1.1.1 EPIDEMIOLOGY

Diabetes is defined by the World Health Organisation (WHO) as a systemic metabolic disorder diagnosed as chronically elevated blood glucose levels, delineated as repeated readings of casual plasma glucose levels higher than 200 mg/dL. Diabetes was reported as the direct cause of 1.6 million global deaths and ranked among the top 10 causes of mortality in 2016(1). The International Diabetes Federation estimated the international prevalence of diabetes in the year 2000 as 4.6%, the estimates in 2019 are 9.3% of the world's population with evidence of exponential increase over the coming decades reaching 10.2% in 2030 and 10.9% by 2045. Furthermore, there is significant higher prevalence in developed countries compared to developing countries, currently at 10.9% and 4% respectively(2). As with all systemic diseases, there is an evident reduction in quality of life and average life expectancy in diabetic patients due to the comorbidities associated and brought on by diabetes. Diabetes has become an increasingly heavier financial burden on the developed countries. Treatment and prevention of diabetic complications and comorbidities is a leading financial burden for all health care systems. While the annual global expenditure is estimated to be 578bn GBP(3), the NHS estimates its spending to be 13bn GBP annually on indirect costs of diabetes complications alone, accounting for more than 10% of the NHS total budget(4,5).

1.1.2 DIAGNOSIS AND COMPLICATIONS

There are three types of diabetes: Type 1, Type 2 and Gestational Diabetes. Gestational diabetes is a state of hyperglycaemia brought on during pregnancy that is associated with adverse effects on both mother and fetus. Type 1 usually presents in prepubescent years of life is an autoimmune disorder in which the pancreatic beta-cells are destroyed, thus insufficient production of insulin to sustain healthy homeostasis of glucose.

Type 2, being the most common and preventable type of diabetes, is caused initially by insulin resistance due to increased desensitisation of insulin receptors found on cells. This in turn leads to several pathogenic pathways including decreased utilisation of circulating glucose, and consequently triggers increased production of glucose by the liver through lipolysis. The eventuality of sustained glucose imbalance causes damage to insulin producing beta cells and glucagon producing alpha cells in the pancreas as they compensate to the cells constant need for glucose alongside the hyperglycaemic state, further hindering the peripheral tissue ability to metabolise glucose. The end result is a cellular state of glucose starvation, an unsuppressed loop of increased glucose and insulin production that releases pro-inflammatory metabolites as a by-product.

The gold standard test for diagnosing diabetes and predicting its complications is an HbA1c blood test; a value of 48 mmol/mol or higher is indicative of a diabetic diagnosis(6). The measurement of HbA1c indicates the proportion of glycated red blood cells due to sustained increased blood glucose over a lengthy period of time. Hyperglycaemia is recognised as a cause of endothelial dysfunction observed in diabetes. The continuous systemic hyperglycaemic state accounts for microvascular and macrovascular complications present in uncontrolled diabetes individuals(7). Thus, HbA1c reflects the risk of vascular complications caused by diabetes. The process through which high degrees of hyperglycaemia leads to cellular injury has been intensively researched. The UK prospective diabetes study showed the distinctive preventative effect of controlling blood glucose levels on reducing the diabetic comorbidities and complications(8).

Diabetic vasculopathy poses the highest risk of causing progressive chronic comorbidities affecting various organs such as the kidneys, eyes and heart in diabetic individuals(9). These comorbidities and complications are the leading cause of death from diabetes(10). Due to their inability to regulate sugar absorption, endothelial cells, mesangial cell and neuronal cells are the most type of cells affected by chronic hyperglycaemic states(11). While it is clinically reported and understood that diabetes increases vascular permeability, the structural molecular pathogenesis of diabetic vascular complications remains incomplete

(12). Various research experiments have been able to provide insight into the structural alteration that leads to the clinical presentation. Imaging techniques have been developed to observe and study these microvascular changes(13,14). The use of vitreous fluorophotometry has been used to detect early effects of diabetes on vascular permeability before patients had clinical presentation of retinal microvascular disease. Retinal capillaries in healthy individuals were impermeable to fluorescence dye, while it demonstrated an increased degree of permeability that was attributed to disturbance on the blood-retinal barrier. Furthermore, this experiment supported the role of a structural component that actively transported negatively charged molecules(15). Other studies looked at paracellular structural proteins that had a role in maintaining permeability function of capillaries but were affected in hyperglycaemic states of diabetes(16).

1.1.3 PATHOGENESIS

Multiple molecular pathogenic pathways are proposed to explain the multitude of damage caused by hyperglycaemia on the vascular endothelium. It is most likely that diabetic vascular damage is the result of an overlap of these interlinked theories(17). The hallmarks of diabetic microvascular disease include thickening of the basement membrane, increased vascular permeability and prothrombotic state (18).

Some of the well understood pathogenic pathways include the formation of Advanced Glycated End-products (AGE) and Reactive Oxygen Species (ROS) due to oxidative stress, the polyol pathway and the activation of Protein Kinase C.

1.1.3.1 Advanced Glycation End Products

Persistent hyperglycaemia causes the formation of AGEs through Maillard reactions between carbohydrates and free amino group of proteins. AGEs are unstable reactive compounds, due to the glycated lysine residue, that play a role in increased vascular permeability and endothelial cell dysfunction in diabetes(19). The binding of AGEs to their specific AGE Receptors (RAGE) acts as a catalyst for a pro-inflammatory and pro-coagulatory cascade(20). Additionally noting the inhibition of specific advantageous AGE

receptors favouring the clearance and breakdown of AGEs in diabetes(21,22). In addition to preventing hyperglycaemic state, other treatment plans were tested to decrease the effect of AGE. Decreasing oxidative stress, inhibiting AGE formation, and breaking down of AGE crosslink in order to improve their removal. However, no clinical trials have been able to demonstrate the efficacy of using such therapeutics, such as aminoguanidine and alagebrium, to significantly decrease the effect of AGE in the progression of diabetic vascular disease(23,24).

1.1.3.2 Aldose Reductase

As hyperglycaemia causes an increased cellular sugar flux, Aldose Reductase (AR) is the enzyme that initiates the irreversible conversion of the excess free glucose to its alcohol counterpart sorbitol through the polyol pathway(25). As the cell lacks the ability to remove sorbitol, which has been ascribed to be a cause of osmotic stress. Osmotic stress plays a direct role in the development of diabetic microvascular disease(26,27). The intracellular accumulation of sugars expedites basement thickening, loss of pericyte and microaneurysm; hallmarks of diabetic micro-vasculopathy(28). Studies that used Aldose Reductase Inhibitor have been unable to prevent or reverse these effects(10).

1.1.3.3 Vascular Endothelial Growth Factor

Vascular Endothelial Growth Factor (VEGF) is a cytokine that has mitogenic and angiogenic properties specific to endothelial cell lines(29), It constitutes of heparan-binding, homodimeric glycoprotein with variable isoforms(30). The gene responsible for the expression of VEGF and upregulation of VEGF binding sites are regulated and induced through various mechanisms that depend on oxygen availability (31), and pro-inflammatory factors (32).

In vivo and in vitro experiments of VEGF have demonstrated its role in increasing angiogenesis (33) as well as increasing vascular permeability (34,35). VEGF has been linked to the early stages of diabetic retinopathy before clinical changes can be observed (36). The upregulation of VEGF is also reported in proliferative stages diabetic retinopathy in human and animal in vivo experimental models, suggesting a strong causative

correlation(37). An experiment demonstrated that the intensity of VEGF staining was proportional to severity of the disease(38). VEGF plays an important role in promoting angiogenesis that leads to the dysregulated vascularisation observed in diabetic retinopathy and its inhibition provides a prospect for treatment and prevention of diabetic complication(39).

Hyperglycaemia has a direct effect on stimulating VEGF expression and release(40). Intermittent hyperglycaemic states cause higher increase in the expression of VEGF compared to persistent hyperglycaemic states, emphasizing the importance of preventing hypoglycaemic states and fluctuating blood glucose levels. Inhibition of ROS production by mitochondria, decreases the expression of VEGF in hyperglycaemic states in vitro, further affirming the interlapping of all the biochemical pathway theories that attempt to explain diabetic complications(41,42).

1.1.3.4 Protein kinase C

Protein Kinase C plays a vital role in cell signalling cascades; thus, its activation occurs in normal physiologic states. It is responsible for controlling proteins downstream of signalling pathways(43). Hyperglycaemia causes an increase in the glycolytic intermediate dihydroxyacetone phosphate that is then reduced to glycerol-3-phosphate, which in turn stimulates the production of diacylglycerol(44). Diacylglycerol, which is upstream of PKC cell signalling pathway causes the chronic activation of PKC in various tissues, including the retina and kidney during hyperglycaemic states(45). Oxidative stress, AGEs and ROS can all potentiate this activation, thus adding to the damaging effect of diabetic vascular disease(46,47). A study found a 90% increase in PKC activity when VEGF was added to endothelial cells to demonstrate its effect on glucose uptake compared to normal growing endothelial cells(48).

1.1.4 SYSTEMIC EFFECT OF DIABETES

Shortly after developing frequent hyperglycaemic states due to diabetes, haemodynamic changes have been observed(49). These changes include increases in blood flow and

pressure reported in the most organs most affected by diabetic angiopathy; the retina and the kidney(50)(51). A well-reviewed concept attributes the systemic effect of diabetes to vasculopathy, which causes dysfunction in the endothelial glycocalyx that impairs its ability to regulate vascular permeability(52).

1.1.4.1 Diabetic Retinopathy

Diabetic vascular retinopathy is the most common microvascular complication of diabetes. It also poses a global financial burden as the most common cause of blindness in adults within the working age in developed countries(53). A systematic literature review done in 2010 to report the global prevalence of Diabetic Retinopathy (DR) established that around 93 million people live with DR, and that 34.6% of diabetics have developed DR through their illness(54). Another study predicted that by 2030, the prevalence of DR will have increased to 191 million globally(55).

Diagnosis of DR is typically made through clinical observations of microvascular lesions in the retina. The clinical stages of DR are divided into non-proliferative and proliferative. One of the earliest studies that studied the vascular complication associated with diabetic retinopathy took place in 1921(56). The hallmarks of non-proliferative DR include microaneurysms, retinal haemorrhages, exudate formation, and changes in venous diameter. In proliferative DR, being the more severe and progressed form, includes intraretinal and preretinal neovascularization(57,58).

DR shares the same molecular pathogenesis with other microvascular complications of diabetes(59,60). The earliest changes in retinal vasculature in states of hyperglycaemia is the dilatation of blood vessels in order to meet the increased metabolic need of retinal tissue(61,62). Loss of pericyte in retinal vasculature is another pathogenic hallmark observed in DR (63,64), which in turn plays a significant role in the earliest vasodynamic clinical sign observed in diabetes(65,66). Furthermore, the blood retinal barrier becomes impaired due to apoptosis of endothelial cells and thickening of basement membrane(67). The loss of endothelial cells and pericytes causes decreased blood flow to capillaries, thus leading to ischaemia and upregulation of VEGF expression by endothelial cells(68). The

involvement of VEGF has a direct effect on vascular permeability as well as an indirect effect through phosphorylation of occludin and ZO-1(69).

At its current state, successful management of diabetic retinopathy include surgical and sustained release pharmacological therapies(70,71). In addition to carrying their own risks and complications, these management approaches have only been able to mitigate the progression of the disease temporarily, with high rates of relapse(72,73). This can be attributed to the gap in our understanding of the changes in the endothelial glycocalyx that lead to the clinical manifestation and diagnosis of the disease.

1.1.4.2 VEGF in diabetes

The vascular changes observed in diabetic retinopathy have been hypothesized to be caused by an excess of a substance produced within the eye in diabetic states(74). In order to produce the effects seen in diabetic retinopathy, the substance must be angiogenic, diffusible and induced in ischaemic states, among other retinal specific characteristics(75). These characteristics are distinguishable in VEGF. VEGF is endothelial specific angiogenic and Vaso-permeable factor that has an affinity to tyrosine kinase activity receptors(76). Previous studies have presented evidence of increased VEGF, among other angiogenic growth factors, production by retinal pigment cells in diabetic states(77)(78). Studies performed on mice and monkeys, in which VEGF production was inhibited by the use of receptor chimeric proteins, showed a decrease in retinal angiogenesis(79)(31).

1.2 VASCULAR WALL STRUCTURE

The basic anatomy of the vascular wall is divided into three layers, each referred to as tunica; tunica intima, tunica media and tunica adventitia. Each layer differs in morphological structure and function(80). The structure of the blood vessel wall originates from the embryonic mesoderm. The thickness of a blood vessel wall is consists of three main layers that vary in thickness depending on the blood vessel type, and the organ it supplies(81,82). Starting with the outermost layer, the adventitia is made up of elastin, collagen, and fibroblasts. It structural components give it the tensile strength to maintain its shape by

resisting excessive extension and recoil while still allowing capacity for expansion and dilatation(83).

The middle layer, the media, consists primarily of smooth muscle cells that present in two categorical phenotypes, the contractile and the synthetic(84). The contractile cells, as the name suggests, provide the contractile strength and ability of the blood vessel. The synthetic cells are important for maintaining the proliferation of the cell depending on the force exhibited on the vessel wall(85).

Lastly, the intima consists of endothelial cells, a basal lamina and a cell free subendothelial layer in all blood vessel types(86). Additionally, a layer of smooth muscle cells as well as various types of white blood cells can be present in big arteries(87).

The layers present in structure of the blood vessel depends on the function of the specific blood vessel(88). Some of these functions include transport of blood throughout the body; whether to sustain high pressure blood flow in arteries or to increase and support blood flow in veins, and transport of solutes and water across the vascular wall in capillaries(89,90). While in arteries, all the layers are present with an abundance of smooth muscle cells(91), capillary vessel walls only have the intima with its endothelial cell layer and basal lamina(92).

The capillary wall structure allows the direct diffusion of small lipophilic molecules and gases(93). Other molecules, such as glucose amino acid and ions, require transport mechanism that depend on facilitated diffusion through specific channels(94). Large proteins are transported into and through endothelial cells by endocytosis and exocytosis. Additionally, intercellular clefts and tight junctions are needed for larger molecules and ions to move across the vascular wall(95,96).

Mass transport, also referred to as bulk flow, involves an efficient transport mechanism that depend on two pressure forces. These two forces, hydrostatic and osmotic pressure, prompt the movement of fluid from a compartment of high pressure to low pressure(97–99). The result of the two forces leads to filtration that causes movement of fluid from intravascular fluid into the interstitial space at the arteriolar end of the capillaries. While it leads to

reabsorption on the venous end of the capillary in which fluid moves back into the intravascular space from the interstitial area(100,101).

1.3 REVISED STARLING PRINCIPLE

The classic Starling principle hypothesized that the movement of fluid across the capillary wall is driven and regulated by the net of four contributing forces: the hydrostatic pressure gradient between the capillary lumen and the interstitium and the oncotic pressure gradient between the capillary lumen and the interstitium. The Starling principle demonstrated that the balance of these four forces is needed to maintain blood volume within circulation. Adding that the capillary hydrostatic pressure decreases as the fluid moves from the arteriolar end of the capillary to the venous end. Thus, indicating a filtration net movement at the arteriolar end and an absorption net movement at the venous end(102). The work published by Starling on fluid absorption across the capillary was widely accepted into the literature but no further experimentation by Starling or subsequent literature was done to apply a demonstration of his hypothesis(103). The first demonstration that provided further evidence of Starlings work was done in 1927 and showed a significant positive linear correlation between fluid filtration or absorption rates through the walls of single capillaries and the hydrostatic pressures fluid(104).

A century after the publication of the Starling principle, a paper was presented that called attention to a few errors in the experiments undertaken to demonstrate the Starling principle when applied to the general vasculature and an absence of the venous reabsorption that was described in the Starlings paper(105). While Starling principle was able to predict and explain the movement of fluid in specific tissue types, i.e. the kidney and intestinal mucosa, it could not establish the same results in the general vasculature(106).

One of the limitations of the classic Starling principle involves the assumption that the fluid moving across the capillary wall forms an ultrafiltrate, thus excluding the relevant movement of macromolecules(107). The steady state described in Starling principle cannot be reached

because an equilibrium between the hydrostatic and colloid osmotic pressure between the plasma and interstitial fluid is never reached due to the movement of macromolecules(106).

Another flaw with the Starling principle is its failure to recognise the role played by the endothelial glycocalyx. The effective osmotic pressure regulating the movement of fluid across the capillary is dependent on the difference in pressure the ultrafiltering layer the glycocalyx structure provides The effective osmotic pressure created by the endothelial glycocalyx varies from the osmotic pressure hypothesized by Starling driven by the difference in pressure across the wall of the capillary as shown in Figure 1.1(108–110).

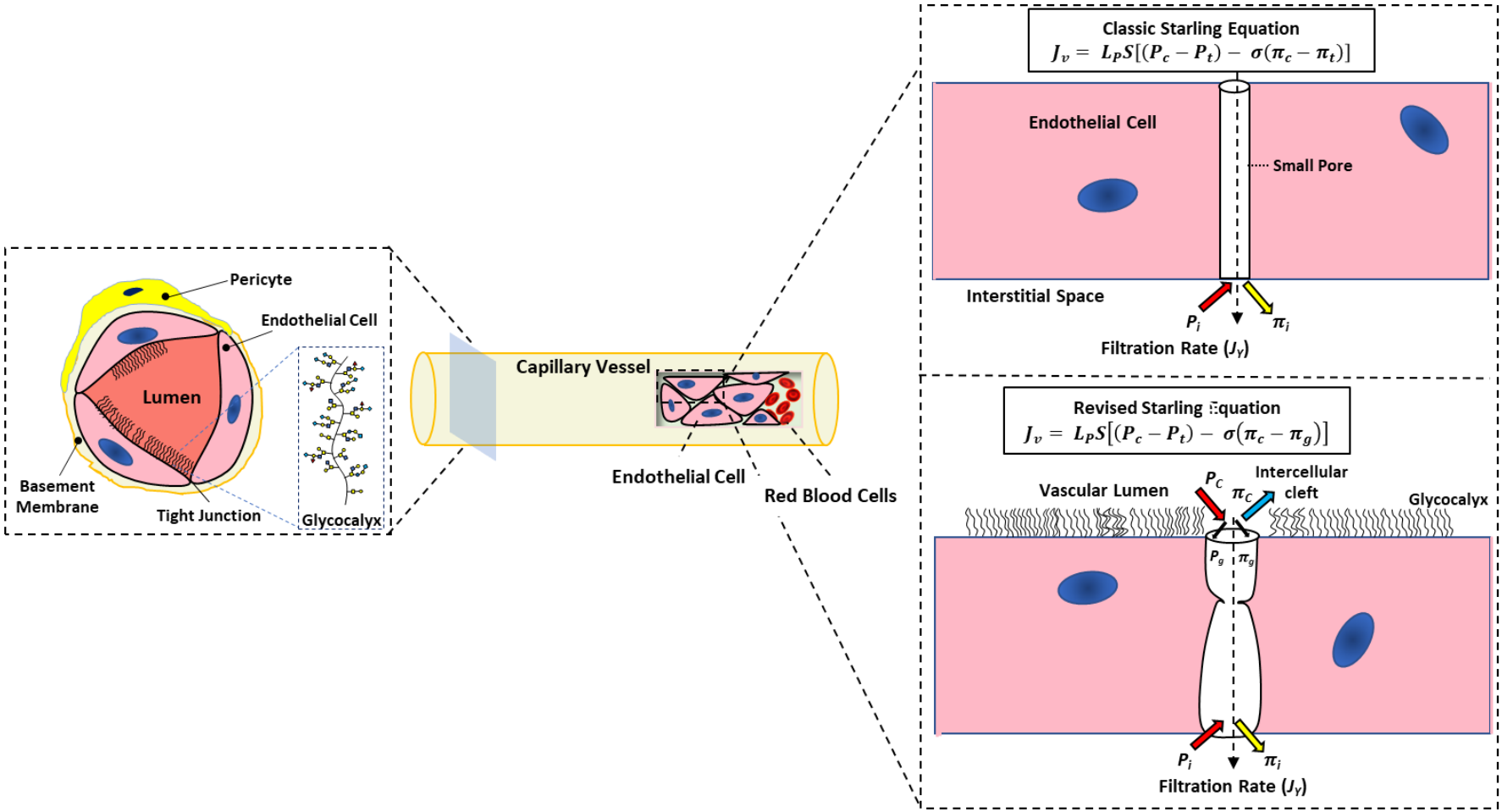

Figure 1.1: Blood Vessel Illustrating Starling Hypothesis and the Endothelial Glycocalyx

a. Shows a cross section of the capillary wall. The endothelial cells are lined with eGLX on the luminal surface and a basement membrane that lies between the endothelial cell and the pericyte.

b. A magnified illustration of the forces that account for the movement of fluid and molecules across the capillary wall. It demonstrates the difference between the classical Starling Hypothesis and the Revised Starling Hypothesis with the eGLX present. Jv= Transendothelial solvent filtration per second, Pc= Capillary Hydrostatic Pressure, Pi=Interstitial hydrostatic pressure, πi= interstitial oncotic pressure, πc= plasma oncotic pressure, Lp= hydraulic conductivity of the membrane, S= surface area for filtration, σ= reflection coefficient.

1.4 ENDOTHELIAL GLYCOCALYX

1.4.1 STRUCTURE AND COMPOSITION OF ENDOTHELIAL GLYCOCALYX

The presence of the Endothelial Glycocalyx (eGLX) was first hypothesized as a porous protein layer that plays a role in the development of oedema in 1940(111). The eGLX is a carbohydrate-abundant coat that lines the inner most luminal layer of vascular endothelium. It is comprised of anchoring core proteins with GAG chains at specific attachment sites forming a mesh of fibrous molecules(112). The main core proteins that form the structure of the eGLX are the syndecans and glypicans (113,114) and the most common occurring GAG chains are heparan sulphate, chondroitin sulphate, both of which covalently linked to glycoproteins, and hyaluronan (115,116). They serve as the contact barrier between the endothelial cell layer and blood contents as they flow through the vessels(117,118). The components of the eGLX varies in different tissue types (119) depending on the function needed by the eGLX (120) through specific core proteins that determine the quantity and location of each GAG chain as shown in Figure 1.2(121).

The sulphate group in the proteoglycans and glycoproteins gives the membrane bound layer a negatively net charge(112). The repelling function of the negative charge is important in controlling and limiting the movement of plasma proteins across the capillary wall, most importantly albumin(122). The eGLX is responsible for maintaining microvascular and endothelial physiology, thus lines all healthy vascular endothelium(123,124). The depth and thickness of the eGLX is varying in different vessel thickness and in different vessel structure(125,126). While it was first postulated that the eGLX has a thickness ranging between 10 to 30 nm(127), succeeding experimentation provided evidence that it occupies a significantly bigger thickness ranging between 0.5 μm to several micrometres(128). Visualising the dimensions of the endothelial glycocalyx is challenging (129) as studies have shown that the structural thickness is significantly underestimated in vitro in comparison to in vivo due to the fragility of its structure (130,131).

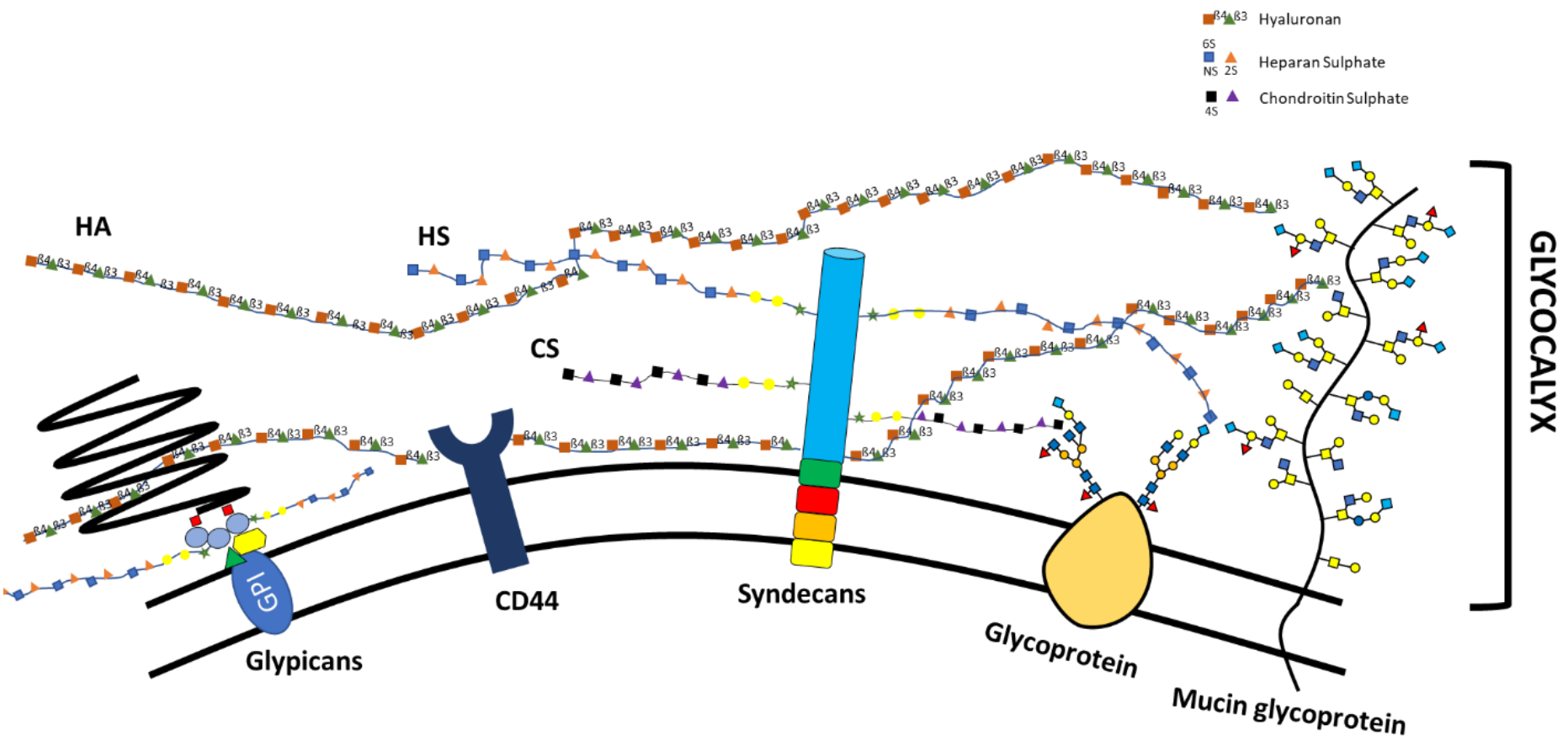

Figure 1.2: Endothelial Glycocalyx Structures.
Illustration of the different components of the endothelial glycocalyx layer; HS (Heparan sulfate), HA (Hyaluronan), CS (Chondroitin Sulphate), Proteoglycans (Syndecan), glycoprotein, glypicans and CD44.

1.4.2 FUNCTION OF THE ENDOTHELIAL GLYCOCALYX:

The eGLX is responsible for maintaining microvascular and endothelial physiology. For starters, the eGLX has an evident role in protecting the endothelial cell layer from mechanical shear stress created by flow of blood(132,133). Another protective capacity provided by the eGLX is limiting the effect of oxidative stress on the endothelial cell layer(134). One mechanism that helps reduce the enzymatic mediators of oxidative stress is the presence of heparan sulphate and hyaluronan, which hinders the effect of oxygen radicals and maintains the availability of the vasoprotective nitric oxide(112,135,136). An experiment demonstrated the upregulation of incorporating sulphated sugars in the composition of the eGLX through a change in size and distribution when exposed to oxidative stress(137).

An important role of cascading effect is the binding of cytokines to eGLX(60). Similar to the effect of cytokines on other cellular mechanisms, cytokines have an effect on the synthesis of eGLX to accommodate for local and systemic physiological and pathological changes(138,139). The eGLX has also been shown to have a role in limiting the extravasation of LDL molecules from the plasma for cellular uptake(80,140).

Regulation of vascular permeability is the most prominent role evident in the pathological states that affect the eGLX(141). The selectivity of the eGLX is based on size and charge of solute (e.g. albumin). The layered structure of the endothelial glycocalyx allows the selective passage of water and solute as they cross through the varying porous sizes(142).

Another important characteristic that enables the eGLX to regulate vascular permeability is its electrostatic negative property(143). Charged dextrans used in experiments have demonstrated that negatively charged molecules are not filtered across the capillary wall, while positively charged molecules become bound and retained by the eGLX to be filtered through the capillary wall(144).

In addition to serving as a mechanical barrier against the inadvertent adhesion of platelets and leukocytes to the vascular wall, the eGLX provides specific binding sites for

anticoagulant enzymes such as antithrombin III and tissue factor pathway inhibitor (145) on heparan sulphate(146).

1.4.3 VISUALIZATION TECHNIQUES USED FOR DETECTION OF THE ENDOTHELIAL GLYCOCALYX

Oxidative stress, caused by hyperglycaemic states, leads to morphological changes within the vascular endothelium. Visualizing the changes that lead to increased permeability is paramount for the development of effective treatment and prevention of diabetic retinopathy(147).

The use of effective imaging techniques poses a crucial opportunity to enhance our understanding of the role of the eGLX in the vascular endothelial. The effect diabetes has on vascular permeability provides a mean of understanding the mechanism and structural composition with which the vascular endothelial layer is able to function. The morphological changes observed in diabetic endothelial models can explain the altered functional ability of the endothelium to maintain homeostasis(148). Understanding the physiological role of the endothelium in maintaining homeostasis and the pathogenesis of diabetic vascular impairment provides an effective and vital breakthrough to better advance management and prevention of diabetic comorbidities. The increased vascular permeability in diabetes affects the molecular transport needed to maintain homeostasis. Novel imaging techniques such as high-resolution electron microscopy can be used to develop 3D electron tomographic reconstruction to better understand the altered compositional and structural change observed in diabetic vasculopathy(147).

Several methods have been utilised for direct visualization of the eGLX. Most commonly through the use of fluorescently labelled lectins that bind to specific sugar molecules on the GAG chains(112).

The first attempts at visualising the eGLX took place in 1966 through the use of ruthenium red as a stain and imaged using an electron microscope. The use of ruthenium red is due to its cationic charge, thus binding to the negatively charged acidic mucopolysaccharides in the

eGLX and resulting in electron densities when osmium tetroxide is present(127). Thereafter came the use of gold colloids and immunoperoxidase labelling (149,150). Followed by the use of positively charged ferritin to provide an outline of the eGLX, which illustrated a thickness much higher than the 20 nm previously viewed and tested its dependence on plasma proteins to maintain its framework(151).

Direct in vivo visualisation of the eGLX was performed to provide an estimated measurement of the thickness of around 0.5 µm. It used a FITC dextran plasma tracer that is not permeable to the eGLX to compare the functional diameter available for blood components to occupy as they flow(128).

Achieving the highest resolution through electron microscopy is limited by the sample preparation method used, as fixation and processing of the sample alters the structural composition(106). The physical and physiological structure of the eGLX makes it fragile and challenging to fix. The eGLX in its innate form is a hydrated gel-like structure (139), loss of the water component will thus lead to a change in the dimensions. When preparing the eGLX for imaging, the tissue undergoes several processes during fixation that may cause its dehydration(152). These include the use of alcohol for dehydration and resin embedding, as well as the general decrease of extracellular components, which may aid in providing a hydrated environment for maintaining the eGLX(153).

Visualising attempts that eliminate the use of dehydrating steps have provided promising results (154–156), however the use of electron microscopy remains lacking in providing the precise and min spatial resolution required to understand the structure of the eGLX. Additionally, the glare caused by the fluorescein dye reduces from the resolution of the image produced and creates imaging artifacts(157).

Finally, it is of importance to discuss the use of high-pressure freezing method to preserve the structure of the eGLX for visualisation. Through the use of rapid freezing methods, water is sublimated. Thus, permits the conservation of the hydrophilic structure and prevents the collapse of molecular structure, all necessary to visualise the eGLX(158). These methods provide higher detection ability of smaller structural changes that are needed to demonstrate

functional roles played by the eGLX and how they are affected in disease states(157). They have provided results closest to the mathematical predictions and in vivo experiments of the eGLX thickness and structure thus far.

1.4.4 VISUALIZATION METHODS

1.4.4.1 Light Microscopy

The first compound microscope, first invented in 1590, were used in visualising biological microorganisms from the start. Soon after, a diverse array of changes allowed for the invention of different types of microscope instruments based on the original technique of a compound microscope(159). While the concept of a confocal microscope dates back to the 1950s, it wasn't used in research laboratories until the 1980s. Since then, drastic improvements to the instrument have allowed the confocal microscope to remain in use(160).

While the use of light microscopy compromises the resolution in comparison to the electron microscope, it allows the visualising of viable hydrated cell structures(161). Thus it provides an advantage when viewing highly dynamic and fragile structures such as the eGLX.

One way of visualising the eGLX using the confocal microscope is through the use of lectins that bind to specific carbohydrate moieties and 3D structures(162). The most frequently utilised lectins in viewing the eGLX are lycopersicon esculentum agglutinin (LEA) and wheat germ agglutinin (WGA)(163). The biggest limitation of using lectins in the case of eGLX is its inability to visualise specific structural and compositional change. Lectins are typically combined with the use of fluorescent dyes to image particular structures that make up the eGLX(164).

Means of visualising the eGLX include using optical microscopy that have been recently developed and utilised include the Stochastic Optical Reconstruction Microscopy (STORM)(165). STORM is one of the few super-resolution imaging techniques that increases the optical microscope imaging spatial resolution by over an order of magnitude down to few nanometres(166). Thus, it has been used to visualise and study biologic

samples at the molecular level(167). The ability to achieve images of biological events using single-molecule-based super-resolution imaging provides vital opportunities to examine molecular scale structural knowledge(168).

1.4.4.2 Electron Microscopy

The 1924 de Broglie theory compared a moving electron to a light wave, alongside a demonstration by Busch that an electron beam can be focused through the appropriate shaping of magnetic or electrostatic fields to create an image led to the development of the technique of electron microscopy(169–171). Electron microscopy (EM) is a technique used to produce high resolution images of the biological and non-biological specimen ultrastructures through a focused beam of electrons(172). The first electron microscope, built in 1932 by Knoll and Ruska (173), lacked a condenser lens and produced lower resolution images than optical microscopes(174).

The ability of electrons to produce high resolution images lies in their very short wavelength property of negligible mass. Furthermore, electrons have low penetrating ability, thus can only be used to visualise ultrathin structure. Specimens and slides must be carefully and critically prepared using the suitable technique, depending on the tissue type, for optimum visualisation(175).

There are two main types of electron microscopes, Transmission Electron Microscope (TEM) and Scanning Electron Microscope (SEM). The difference lies in the ability of the TEM to, as the name suggests, be transmitted through the structure it is illuminating to produce a 2D image of the internal features(176). TEM through interpretation of loss events, provides the most powerful combination of spectral and energy resolution(177). SEM however scans the surface of the structure, usually of thicker depth, to produce a 3D image. In the case of endothelial glycocalyx, TEM has been the method of viewing since the first visualisation attempts(127,178,179). Different techniques have been used but they all involve the use of a heavy metal and usually perfusion fixing rather than post staining. The use of SEM was limited by low resolution(180,181).

The first image produced of the Endothelial glycocalyx by TEM showed a gap of thin filament between the red blood cells circulating and the endothelial cell layer. The thin filament, described as scanty material, seemed to also fill the space junction between the endothelial cells(182). Since then, several techniques of staining and fixation methods have been developed and attempted to provide better visualisation and understanding of the endothelial glycocalyx(125,183). Stabilisation methods that use cationic probes have advanced imaging of the eGLX. These include ruthenium red (184) and alcian blue (185), which improve the reduction of osmium, thus increasing the eGLX polysaccharide electron density(186).

1.5 BASEMENT MEMBRANE

Three decades after the discovery of the vascular changes observed in diabetic retinopathy, a study described the increase in thickness of the vascular wall with a higher intensity in basement membrane staining(187). After which the development of electron microscopes enabled the first investigation of the basement membrane in diabetic states in muscle tissue(188). The findings then prompted a streptozotocin induction of diabetes in rats to study the changes of basement membrane(189). All vascular studies in diabetic retinopathy provided evidence of increased basement membrane thickness as the earliest and most prominent vascular structural changes(190–192).

The observation has led a new approach of experiments to attempt to correlate the increased permeability with the paradoxical basement membrane thickening(193,194). Deposition of extracellular matrix has been recognized as one of the mechanisms that leads to the increase in thickness of the basement membrane in hyperglycaemic states. Studies showed a compositional change in the basement membrane in diabetic tissue through the upregulation of Fibronectin and Collagen IV expression(195). The role of the basement membrane is suggested to be compromised in diabetic pathogenesis due to changes in composition. The cross linking and glycation of its filaments into bundles that contributes to the increased permeability(193). Thus far, evidence has suggested the increase in thickness has a contributary role in the development of increased permeability. The impairment in the

ultrafitering barrier on the endothelial lining has been discussed by many as the possible cause of basement membrane changes(196,197). The hypothesis we address in our experiments is the effects of changes in the eGLX on the basement membrane thickness.

1.6 SPHINX-31

Vascular endothelial growth factor (VEGF) A is a highly specific endothelial cell inducer of angiogenesis. Additionally, VEGF regulates the synthesis and cleaving of glycosaminoglycans that constitute the eGLX(198). Studies have supported evidence of the critical role it plays in development of neovascular eye diseases, including diabetic retinopathy(199,200). There are different isoforms of VEGF-A, each with a different role. The alternative splicing of the 8 exon VEGFA gene determine which isoform is synthesized(201). The two isoforms most relevant to diabetic retinopathy include the pro-angiogenic VEGFA165a and anti-angiogenic VEGFA165b(202). An imbalance favouring VEGFA165a synthesis leads to excessive angiogenesis observed in diabetic retinopathy(203). Furthermore, VEGFA binds to VEGF Receptor 2 (VEGFR2) induces its phosphorylation and activates intercellular signalling cascades, that are essential for endothelial cell survival, proliferation and motility(204). Fast effects of VEGFR2 phosphorylation include increased permeability through destabilization of endothelial cell junctions such as VA-Cadherin(205). Other slower acting effects of VEGFR2 include the protective and restorative activity on the eGLX(206).

Several Serine-Arginine protein are responsible for the regulation of VEGF splicing, one of which being serine arginine-rich splicing factor 1 (SRSF1).(207) SRSF1 is phosphorylated by the Serine-Arginine Serine Kinase (SRPK1) gene(208). SPHINX31 is an SRPK1 inhibitor, thus has been suggested as a potential therapeutic agent in various vascular diseases such as diabetes(209).

Previous studies have been able to provide evidence of its efficacy in restoring a functional balance between pro-angiogenic and anti-angiogenic protein(208). It's pharmacokinetic properties as well as its potency as a topical agent in the eye present an opportunity for

advancement a suitable treatment for different diabetic complications(210). The purpose of this study is observe its effect on diabetic retinopathy as a topical agent.

1.7 EXT GENES

Exostosin Glycosyltransferase 1 (EXT1) and Exostosin Glycosyltransferase 2 (EXT 2) are protein coding gene located on chromosome 8. The EXT proteins are reported to have a vital role in formation and elongation of the Heparan sulphate glycoprotein backbone composed of alternating glucuronic acid (GlcA) and N-acetylglucosamine (GlcNAc) units. The role of EXT1 involves encoding for an endoplasmic reticulum-resident type II transmembrane glycosyltransferase necessary for the chain elongation step of heparan sulphate biosynthesis(211–213). Mutation of EXT1 is reported in hereditary multiple exostoses type I. Due to the gene's tumour suppressor role, loss of its function leads to formation of multiple osteochondromas and affecting the development of bone leading to skeletal deformities, including limb length discrepancy(214,215). Alternatively, experiments involving EXT2 mutations did not exhibit negative effect on the production and function of Heparan Sulphate as observed in EXT1 mutations. The glycosyltransferase activity of a fully functioning EXT1/EXT2 protein complex bring about more heparan sulphate production than the sum of EXT1 or EXT2 proteins when present separately(212). It has been hypothesised that EXT2 gene dose not have direct involvement in the hepran sulphate glycoprotein chain elongation process but rather in enabling the folding and transportation of necessary proteins to the Golgi apparatus complex by EXT1(216). Additionally, studies on individuals with EXT1 mutations have reported their role in maintaining endothelial homeostasis through their ability to increase Nitric Oxide bioavailability(217).

This finding supports the compositional function played by heparan sulphate glycoprotein within the endothelial glycocalyx in flow-mediated dilatation(218,219).

The biological function of heparan sulphate is determined by the location of the sulfate groups and the length of the polysaccharide chain. Thus different heparan sulphate proteoglycans differ in specific binding sites for different specific proteins, while other

proteins bind non-specifically to negative regions on the polysaccharide chain(220). Even though the structure of heparan sulphate proteoglycan chain is cell-specific, it remains dynamic and responsive. It is adjusted through cell signalling process to the developing cellular needs and surrounding(221).

The role of the EXT genes is involved in catalysing the initiation and chain elongation on a proteoglycan backbone. It works alongside N-deacetylase/N-sulfotransferase and O-sulfotransferase involved in chain sulfation. The glucosaminyl N-deacetylase/N-sulfotransferase act as the first modification enzymes that initiate the work on the growing heparan sulfate polysaccharide chain along the proteoglycan backbone(222). EXT1 and EXT2 genes carry out several in vitro glycosyl transferase activity (212,223) by acting as polymerizing enzymes that define the sulphation pattern. The end result pattern of the heparan sulphate proteoglycan will determine which of the target molecules involved in the function of the eGLX are to be able to bind(224,225).

The role of heparan sulphate chain and its pattern has been previously assessed in states of vascular pathogenesis through observation of changes in the eGLX as a functioning barrier(226,227). Gene targeting can be used to inhibition EXT1 gene to further understand the role of heparan sulphate as a core protein of the eGLX(221). Additionally, heparan sulphate proteoglycan has been reported to have a functional role as a VEGFR2 co-receptor by facilitating its angiogenic activity(228).

1.8 CRE/LOX SYSTEM

The CRE/LOX system is made up of two key components, the Cre recombinase and the LoxP as the recognition site(229). The components are produced, extricated, and adapted from P1 Bacteriophage. The components do not occur naturally in any other species, thus acts can be controlled to act on specific intended genes. The loxP is made up of 13 (x2) base-pair recognition sites separated by an 8 base-pair spacer region(230,231). The loxP component are always used in pairs that flank the selected gene(232). The Cre is inserted in a gene that is expressed in specific tissue to enable tissue selectivity of gene targeting. In

the case of EXT1 gene expression in endothelial cells, VE-Cadherin is selected as the tissue specific promoter for the Cre location(233).

The direction of the two loxP components in relative to eachother determines the gene expression alteration. While same direction loxP components lead to irreversible excision of the targeted gene that lies in between, oppositely orientated loxP components lead to reversible inversion of the targeted gene sequence that flips back and forth indefinitely(234).

1.9 AIMS AND OBJECTIVES

The importance of the eGLX in maintaining the capillary wall as an imperfect semipermeable membrane needed to form the ultrafiltrate and maintain equilibrium between intravascular and extravascular fluid compartments has been well reported(106,235). The evidence has been supported by the effect of damage to the eGLX seen in disease states on increasing permeability(236,237). However, there remains a gap in our knowledge of the structural change in the eGLX that causes the increased permeability. Therefore, the scope of this research will aim to explain some of underlying causes that lead to the increased permeability observed in diabetic vasculature.

1.9.1 STRUCTURAL CHANGE OF EGLX

The structural changes in the endothelial glycocalyx that lines the vascular endothelium in diabetic capillaries will be thoroughly discussed and investigated. The retinal capillaries will be the focus of visualising these changes. A range of advanced imaging techniques and tissue preservation methods will be employed and tested to visualise these structural changes. These include transmission electron microscopy and high pressure freezing. The LaDy GAGa staining method, has provided the most valuable tool established to visualise the structural change, will also be utilised.

Images will then be analysed using ImageJ (238) for a change in depth and percentage coverage of the eGLX. The images are categorised based on being perfused or not perfused, then subcategorised on whether the eGLX is present lining the endothelial cells or having been shed due to perfusion. The eGLX's role in permeability must be analysed

alongside other vascular wall permeability barriers, including tight junctions and basement membrane. Thus, the thickness of the basement membrane in retinal capillaries will also be measured.

Based on preliminary data (Figure 1.3) previously carried out, we believe there is a decrease in depth and percentage coverage of the eGLX but no change in the thickness of the basement membrane. The data used is from diabetic mice, see Appendix I for an example of the experimental plan.

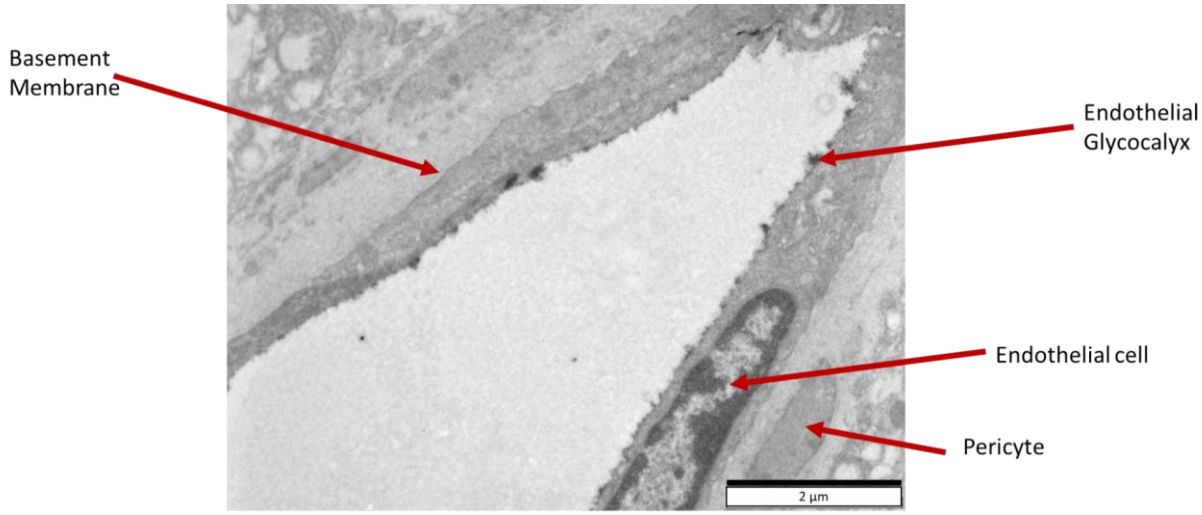

Figure 1.3: Transmission Electron Micrograph of Retinal Capillary.
A transmission electron micrograph showing the presence of endothelial glycocalyx perfusion fixed and stained with the LaDy GAGa method in a diabetic mouse sample. Endothelial glycocalyx is visualised by the appearance of dark staining with the basement membrane present between the endothelial glycocalyx and the pericyte.

CHAPTER 2: METHODOLOGY

2.1 TREATMENT OF MICE

For this study, ethical approval was required as experiments involving mice took place. All experimental animals were treated in accordance with the ARVO statement for the Use of Animals in Ophthalmic and Vision Research at the University of Nottingham (UoN) Biological Services Unit (BSU) under the UK Home Office licence PPL 30/3184 for the diabetic/SPHINX31 experiments and Home Office licence P3E735452. Thus, the most compassionate ways to cull the mice was ensured and in-vivo work was carried out by trained and certified individuals (Claire Allen & Penny Lohrer).

2.2 DIABETIC AND SPHINX-31 TREATED EXPERIMENT

30 Female DBA2J mice were used; 15 served as non-diabetic controls and 15 mice were randomly selected to become diabetic. After diabetic status was achieved, 4 of the diabetic mice were randomly selected for a SPHINX-31 treatment as a pilot study to observe its effect on permeability. Randomised selection of the mice treatment was implemented by blind selection of a treatment option from an envelope for each mouse.

The experiment only included female mice to eliminate any sex-based differences. Female mice were selected to decrease the weight increase likelihood that is observed in male mice, as weight is a direct confounding factor in diabetes. Female mice provide less varying weight measurements as experimental subjects. While it has been previously reported that female mice are resistant to diabetic induction with STZ, more recent studies have reported no difference in diabetic progression between the sexes(239). The mice were age and weight matched at 22 weeks and over 20 g, respectively. The only exclusion criteria was a weight below 20 grams and lean mice were chosen to ensure that diabetic state was a result of STZ treatment exclusively.

2.2.1 INDUCING DIABETES

On day 0, diabetic induction of the diabetic mice was started by an intraperitoneal injection of Streptozocin (STZ). STZ acts as an islet cell ablating agent that is taken up by the GLUT2

transporter on pancreatic β cells by having a structure similar to glucose(240). Uptake of STZ by β cells lead to its alkylation of its DNA, resulting in inflammation and consequently an infiltrative immune response of lymphocytes that destroys them. A lack of insulin producing β cells mimic a state of insulin dependent diabetes, thus causing hyperglycaemia. Diabetic induction by STZ is more feasible than the use of genetical or viral induction and more favourable than chemical induction by alloxan for having a wider diabetogenic dose(241).

STZ dose was prepared by dissolving 10 mg of STZ in 2 ml of 0.1 M citrate buffer solution with an adjusted pH of 4.5 to create a 5mg/ml STZ solution. The doses were prepared, filter sterilised and stored on ice for 20 min before being administered.

A dose of 40mg/kg was given to each mouse in the diabetic and SPHINX-31 treated group. To induce diabetes more effectively, STZ was given after a 6-hour fasting period to increase the uptake rate by β cells. In order to prevent death from hypoglycaemic state due to the rapid glycaemic fluctuation, a 10% sucrose was given alongside food after each dose. STZ doses were repeated up to 5 times until hyperglycaemia (blood glucose > 15 mM) was achieved. The use of several smaller doses of STZ was found to decrease remission rates of diabetes (242) and avoids the risk of toxicity to the kidney(243). The welfare and weight of the mice was monitored daily during this period.

2.2.2 Monitoring Diabetes

2.2.2.1 Blood Glucose Levels

Blood glucose level was measured prior to administering of STZ and consistently throughout the experiment to ensure that diabetic state was achieved. Blood samples were taken through a venous puncture with the use of a 25-gauge needle and glucose measured using an Accu-Check glucose monitor. Successful induction of Type 1 Diabetes was set at a blood glucose measurement > 25 mmol/l.

2.3 EXT1 Knockout Experiment

To ensure the activation of the EXT1flox/flox with Tamoxifen, two control groups was used. To establish that the observed results were due to the controlled and selective Cre activity

rather than background expression of the loxP component independent from the Cre, a control group was needed lacking a Cre component ($Ext^{flox/flox}$:$VE^{wt/wt}$ + Tamoxefen). The first control group was therefore homozygous with the loxP pair components $EXT1^{flox/flox}$ gene but without the Cre present. Thus, the EXT1 gene were expected to be expressed as in the general strain population.

Furthermore, for experimental purposes that require data before and after the effect of the gene targeting, the Cre component was controlled by an inducible promoter or regulator. In which case, the Cre component was not expressed until the promoter is added, thus setting the Cre/lox in effect. In order to ensure the controllability of Cre activity, a second control group was necessary that contained the Cre component but was not given the inducer ($Ext^{flox/flox}$:$VE^{cre/wt}$ + Vehicle).

The second control group had a genotype of $EXT1^{flox/flox}$ with the Cre present in the VE-Cadherin. All of which identical to the experimental group. However, this group was not given a Tamoxifen dose to induce the gene inhibition by the Cre.

Previous studies have targeted heparan sulphate synthesis through the use of the loxP-Cre activated system in different cell-types (e.g. bone and central nervous system) specific(244). Confirmation of the success of heparan sulphate inhibition in Cre activated experimental groups in these studies was achieved by the use immunocytochemistry with a monoclonal antibody that binds to heparan sulphate(245). Additionally, these studies demonstrated the incompatibility of EXT1 null phenotypes with life, where all experimental animal subjects led to fetal lethality due to gastrulation abnormality(246). Thus, emphasizing the advantage of using the Cre/lox system to produce selectively heterozygous inhibition of one copy of the EXT1 gene.

For the purpose of this study, VE-Cadherin was selected as the Cre driver for being a strictly endothelial cell specific adhesion molecule(233). Genetic testing was performed to confirm the genotype of each mouse conforms with their experimental group. However, genetic testing is unable to confirm inhibition of the EXT1 gene or Cre specificity to endothelial cells.

2.4 ALBUMIN DETECTION

Weekly urine samples were obtained starting from Day 0. Each mouse was isolated in a metabolic cage with water for fluids and an enrichment diet until a minimum amount of 50 µl of urine was obtained for analysis. Albumin Creatinine Ratio (ACR) was measured using Enzyme-Linked Immunosorbent Assay (ELISA). Mouse albumin specific capture antibody added to 50 µl of urine in wells at a concentration of 1:10,000. Albumin specific biotinylated detection antibody was then added to the well before being washed thrice to remove unbound excess antibody. Streptavidin-Peroxidase Conjugate and TMB (3,3',5,5'-tetramethylbenzidine) were added to the wells and incubated for 20 mins at room temperature. A stop solution of Sulfric Acid turns the solution yellow on acidification, with the density of the colour being proportional to the concentration of albumin in urine. A measurement of the density was taken to ensure that albuminuria, a complication of diabetes, had occurred, thus reflecting the progression of the disease.

2.5 FUNDUS FLUORESCEIN ANGIOGRAPHY

It is predicted that retinal vascular permeability will start increasing from Day 14 and further progress the following 2 weeks(247). To observe the change in retinal vascular permeability predicted to occur after inducing diabetes, Fundus Fluorescein Angiography (FFA) was performed at Day 0 and Day 21 on all mice. Mice were anaesthetised with a solution of Ketamine (50mg/kg) and Medetomidine (0.5mg/kg) and eyes dilated with phenylephrine hydrochloride (2% w/v) and Tropicamide (0.5% w/v).

2.6 EUTHANASIA AND PERFUSION FIXING

The mice were euthanised using a lethal dose of sodium pentobarbitone (Lethobarb, Ayrton Saunders Ltd, Liverpool, UK) and kept on a heat pad for 20 min or until terminally unconscious. The abdominal aorta was clamped below the renal branches to ensure that the buffer was directed to the kidneys and did not accumulate in the tail. The diabetic and non-diabetic group of mice were euthanised on week 8, while the SPHINX-31 (Figure 2.1) and EXT1 (Figure 2.2) treated mice on week 12. Four different buffer solutions (Table 2.1) were

made. An incision was rapidly made in the thorax to enable intracardiac perfusion fixation using the LaDy GAGa method. Next, the left side of the heart was perfused at 60mmHg pressure using a blunt 24-guage needle with Buffer 1 (room temperature, pH 7.5) to flush with the positively charged lanthanum and dysprosium ions ,which bind to and stain negatively charged glycosaminoglycans(248). Followed by, perfusion of Buffer 2 (room temperature, pH 7.5) until the mice were stiff.

The use of heparan as an anticoagulant was avoided in all buffer solutions during perfusion to prevent any damaging reaction with the eGLX or reacting with lanthanum and preventing it from staining the eGLX. Fixing the tissue inactivates proteolytic enzymes present in tissue, which may degrade and decontaminate it.

1L of Mammalian Ringers solution (Buffer 0) consisted of:

6.72g of NaCl

0.42g of KCl

0.24g of $CaCl_2$

1.80g of Glucose

1.31g of HEPES

900ml double distilled water

Table 2.1: The composition of the buffers used for perfusion fixing of the mice.

Buffer 1	**Buffer 2**	**Buffer 3**
100ml Buffer 0 0.5g $LaNO_3.6H_2O$ 0.5g of $DyCl_3.6H_2O$	Buffer 1 2.5% Glutaraldehyde 2% Sucrose	Buffer 0 2.5% Glutaraldehyde 2% Sucrose

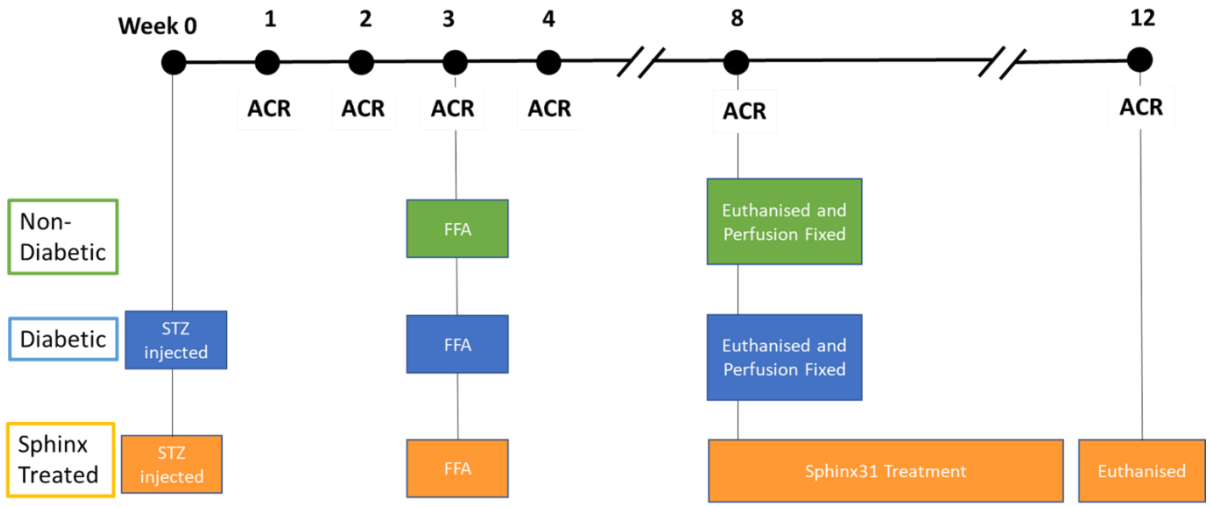

Figure 2.1: Diabetic/SPHINX-31 Pilot Study Experiment Timeline.

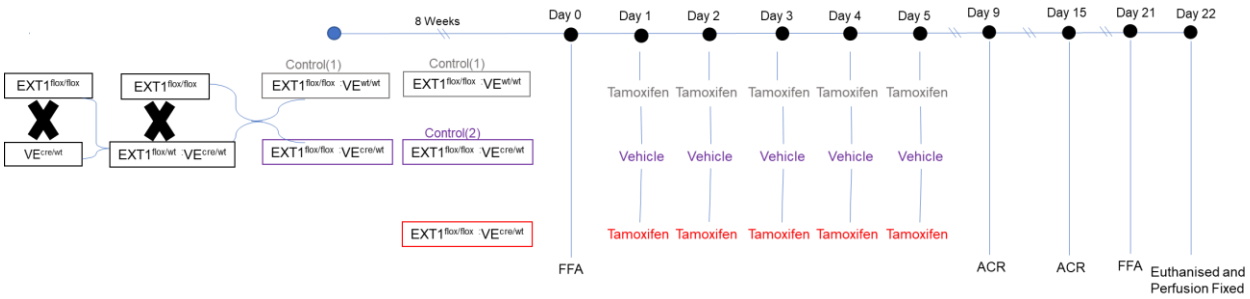

Figure 2.2: EXT1 Pilot Study Experiment Timeline and Breeding Genotypes.

2.7 Tissue Sectioning

Excision of both eyes was performed using surgical scissors and fine forceps. The right eye was then isolated in Buffer 3 (pH 7.5) in a 12-well plate on ice. While the left eye was immersed in phosphate buffered saline (PBS) in 1.5 ml falcon tubes and placed on ice. The purpose of the PBS was to preserve the osmotic conditions and prevent the tissue from drying out while the ice was necessary to slow down the enzymatic degradation of the tissue. The left eye was then dissected into 4 separate petals under a light microscope. 2 petals were immersed in Mammalian Ringer's before being scheduled for high pressure freezing the same day, 1 petal was fixed in paraformaldehyde (PFA) for cryosectioning and the final petal was also fixed in PFA and scheduled for Isolectin B4 staining at a later date.

2.8 Resin Embedding

In preparation for samples to be imaged by TEM, they were embedded in resin to enable sectioning at 70 nm thickness. The fixed eye tissue was isolated, washed with cacodylate and transferred into 0.1M sodium cacodylate buffer (pH). The next step involved the fixing of lipids and staining the sample using 1% Osmium Tetroxide (OsO_4) for 1 hour. Followed by a rinse with 0.1M sodium cacodylate buffer and a second rinse with 18.2MΩ deionised water (ddH_2O) to discard of potential artefacts. The tissue samples were then left overnight in Uranyl acetate at 4°c to be stained and achieve further contrast. The use of Lead citrate was excluded from the process to avoid the loss of eGLX visibility. After which, they were washed twice with ddH_2O for at least a min to remove excess uranyl acetate.

The dehydration process involved a series of 20 minutes immersion sessions in ascending ethanol solutions (70%, 90%, followed by a triple wash of 100% ethanol) to allow the transitional replacement of the water content of the tissue. Propylene oxide, while insoluble in water is soluble in ethanol and was used to transfer to epoxy resin (itself with limited ethanol solubility). Propylene oxide was used to act as a transition solvent between the alcohol dehydrations and epoxy resin (Araldite). Starting by 100% propylene oxide, followed by 1 hour in 2:1 propylene oxide: resin, 1 h in 1:1 propylene oxide: resin, 1 h in 1:2 propylene oxide: resin, ending with 100% resin left overnight. They were then moved into suitable plastic moulds filled with 100% resin and polymerised for 48-72 hours at 60°C. Once polymerized, the resin block is sufficiently hard and inert, allowing thin sectioning of the tissue.

2.9 IMAGING

The samples were dried before going to the TEM (Technai T12 Biotwin), where micrographs were captured under 100kV. Using the TEM, the 70nm thick sections of the retina with the choroid still intact were examined and imaged. Low magnifications of 1050x with a 62 x 85 µm field of view were used to image the whole thickness of the retina to form a full thickness image to demonstrate the different anatomical layers that constitute the retina (Figure 2.3). Low magnification of 2,250x was also used to scan through the tissue sample and locate the

blood vessels. Once a blood vessel is identified, various higher magnifications typically in the ranges of 16,500x and 60,000 x with a 1 x 1.5 µm field of view were used as necessary to provide images for analysing the basement membrane and endothelial glycocalyx, respectively. Additionally, it was necessary to use the suitable higher magnification to identify endothelial cells, pericytes and intercellular spacing. The endothelial glycocalyx was distinguished by a visible dark stain. While all layers where inspected for blood vessels, they were most prominent in the Nerve Fiber Layer. Additionally, as part of the eGLX project, images of capillaries were taken from other organs (Figure 2.4).

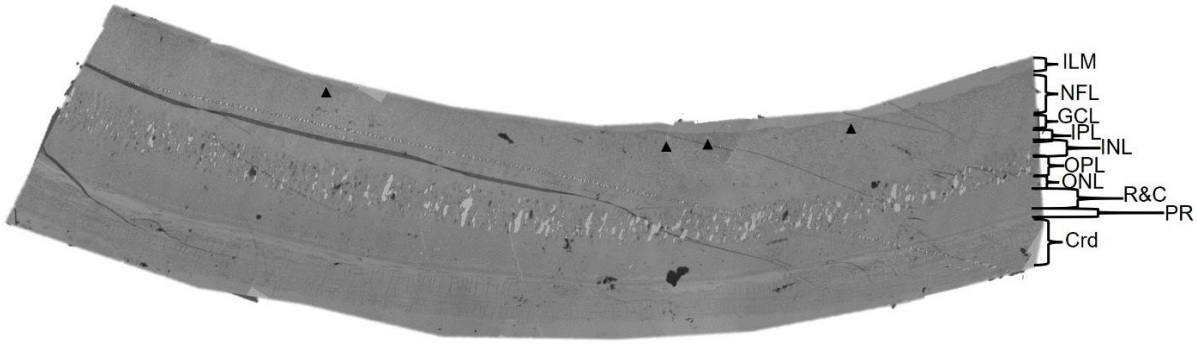

Figure 2.3:Montage of the Full Thickness of Retina Demonstrating the Different Layers
TEM images of perfusion fixed retinal capillary from DBA2J female mice showing the different layers of the retina including: Inner Layer Membrane (ILM), Nerve Fibre Layer (NFL), Ganglion Cell Layer (GCL), Inner Plexiform Layer (IPL), Inner Nuclear Layer (INL), Outer Plexiform Layer (OPL), Outer Nuclear Layer (ONL), Layer of Rods and Cones (R&C), Pigmented Layer (PR), and Choroid (Crd).
▲ *indicates location of capillary vessels imaged for analysis in the Nerve Fiber Layer.*

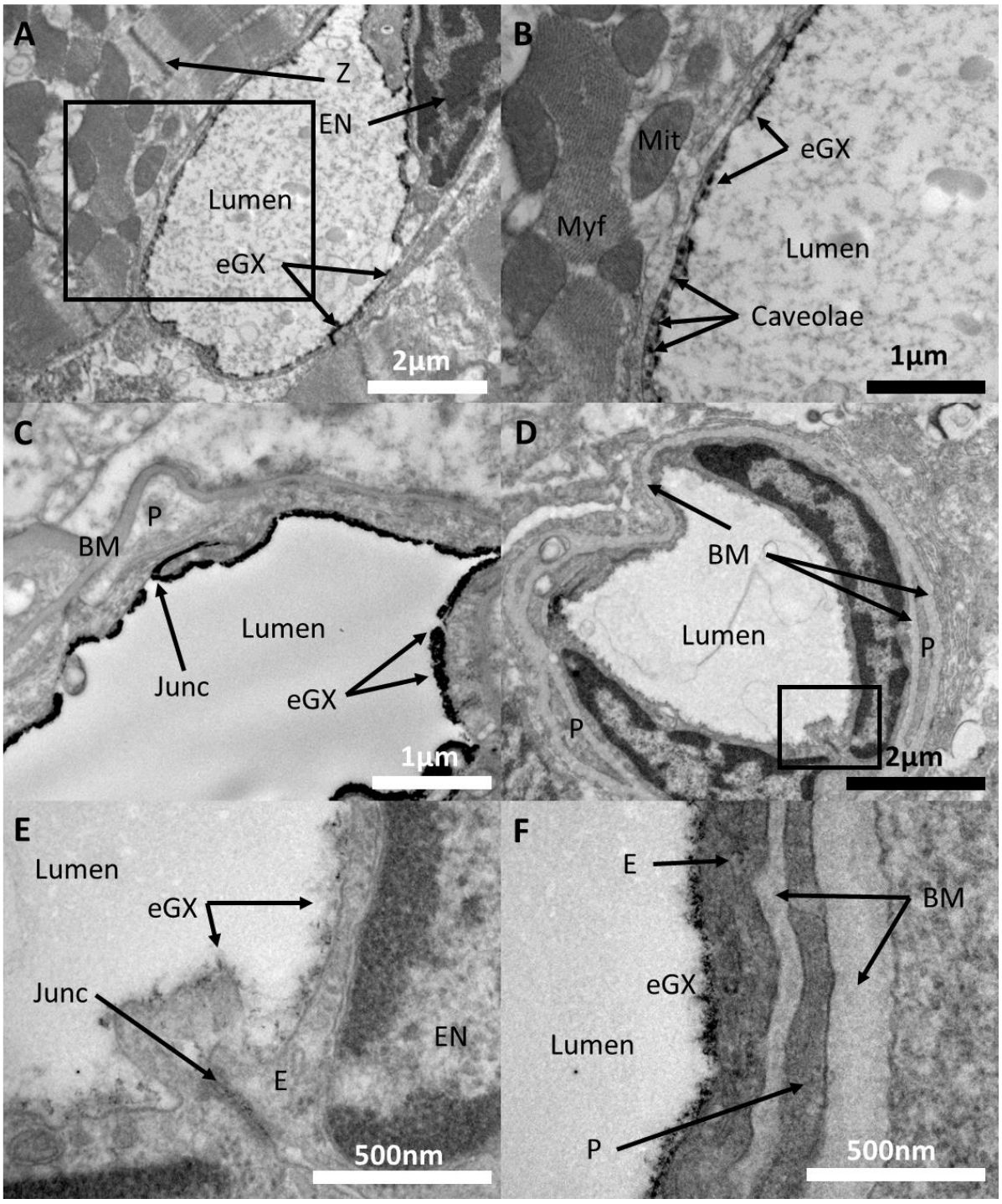

Figure 2.4: Endothelial Glycocalyx in Different Tissue Types

Images A-F are TEM images of perfusion fixed capillaries from DB2J female mice (A) an example of a heart muscle tissue capillary of a diabetic mouse. Figure (B) a higher magnification of heart tissue that demonstrates the presence and staining of eGLX.. Figure (C) an example of a brain tissue capillary of a diabetic mouse. Figure (D) an example of a retinal tissue capillary of a diabetic mouse. Figure (E) is a higher magnifiction of retinal to demonstrate the presence and staining of eGLX. Figure (F) an example of a retinal tissue capillary of a diabetic mouse.

endothelial glycocalyx (eGX), Endothelial Cell (E), Endothelial Cell Nucleus (EN), Junction (Junc), Basement Membrane (BM), Pericyte (P), Mitochondria (Mit), Z line (Z), and Myofibrin (Myf).

2.10 IMAGE ANALYSIS

All images were analysed using ImageJ software(238)(https://imagej.net). Low magnification micrographs were essential to capture whole blood vessels needed to measure things such as % coverage of glycocalyx on endothelium and basement membrane thickness, while high magnification micrographs were essential to capture close detail of structures as tight junctions and the properties and appearance of the glycocalyx both associated with and detached from the endothelium. The variety in images allows a thorough comparison between diabetic mice to controls.

Blood vessel images were grouped into well-perfused and non-perfused depending on the presence of blood cells within the lumen. The well perfused were then categorised based on whether any eGLX remained intact and attached to the endothelial surface of the lumen into excessively-perfused when lacking in intact eGLX and sufficiently-perfused when the eGLX was visibly intact and attached the endothelial surface. The non-perfused and the excessively-perfused vessels were eliminated from the images used for eGLX analysis due to the inability of the LaDy GAGa method to stain it for suitable visibility. (Figure 2.5)

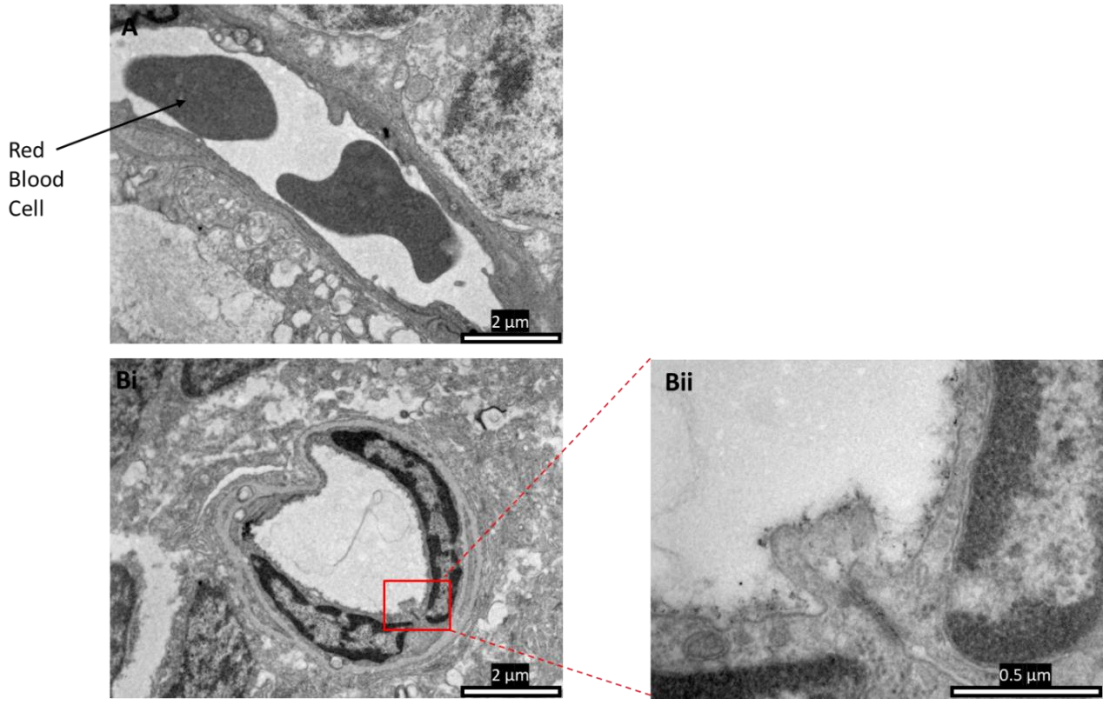

Figure 2.5: Categorising Retinal Capillaries.
Images A, Bi and Bii are TEM images of perfusion fixed retinal capillary from DB2J female mice (A) an example of a non-perfused vessel of a diabetic mouse (Bi) a standard perfused control (non-diabetic) retinal capillary. (Bii) illustrates the visibility of the endothelial glycocalyx in a perfused vessel.

2.10.1 ENDOTHELIAL GLYCOCALYX PERCENTAGE COVERAGE

The freehand tool on ImageJ was used to draw a distinctive line the luminal surface of the blood vessel to quantify its luminal total surface area. Next, the freehand tool was used to mark the luminal surface where the eGLX was present and adherent to the surface to quantify the length covered by the eGLX. The eGLX coverage was then calculated as a percentage using the following equation:

$$\text{eGLX Percentage Coverage } (\%) = \frac{\text{Length of Endothelial Surface Covered by eGLX } (\mu\text{m})}{\text{Length of Endothelial Surface } (\mu\text{m})} \text{x}100$$

2.10.2 BASEMENT MEMBRANE THICKNESS

In order to calculate the mean basement membrane thickness for each mouse, a minimum of 5 blood vessels were imaged. To avoid local variation more than 100 individual perpendicular lines were drawn across the basement membrane, chosen at random and spaced at 0.1 µm intervals, for each blood vessel. Care was taken to ensure the shortest distance across the basement membrane, though as manually it is conceded that there will be a systematic overmeasurement of a couple of pixels (typical distance) which is far lower than the variation within a mouse, and present across all mice groups.

2.11 RETINAL ENDOTHELIAL CELL CULTURE AND VE-CADHERIN IMMUNOFLUORESCENCE STAINING

2.11.1 CELL CULTURE

The cells were cultured in Dulbecco's modified Eagle's medium containing 20 mM sodium bicarbonate, 15 ng/ml-1 endothelial cell growth factor (ECGF), 10 U/ml-1 heparin, 100 U/ml-1 penicillin, 100 mg ml-1 streptomycin, 2.5 mg ml-1 amphotericin B, and 20 % fetal bovine serum (growth medium-A) at 37°C in a humidifed atmosphere of 5 % CO2/air. After cell attachment the temperature was reduced from 37 to 33°C to activate SV 40 large T-antigen and the culture medium is changed to DMEM containing 20 mM

sodium bicarbonate 15 ng/ml ECGF, 100 U/ml penicillin, 100 mg/ml streptomycin, and 10% FBS (growth medium-B).

The colonies of the other cell types, such as pericytes and fibroblasts, were removed by aspiration. Following two or three passages, cells were cloned from a single cell by colony formation and isolated twice from other cells using a penicillin cup. Cells were grown in Endothelial Basal Medium −2 (EBM-2) (LONZA New Orleans, LA, USA) containing hydrocortisone. At 80–90% confluence, retinal endothelial were transferred to serum starved-medium (1% serum) for 24 hours incubation.

2.11.2 VE-CADHERIN IMMUNOFLUORESCENCE STAINING

Cells were grown overnight on cell culture plate at initial seeding density of 4 × 104 cells per cm2 . The cells were then covered to a depth of 2–3 mm with 4% PFA diluted in PBS. The cells were left to fix for 15 min at room temperature. Fixative was aspirated, rinsed three times in PBS for 5 min each. The specimen was blocked using a blocking buffer (PBS / 5% BSA) for 60 min then aspirated. The diluted primary antibody (0.2% BSA (1:200) was applied and incubated on the specimen for 1 hr. Rinsed with PBS 3 times, then incubated in fluorochrome-conjugated secondary antibody (Alexa Fluor 488-labeled) diluted in PBS / 1% BSA for 1–2 h at room temperature in the dark. Rinsed three times with PBS for 5 min. Hoescht (1:10000) with Mitotracker was applied and left overnight at room temperature. Leica confocal microscope was used for imaging of figure 3.9.

CHAPTER 3: DIABETIC RESULTS

3.1 IN VIVO EXPERIMENTS

In order to quantify the increase in retinal vascular permeability, a major retinal vessel was selected and the mean fluorescence intensity within that vessel was recorded 15 frames per seconds (fps) for a 3 minutes video and compared with nearby tissue (which includes unresolved capillaries). A preliminary time course was used to for the graph. The graph was then adjusted according to the regions where there was detectable tissue fluorescence. Any major vessel saturation was excluded from analysis. A random point (rectangular in shape) was selected within the major vessel to represent the fluorescent intensity and another random point (of equal dimension) was selected outside the major blood vessel while ensuring no visible distinct vessels where observed within that point.(247) The equation used to calculate the permeability assumes the surface area available for exchange is the same in both experimental groups (Figure 3.1).

$$P_{Flourescein}^{t=0} = \frac{d < I_{V_1} >}{dt} \cdot \frac{V_{con}}{2\pi r . L_{con} . < I_{A_2} >} - \frac{r}{2 < I_{V_2} >} \cdot \frac{d < I_{V_2} >}{dt}$$

Figure 3.1: Fundus Fluorescent Angiography Equation.
Vascular permeability was calculated using the equation provided (229). Due to the regions of interest being a mixture of capillaries and interstitum knowing the vascular spacing and mean size is important for full quantification. Iv1=fluorescent Intensity of tissue imaging volume, Iv2= fluorescent Intensity of major vessel imaging volume, P t=0 fluorescent= initial fluorescent permeability, Lcon= length of vessel in confocal, Vcon= volume measured in confocal post-euthanasia to contain all the depth field of the vessel plexuses, r= mean radius of the vessel.

Fundus Fluorescent Angiography was used to calculate permeability on Day 0 of the experiment and again on Day 21 (Figure 3.2), when diabetic status was achieved through Streptozocin and confirmed with blood glucose levels higher than 25 mmol/l.

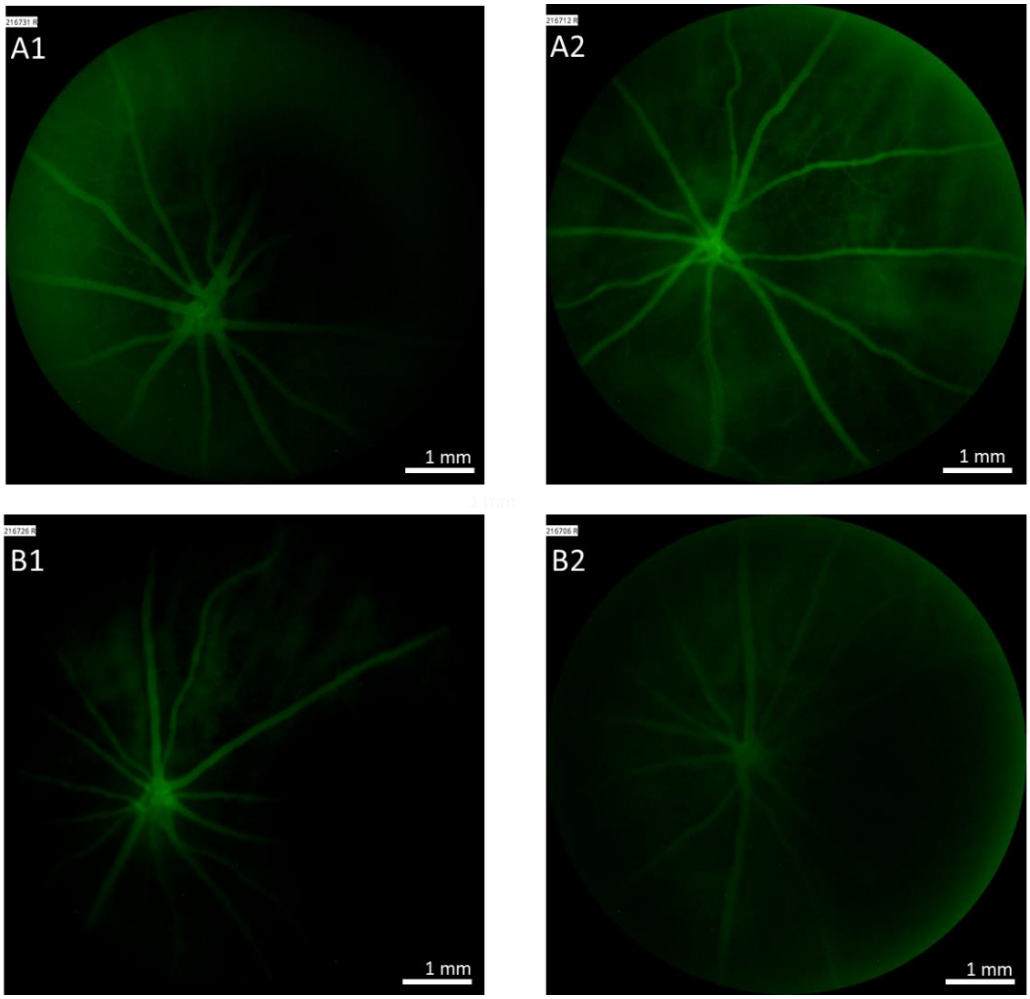

Figure 3.2: Fundus Fluorescent Angiography
The mean intensity of NaF in the retinal tissue and a main retinal vessel were measured every 200 frames for 3 min. A1) Nondiabetic fundus at Day 1. A2) Nondiabetic fundus at Day 21. B1) Diabetic fundus at Day 1. B2) Diabetic fundus at Day 21.

Non-diabetic mice showed no significant difference in retinal vascular permeability when comparing Day 0 and Day 21 ($p=0.38$). The diabetic group of mice, which at the time included the Sphinx 31 treated group, followed the predicted trend of having increased vascular retinal permeability 21 days after inducing diabetes. (Figure 3.3)

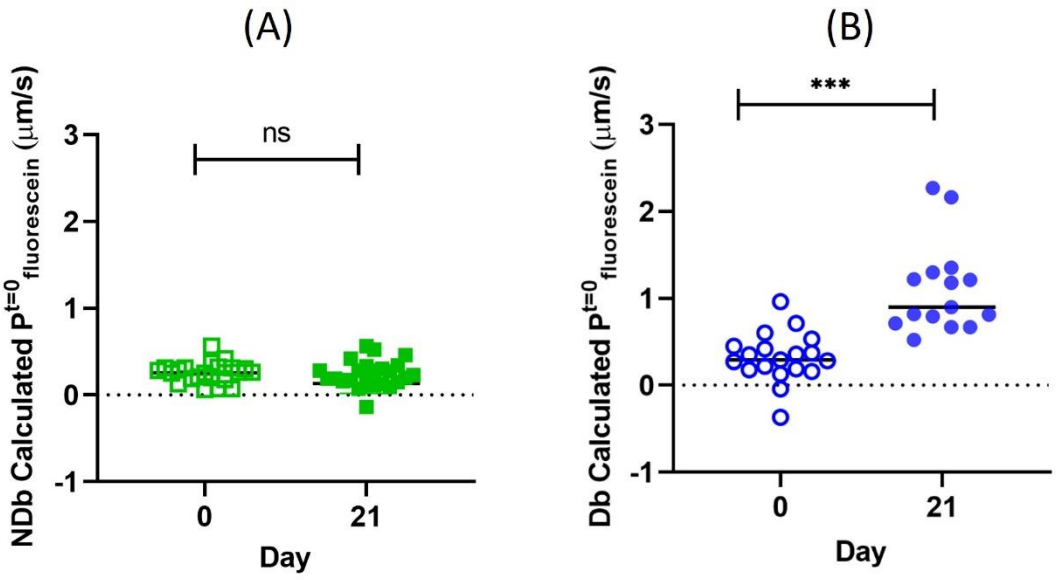

Figure 3.3 Permeability Data
*(A) No significant difference in permeability in the Non-Diabetic group after 21 days. (B) Change in retinal vascular permeability in Diabetic group is statistically significant. *** p<0.0001 using unpaired t-test.*

As expected, the levels of Urine Albumin/Creatinine ratio (ACR) increased after diabetic induction of the diabetic and Sphinx-31 treated group with Streptozocin (Figure 3.4). At week 15, treatment with Sphinx31 reverses the ratio to the normal range expected. The linear fit between 9 weeks and 15 weeks was extrapolated to 18 weeks to reflect the expected measurement if the mice had been left alive. ACR ratio was significantly different between Diabetic group at 15 weeks and Sphinx31 group at 18 weeks ($p<0.005$). Unpaired t-test was used to determine significance (**$p<0.0005$).

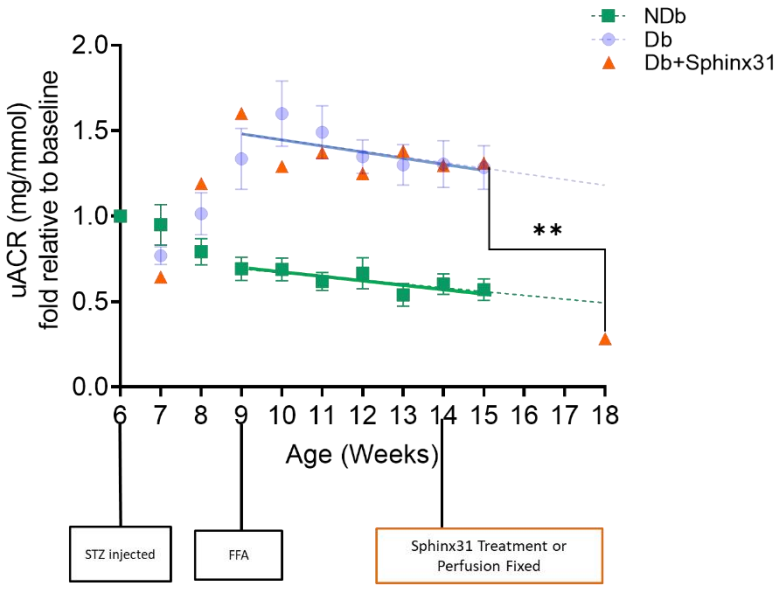

Figure 3.4: Urine Albumin Creatinine Ratio Increases After Diabetic Induction and is Reversed with SPHINX-31 Treatment.
*Diabetic Albumin Creatinine Ratio is increased in Diabetes and reversed after Sphinx31 Treatment. ** p=0.0010 using unpaired t-test*.

Basement membrane thickness was measured in a minimum of 5 different blood vessels for each mouse with the average taken to represent each mouse measurement. More than 100 individual lines were drawn across the basement membrane, chosen at random, for each blood vessel (Figure 3.5). At 8 weeks post diabetic induction, at the time of culling, there is a significant increase in basement membrane thickness in the diabetic mice (0.38±0.11) compared to the non-diabetic group (0.16±0.03) of mice ($p<0.00001$). Sphinx-31 (0.13±0.03) treated mice on the other hand, had values similar to the non-diabetic group, and significantly lower values than the diabetic group ($p<0.0001$). The diabetic group also had the highest standard deviation compared to the other two groups. The data is summarised in Figure 3.6.

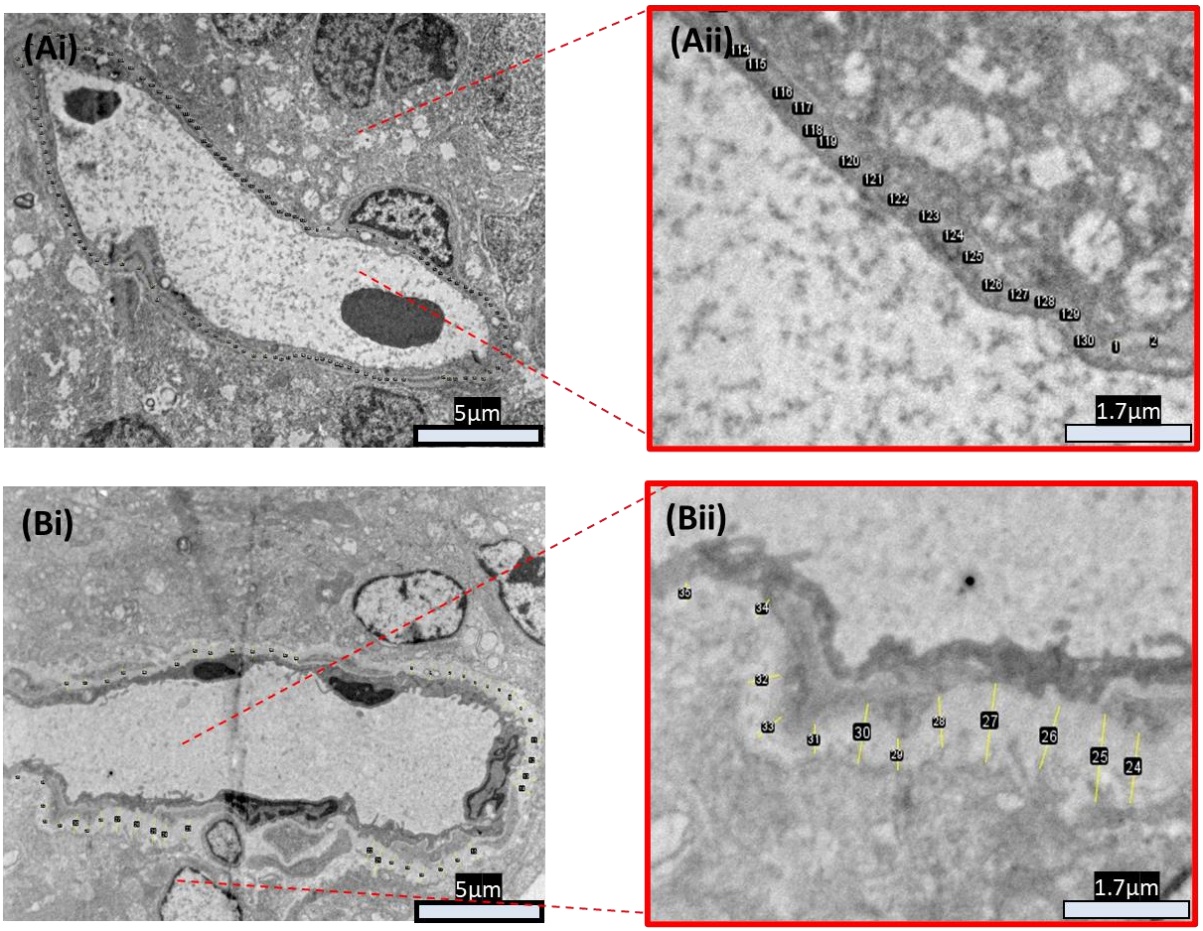

Figure 3.5: Basement Membrane Thickness.
*TEM images of perfusion fixed retinal capillary from DB2J female mice **(Ai)** non-diabetic retinal capillary **(Bi)** standard diabetic capillary that shows thickening of the BM. **(Aii)** & **(Bii)** are digital zooms to illustrate how the BM thickness was measured in the images.*

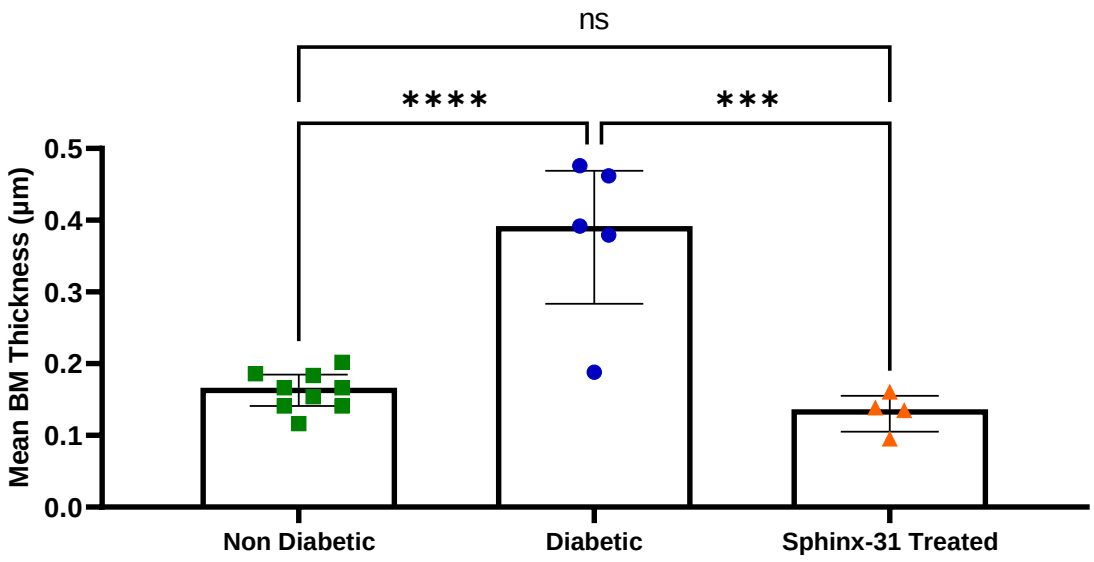

Figure 3.6: Increased Basement Membrane Thickness Measurements in Diabetic Group Compared to Control and SPHINX-31 Treated groups.

*The graph demonstrates the difference between the three groups of mice with the SD bars. ***p=0.0001 **** p<0.0001. One-way Anova was used to measure statistical significance and Tukey's multiple comparison as post hoc test.*

From the mice included in this experiment, 14 were perfusion fixed with the LaDy GAGa method. All 4 diabetic perfusion fixed mice had visibly stained endothelial glycocalyx, but only 7 of the 10 non-diabetic perfusion fixed mice had visibly stained endothelial glycocalyx (Table 3.1). No Sphinx-31 treated mice were perfusion fixed due to COVID-19 restrictions that impacted the separate day of culling. Therefore, no Sphinx-31 treated mice were included in the endothelial glycocalyx results.

Table 3.1: Proportion of Mice with Visibly Stained Endothelial Glycocalyx Blood vessels From the total Number of Perfusion Fixed Mice.

	Perfusion Fixed Mice	**Well Perfused Blood vessels w/ eGLX**
Non-Diabetic	10	7
Diabetic	4	4

While all mice in the Non-Diabetic and Diabetic Groups were Perfusion Fixed, not all had sufficiently stained eGLX to allow data analysis. Only 7 mice from the control (Non-Diabetic) group had visibly stained eGLX. All diabetic mice had visibly stained eGLX.

Only well perfused vessels that provided visibly stained and attached eGLX were used for image analysis. A minimum of 10 different locations across multiple blood vessels were used to calculate an average for each mouse. For the measurement of endothelial glycocalyx coverage, the percentage coverage was taken by measuring the proportion of the endothelial surface that was covered by a visibly stained and attached eGLX (Figure 3.7). A line was hand drawn to cover the whole length of the endothelial surface, and separate individual lines were drawn to mark the length that was covered by the eGLX. equation in Section 2.10.1 was used to calculate the eGLX percentage coverage.

There was a significant decrease in the eGLX percentage coverage in the diabetic group (69.57±8.33) compared to the non-diabetic group (52.22±2.73) with a mean difference of 25.56 ± 5.422(unpaired t-test showed $p<0.001$) as shown in Figure 3.8.

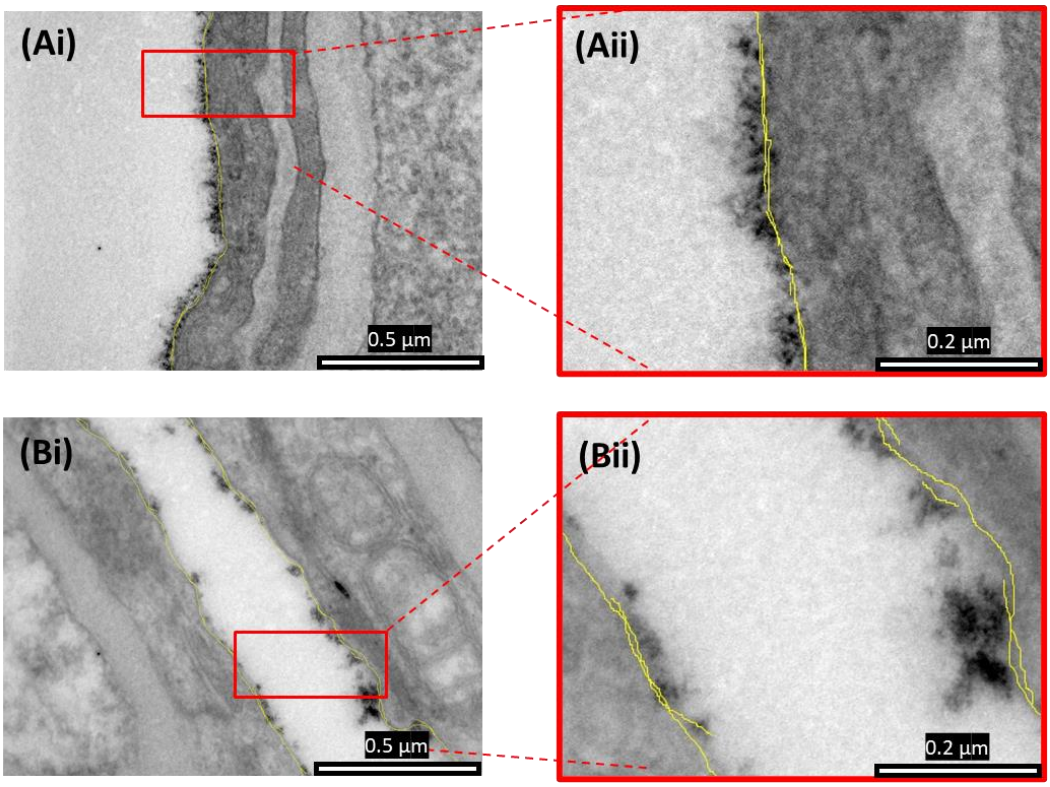

Figure 3.7: Endothelial Glycocalyx Percentage Coverage.
(Ai) & (Bi) TEM images of perfusion fixed retinal capillary from DB2J female mice (Ai) non-diabetic retinal capillary (Bi) diabetic capillary showing a decrease in the percentage coverage of the eGLX (Aii/Bii) are digitally zoomed to illustrate how the eGLX coverage was measured.

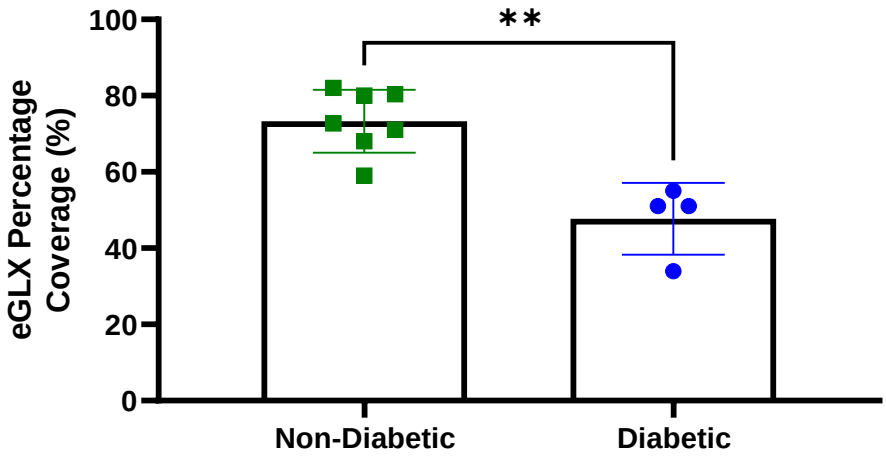

Figure 3.8: Endothelial Glycocalyx Percentage Coverage Difference between Groups.
The graph demonstrates the difference between the two groups of mice with the error bars. Unpaired t-test was used to measure statistical significance. (**) p ≤ 0.01.

The eGLX maximum height was measured as the highest point visible of a stained eGLX cluster. Due to the decreased percentage coverage observed in the diabetic group, the measurement was less representative of the adherent eGLX for that group. Therefore, a

surrogate measurement for indication of total eGLX content was calculated by multiplying the maximum height by the percentage coverage of eGLX. An unpaired t-test showed no significant difference between the two groups (p>0.05) as shown in Figure 3.9. The lack of significance indicates the extra height is likely to be trapped eGLX from shedding or in the diabetic case, weaker binding. Confirmation would require a more systematic approach using an improved quantification for total content.

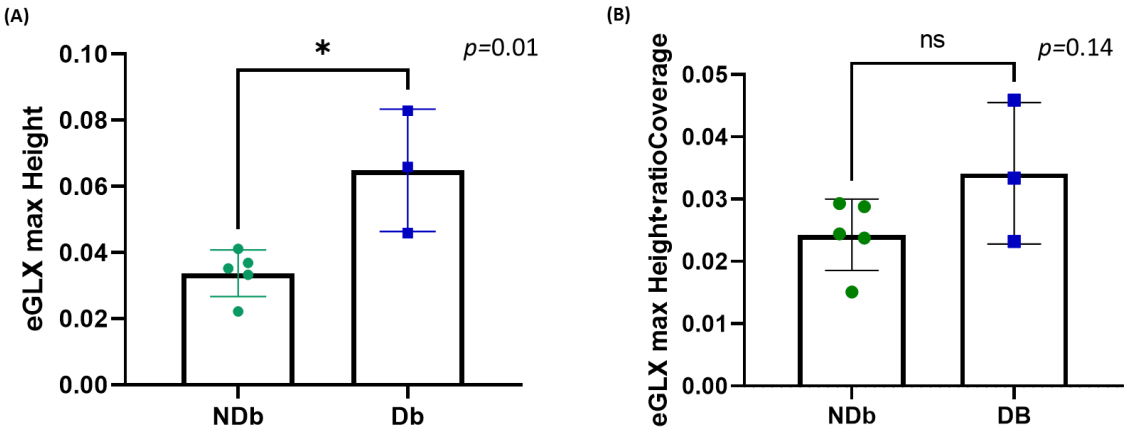

Figure 3.9: eGLX Maximum Height increases in Diabetic Mice using the LaDy GAGa Staining Method.
The graph demonstrates the difference between the two groups of mice with the error bars. Unpaired t-test was used to measure statistical significance. (ns) p > 0.01 (*) p < 0.05

3.2 IMAGING COMPOSITIONAL CHANGES IN ENDOTHELIAL GLYCOCALYX

Retinal endothelial cells was fluorescent stained for VE-Cadherin and imaged using an optical microscope to observe potential changes in tight junction in diabetic vasculature. Furthermore, EXT1 Knockout mice was used to examine the change in linking junctions and eGLX.

Figure 3.10 is an example of VE-Cadherin stained for on retinal endothelial cells. However, the cells proved as unviable for the desired experiments because they were too late of passage. We were expected to conduct the experiment again as a co-stain with ZO-1 on a lower passage to provide the images needed for analysis but were unable to do so due to lack of time and COVID restrictions.

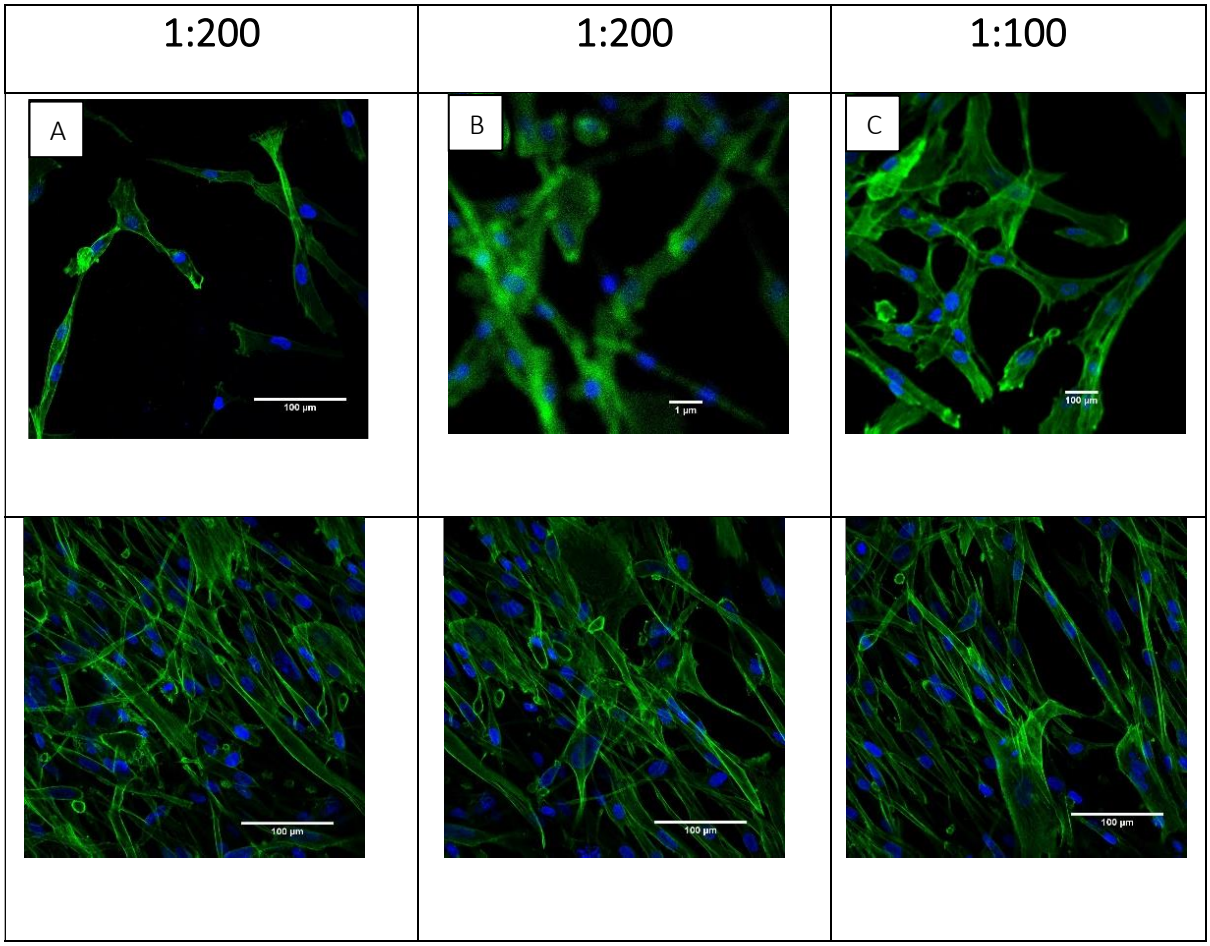

Figure 3.10: VE-Cadherin stain in Human Retinal Epithelial Cells
20x lens stained for Cadherin antibody, with secondary antibody Alexa Fluor 488-labeled and Hoescht. Image A and B are two different wells stained with a primary antibody dilution of 1:200. Image C was stained with a primary antibody of 1:100. Image D & E are a Z stack of the two wells stained with the 1:200 dilution of primary antibody. Image F shows a Z stack of the cells stained with a primary antibody dilution of 1:100.

CHAPTER 4: EXT1 RESULTS

A minimum of 7 blood vessels were imaged and analysed to measure the thickness of the basement membrane (Figure 4.1). An average of the two blood vessels was used to represent the value for each mouse. The measurements provide preliminary evidence that there is an increase in the basement thickness when the EXT1 inhibition was activated. Tukey's multiple comparison test was used; the increase is statistically significant compared to the vehicle control group (p<0.05), but not statistically significant compared to the control group that lacked the Cre (p=0.072) as demonstrated in Figure 4.3.

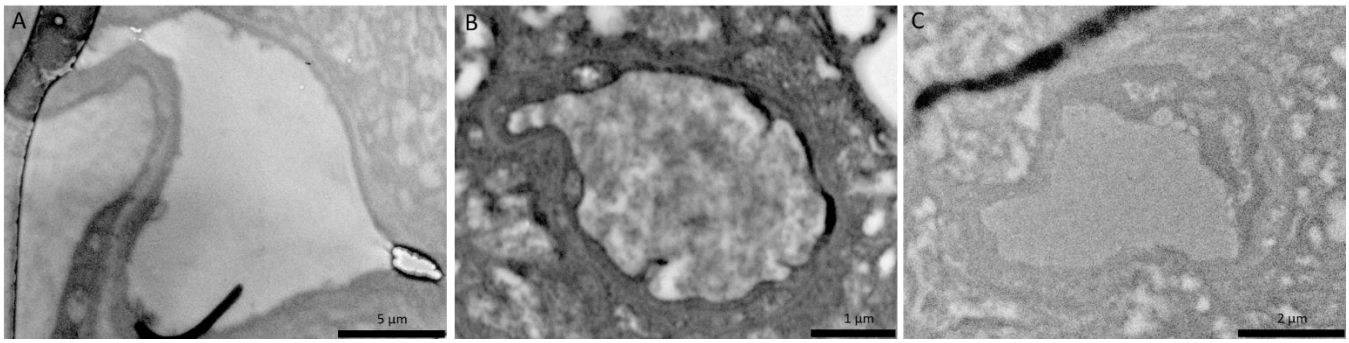

Figure 4.1: TEM Images of Standard Retinal Blood Vessels from each Group of Mice in the EXT1 Experiment
TEM images of perfusion fixed retinal capillary from C57BL/6J female mice.
A. $Ext^{flox/flox}$:$VE^{wt/wt}$ + Tamoxefen
B. $Ext^{flox/flox}$:$VE^{cre/wt}$ + Vehicle
C. $Ext^{flox/flox}$:$VE^{cre/wt}$ + Tamoxefen

Urine Albumin and Creatinine assays were taken on weekly basis from all mice and used to calculate the ACR. The different groups presented no significant trend in ACR change through the timeline of the experiment. Tukey's multiple comparison test was used to test for significance (p>0.9). (Figure 4.2)

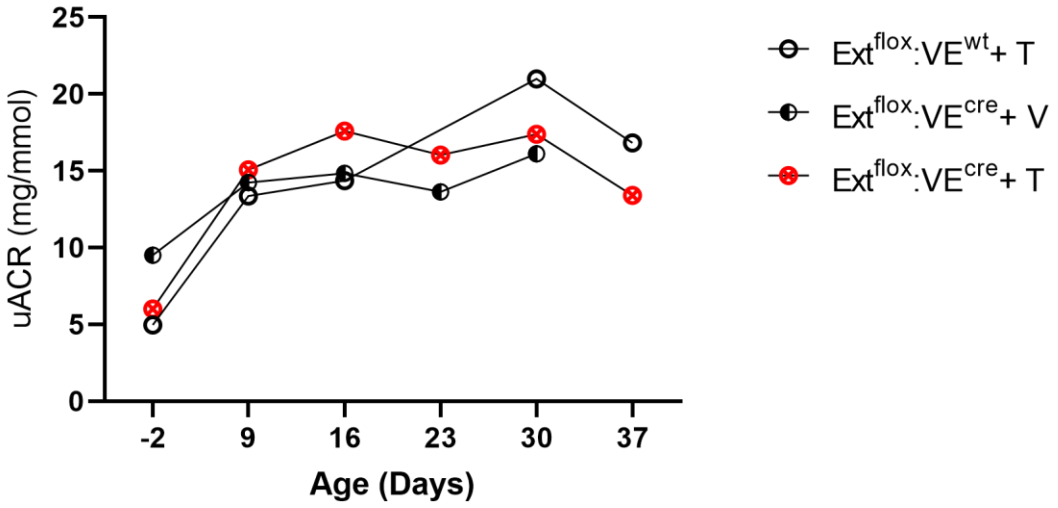

Figure 4.2 Urine Albumin Creatinine Ratio Shows no Significant Change in EXT1 Knockout Mice
The Albumin Creatinine Ratio didn't display a significant difference between the different groups.

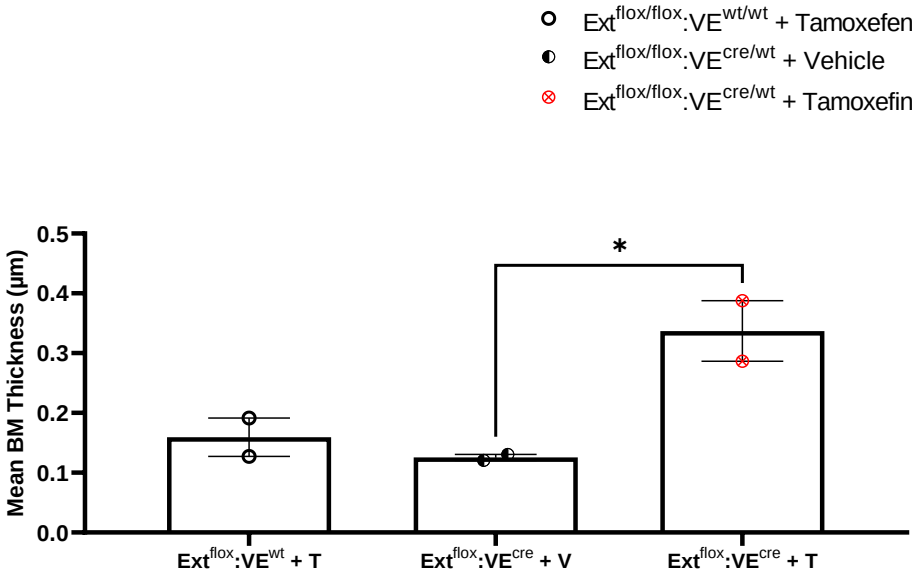

Figure 4.3: Basement Membrane Thickness Measurements is significantly increased in Ext$^{flox/flox}$:VE$^{cre/wt}$ + Tamoxefen mice
The graph demonstrates the difference between the three groups of mice with the SD bars.

Ext$^{flox/flox}$:VE$^{cre/wt}$ + Tamoxefen group showed a significant increase in basement membrane thickness compared to the Ext$^{flox/flox}$:VE$^{cre/wt}$ + Vehicle group. (Figure 4.3)

The set of results from the two experiments are presented on the same graph for comparison (Figure 4.4). The graph illustrates the similarity in basement membrane thickness measurement between the diabetic (0.38± 0.12) and the Ext$^{flox/flox}$:VE$^{cre/wt}$ +

Tamoxefen group (0.34± 0.07), relative to the control groups in the experiments. $Ext^{flox/flox}$:$VE^{wt/wt}$ + Tamoxefen (0.16± 0.05) $Ext^{flox/flox}$:$VE^{cre/wt}$ + Vehicle (0.13± 0.01) and Non-Diabetic (0.16± 0.03) . The results of Tukey's multiple comparison test show a significant difference between the Diabetic and the $Ext^{flox/flox}$:$VE^{cre/wt}$ + Tamoxefen, and all the control groups (*p<0.05) (**p<0.005) (***p<0.0005).

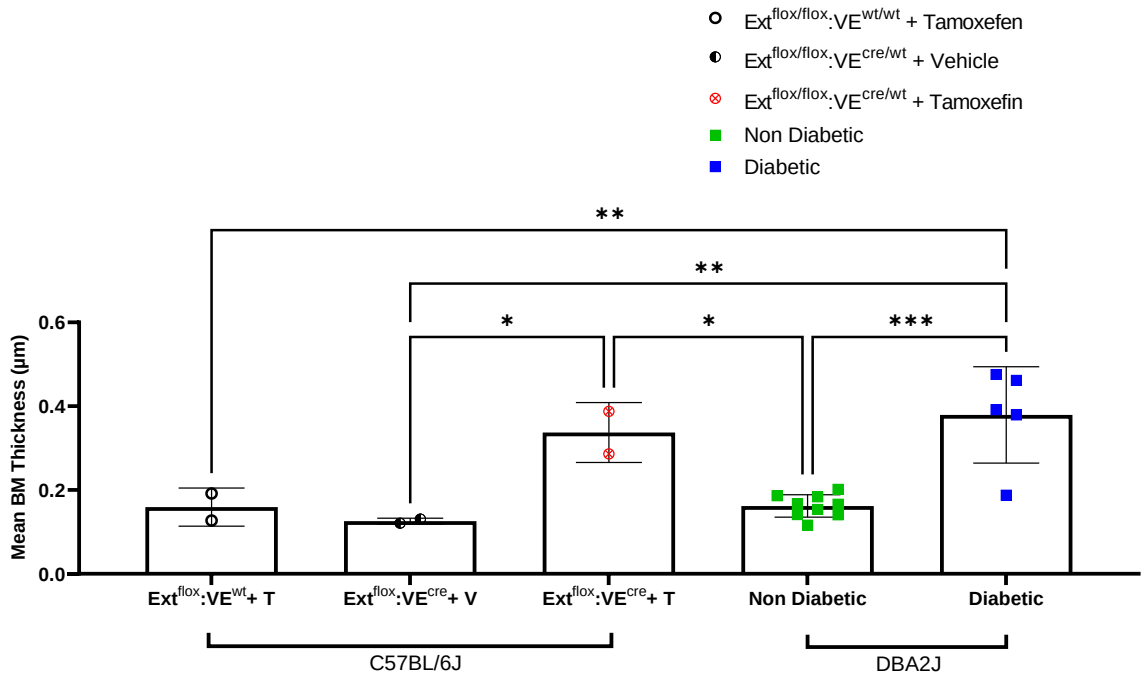

Figure 4.4: Basement Membrane Thickness Measurements is significantly increased in Extflox/flox:VEcre/wt + Tamoxefen mice compared to Non-Diabetic Mice from the diabetic comparison.
The graph demonstrates the difference between the five groups of mice with the SD bars.

All 6 mice included in the experiment were perfusion fixed, but only 4 of which had visibly stained endothelial glycocalyx suitable for analysis. Compared to the two control groups, the $Ext^{flox/flox}$:$VE^{cre/wt}$ + Tamoxifen had less eGLX percentage coverage, however a Tukey's Multiple Comparison Test showed no statistical significance as shown in Figure 4.5.

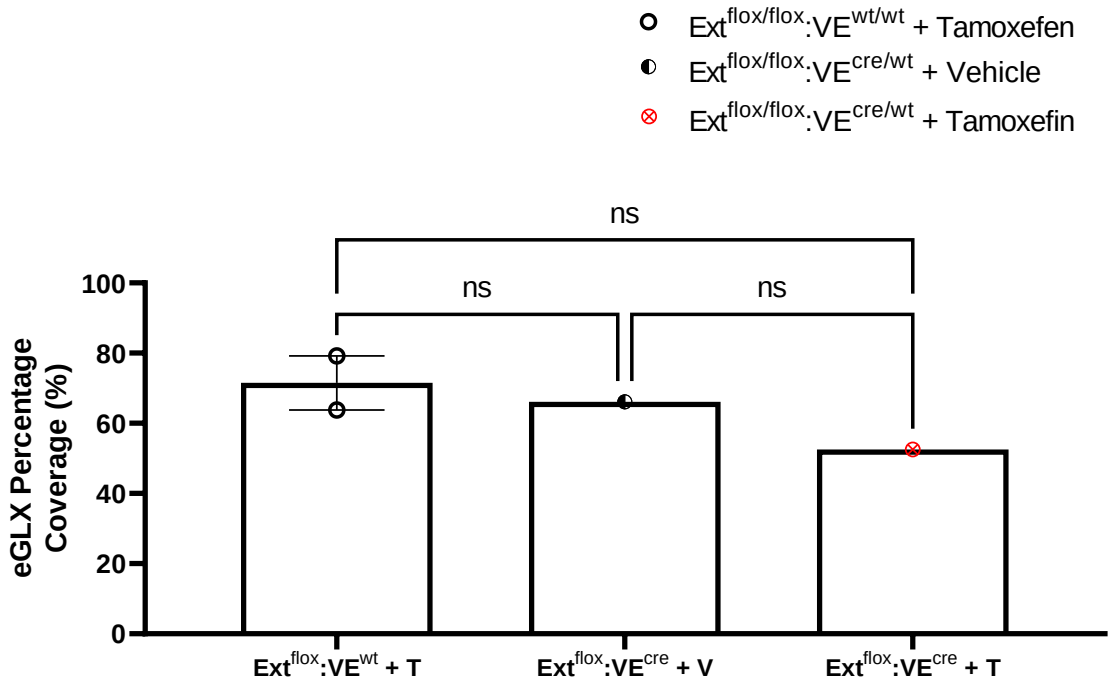

Figure 4.5: Extflox/flox:VEcre/wt + Tamoxefen mouse had less Endothelial Glycocalyx Percentage Coverage compared to the control groups.
The graph demonstrates the difference between the three groups of mice with the SD bars.

CHAPTER 5: DISCUSSION

5.1 GLYCOCALYX STAINING METHOD

Achieving diabetic status was fundamental to correlate diabetic retinopathy and diabetic kidney disease with the eGLX structural changes proposed in the hypothesis. The sets of data in the EXT1 pertaining to the development of diabetes followed the predicted trends to demonstrate the progression of diabetes and its vascular complication of increased permeability.

All staining attempts in the experiments used the LaDy GAGa staining method. The set of data obtained from eGLX percentage coverage study provides evidence of the capability and efficiency of the LaDy GAGa staining method to demonstrate the changes previously reported in the literature.(249) While the mean maximum height analysis demonstrated the limitation of the LaDy GAGa technique to support previously evident observations of the decrease in volume of the eGLX in diabetix vessels(60).

For the purpose of the data attempted from the samples, the staining method provided is deemed adequate and suitable. One issue that arose from the use of the LaDy GAGa included its inability to ensure all blood vessels imaged under TEM presented visibly stained eGLX. This has been attributed to the perfusion fixing technique rather than the stain used. While perfusion fixing, some blood vessels didn't receive enough pressure to flush the lumen contents and allow staining of the eGLX. In other cases, the high perfusion pressure reaching the blood vessel lumen flushed the eGLX along with its contents. The perfusion fixing technique is unable to control or maintain consistent pressure throughout the vascular system. Even though not all blood vessels had visibly stained eGLX, it was able to provide a statistically significant number.

Another aspect to be considered when interpreting the results is the angle of sectioning the retinal tissue. While care was taken to ensure vessels used had what appeared to be a normal cross section, normally by visual judgement of the endothelial layer there was no mean of ensuring the angle precision. The normal method of checking the lipid bilayer is

visible could not be used for all specimens due to staining quality. We therefore expect a systematic over estimate for measurements, although this would be similar between groups.

It should be noted that diabetic blood vessels demonstrated higher proportion of detached eGLX that clumped in groups over the endothelial surface. The effect of which could be a reason for the decrease in percentage coverage evident in the diabetic group. An important progression this observation requires an understanding of the effect of hyperglycaemia that renders the eGLX more susceptible to detachment, and whether that structural change plays a role in the increased permeability. Accordingly, indicating a difference in composition and structure that occurs as a result of diabetes.

As part of the two experiments, in addition to the EM sections imaged and analysed, retinal tissue sections have been prepared for different methods of visualisation. These include cryogenic sections for immunofluorescne staining for WGA and R18, isolectin B staining and high pressure freezing for mass spectroscopy. The former two retinal petals were placed in 5% parafolmaldehyde and the later was left in mammalian ringer's solution until it was high pressure frozen within a few hours of culling the mice.

Mice lacking in visibly stained eGLX could be to extensive damage caused to the eGLX at earlier stages of tissue handling, before fixation, as the capillary vasculature is extremely delicate(127).

While the depth and size of eGLX diminishes during fixation, thus giving an underestimated value to the size of the eGLX *in-vivo*, this reduction will be consistent across all experimental groups(250).

Techniques that involve various methods to ensure the preservation of the hydrated-gel-like structure of the eGLX (i.e. HPF), localising areas of interest (i.e. cryo-correlative microscopy), decreasing the thickness of samples (i.e. cryo-FIB) and 3D imaging techniques (i.e. ORBI SIMS) are vital for further advancements in our knowledge of the structure and composition of the eGLX.

5.2 DIABETIC EXPERIMENT

In terms of retinal permeability, the data set from the diabetic and SPHINX-31 treated mice presented diabetic values double those of the control group. The oncotic pressure within the subglycocalyx space that overlies the intercellular junctions, maintains the oncotic pressure gradient opposing water and solute flow(251). Therefore, the increased permeability to small molecules in the diabetic group is in line with what has been reported in states of loss of function of the eGLX(252)(253). All of which supports the hypothesis that the damaging effect of the hyperglycaemic states on the eGLX is the fundamental cause of the increased permeability. However, it doesn't provide conclusive evidence for the direction of causality.

While an increase in basement membrane thickness has been widely well established in diabetic state, the ambiguity lies in the process that leads to the increase. It has been previously postulated that hyperglycaemic state causes the increase in thickness which in turn is the primary cause of the increase in permeability. Understanding the structure and function of the eGLX provides a different perspective that better explains the increase in permeability.

If the Sphinx-31 treatment is to be assumed as correcting the impairment in eGLX function, then its ability to reverse basement membrane thickening indicates the role played by the eGLX in the progression of diabetic vasculature.

The diabetic experiment set of data for basement membrane thickness includes a diabetic mouse outlier value that fits within the control mice range of values. The mouse (216705) was confirmed to have developed diabetes through the regular glucose tests and has presented diabetic range values in all other parameters, including an FFA value above the diabetic mean (1.35 µm/s).

We were also unable to obtain eGLX data from that mouse. One interpretation for the value of basement membrane thickness could be due to a fault in perfusion fixing or embedding that led to membrane thickness collapse and flushing of the eGLX. More likely is this mouse was not affected by diabetes in the same way.

5.3 EXT1 PILOT STUDY

The EXT1 Knockout pilot study provides promising insight on potential evidence of the effect of a dysfunctional eGLX on basement membrane thickness. While the values statistical significance are statistically weak due to an inadequate sample size, they show a trend that depicts the expected results to confirm the hypothesis of this research. Thus far, the EXT1 pilot study values of increased basement membrane thickness and decreased eGLX percentage coverage in $Ext^{flox/flox}$:$VE^{cre/wt}$ + Tamoxefen group show a similar trend of values observed in diabetic mice. The results indicate that the effect of the functional loss of heparan sulphate synthesis and elongation on the eGLX structure is similar to that caused by diabetic state.

While it was previously assumed that hyperglycaemia leads to increased basement membrane thickness which in turn causes the increase in permeability, the results of the two experiments present evidence that supports a different explanation. The EXT1 lacked the hyperglycaemic microenvironment of oxidative stress that is described to cause the damage on the basement, yet the values present a trend of increased basement membrane with the loss of the eGLX. The increased permeability to small molecules in the diabetic experiments is in line with what previous literature has reported after the loss of the eGLX.(253) The sets of results from the two experiments taken together build on the evidence that support the hypothesis that links the impairment in eGLX as the root cause of diabetic microvasculature changes (e.g. increased basement membrane thickness).

In other words, the results indicate that the increase in basement membrane thickness is due to increased water content within the basement membrane, caused by the oncotic imbalance rather than deposition of extracellular matrix as previously assumed(195).

In addition to inhibition of heparan sulphate on the endothelial cell's luminal surface, EXT1 $^{flox/flox}$ is also expected to inhibit heparan sulphate production underneath the endothelial cell, adjacent to the basement membrane. Endothelial cells have been reported to be responsible for the synthesis and deposition of basement membrane proteins essential for maintaining permeability(254). However, loss of eGLX doesn't necessarily mean the junctional strands

within the intercellular clefts remain intact. In the context of EXT1 knockout experiment, the set of results nullify an alternative hypothesis that involves a dysfunction in junctional strands that lead to the increase in basement membrane thickness.

The quality of the images obtained from the EXT1 pilot study (*in-vivo* finished mid-August 2021) did not meet the quality standard of the diabetic mice in terms of high resolution at higher magnification. The inferior quality is expected to be due to insufficient incubation time in embedding steps to ensure embedding steps are fully able to permeate the deeper eye tissue. Therefore, modifications will be done on the embedding protocol to allow for longer incubation periods in the full EXT1 experiment (in-vivo finishes mid October 2021).

Fluorescent Fundus Angiography data has been obtained *in vivo,* however they were not ready for analysis during the timescale of this project.

The use of conventional genetic knockout methods, which involve inhibition of selected genes early in embryonic development, provide experimental results of a biological system that has adapted to the inhibition. The Cre/lox system on the other hand is more likely to provide results that correspond to the acute stage of adaptation to the induced inhibition, similar to the pathogenic process of diabetes that leads to diabetic retinopathy.

Finally, it should be noted that a Cre driver (VE-Cadherin) efficiency is limited by the specificity of the promotor used (Tamoxifen in this case) and the Cre recombinase within the targeted endothelial cells. Thus, the Cre/lox system will not be 100% efficient at inhibiting HS synthesis in a given cell type while limiting the effect on other cell types through the use of VE-Cadherin(255).

CHAPTER 6: FUTURE WORK

The aim of the study was to provide evidence on that the changes in permeability in diabetic retinopathy, which then affects the ultrastructure of the basement membrane, can be fully explained by loss of the endothelial eGLX. While the results of the study support the

hypothesis, additional studies are needed to confirm that our data are a direct result of the experimental design.

Evidence on the role of the eGLX in basement membrane expansion can be further supported by ensuring there are no changes in the endothelial cells structural junctions in the $Ext^{flox/flox}$:$VE^{cre/wt}$ + Tamoxefen group (the knockout group). Demonstrating that loss of eGLX didn't cause changes in structural junctions provides evidence that the physical absence of the eGLX lead to the increase in basement membrane thickness. Additionally, it ensures that inhibition of HS production and elongation by EXT1 gene led to the only change targeted in the experiment; loss of endothelial eGLX rather than an alternative biochemical process that disrupts the endothelial cellular layer.

Furthermore, the content layer of the expansional (EXT1 experiment) and contractional (SPHINX-31 experiment) basement membrane needs to be further studied to confirm it is due to the movement of water rather than deposition of fibrous matrix. A 3D reconstruction of the layer through the use of Electron Tomography would be effective in demonstrating the content and compositional change in case of pore structure changes(248).

Additionally, ensuring the heparan sulphate content was mainly changed on the luminal surface of the endothelial cell surface can be confirmed through different methods. One of which is the use of a membrane dye that stains for heparan sulphate, and further quantifying its presence above the endothelial cell surface as well as below. A different approach could be the use of Time of Flight Secondary Ion Mass Spectrometry (ToF SIMS) to analyse the content of the different glycosaminoglycan chains for a change in heparan sulphate between the control and experimental groups(256).

CHAPTER 7: CONCLUSION AND SUMMARY

While our understanding of the function, structure, and composition of the eGLX remains limited, the pathogenic states, such as diabetes, provide incisive evidence of its importance in maintaining a dynamic permeability homeostasis. Given the burden diabetic microvascular complications pose on quality of life and deterioration of health, understanding the ultrastructural sequence of events that lead to their development is vital.

Separately, each eGLX visualisation technique remains lacking in providing the data needed to build conclusive evidence. The LaDy GAGa staining method provides an efficient method of quantifying the change of adherent eGLX structure. Various obstacles were overcome in developing quantifiable evidence through the use of the LaDy GAGa technique. Some of which include changes to perfusion fixing technique to ensure the best manner of preserving the tissue and preventing further changes or damage caused by the use of heavy metals for fixing. Embedding protocols have been altered to suit future experiments for better preservation of tissue for imaging.

Furthermore, SPHINX-31 shows promising results as a therapeutic drug in reversing a microvascular complication of diabetes rather than just blocking onset. Despite the hopeful results, extensive efforts need to be made in understanding the drug's physiological mechanism of action and other pharmacological properties.

The EXT1 pilot study presented sufficient data to allow for improved protocols with a bigger number of mice to provide conclusive evidence of the role played by heparan sulphate in the structure and function of the eGLX. It also gave indications of the function of the eGLX in the process of events that lead to basement membrane thickening,

.

APPENDIX I: EXPERIMENTAL PLAN FOR DBA2J

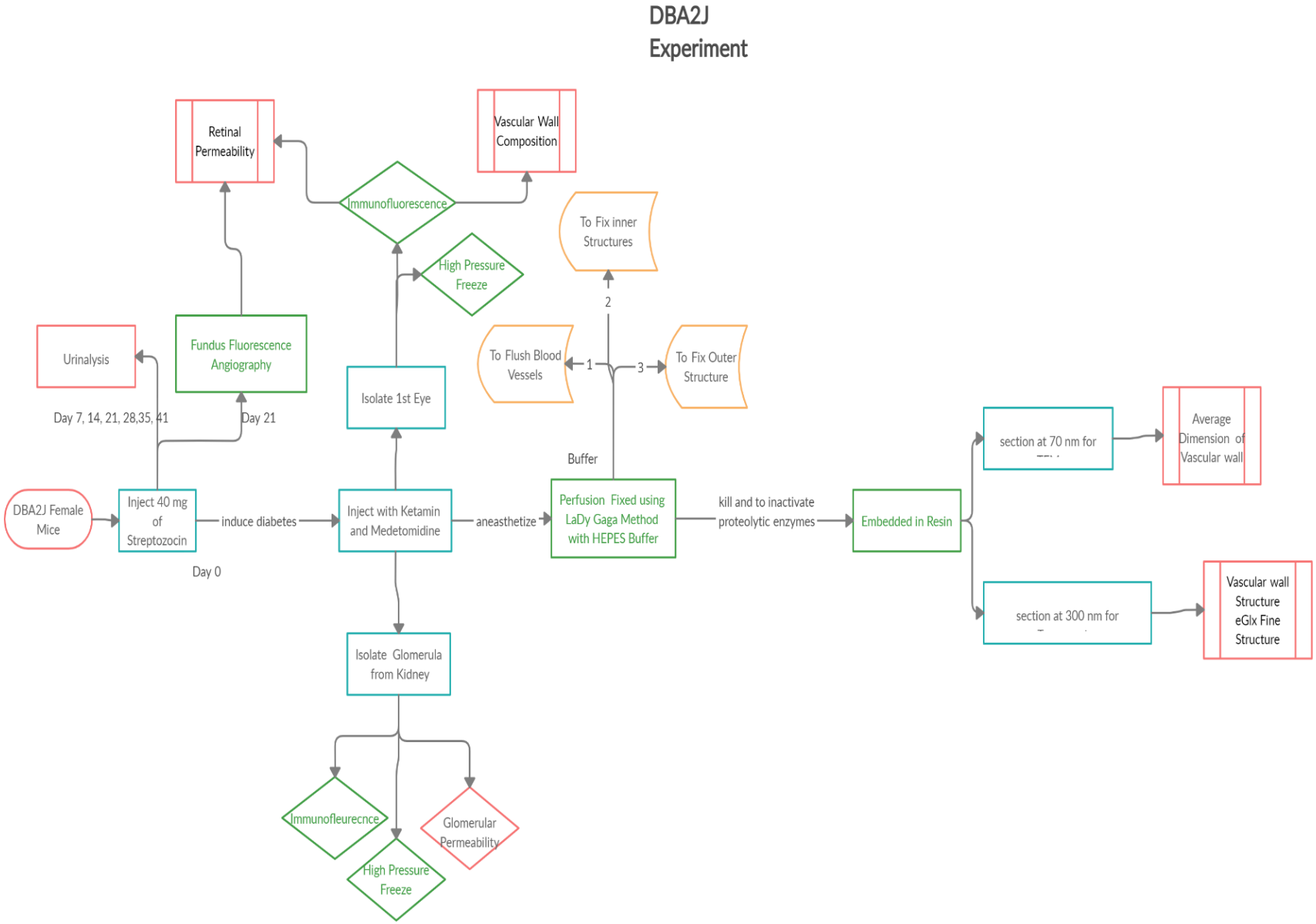

APPENDIX II: PG TRAINING COURSES

Course Name	Date	Duration	Points Awarded	
Copyright Condensed - a short introduction to copyright for your research (webinar version)	16/02/2021	0.5 Days	1.0	Confirmed
Introduction to Flow Cytometry (online) - All Faculties	11/02/2021	0.5 Days	1.0	Confirmed
An Introduction to the UK Data Service	28/01/2021	2 hours	1.0	Attended
Introduction to Responsible Research & Innovation (Moderated Online)	25/01/2021	14 Days	6.0	Attended
Good Laboratory Practice: Techniques (Faculty of Medicine and Health Sciences)	11/12/2020	0.5 Days	1.0	Attended
Critical Appraisal of the Scientific Literature: Clinical Focus (Faculty of Medicine & Health Sciences)	10/12/2020	0.5 Days	1.0	Attended
Approaches to Qualitative Evidence Synthesis - online (Faculty of Medicine & Health Sciences)	07/12/2020	5 Days	1.0	Attended
Biomedical Imaging in Research - online (Faculty of Medicine and Health Sciences)	03/12/2020	3 hours	1.0	Attended
Maths in the Lab - online (Faculty of Medicine and Health Sciences)	27/11/2020	0.5 Days	1.0	Attended
Exploring Ethics in Research (Faculty of Medicine and Health Sciences)	23/11/2020	0.5 Days	1.0	Attended
Introduction to Statistics with SPSS - online (Faculty of Medicine and Health Sciences)	18/11/2020	2 Days	2.0	Attended
Computational modelling in critical illness - online (Faculty of Medicine and Health Sciences only)	17/11/2020	0.5 Days	1.0	Attended
Introduction to Flow Cytometry (online) - All Faculties	04/11/2020	0.5 Days	1.0	Attended
Understanding your research degree (standalone online learning course)	01/10/2020	1 Day	2.0	Attended

REFERENCES

1. WHO. The top 10 causes of death [Internet]. 2018 [cited 2020 Jun 14]. Available from: https://www.who.int/news-room/fact-sheets/detail/the-top-10-causes-of-death

2. Saeedi P, Petersohn I, Salpea P, Malanda B, Karuranga S, Unwin N, et al. Global and regional diabetes prevalence estimates for 2019 and projections for 2030 and 2045: Results from the International Diabetes Federation Diabetes Atlas, 9th edition. 2019 [cited 2020 Jun 14]; Available from: https://doi.org/10.1016/j.diabres.2019.107843

3. International Diabetes Federation. IDF DIABETES ATLAS. 9th ed. IDF; 2019.

4. Diabetes.org.uk. THE COST OF DIABETES REPORT. 2014.

5. Hex N, Bartlett C, Wright D, Taylor M, Varley D. Estimating the current and future costs of Type1 and Type2 diabetes in the UK, including direct health costs and indirect societal and productivity costs. Diabet Med. 2012;

6. Fox J. Oxford Textbook of Endocrinology and Diabetes (2nd edn). Ann Clin Biochem. 2012;49(4):414.

7. Dogné S, Flamion B, Caron N. Endothelial Glycocalyx as a Shield Against Diabetic Vascular Complications: Involvement of Hyaluronan and Hyaluronidases. Arterioscler Thromb Vasc Biol [Internet]. 2018/06/07. 2018 Jul;38(7):1427–39. Available from: https://pubmed.ncbi.nlm.nih.gov/29880486

8. King P, Peacock I, Donnelly R. The UK prospective diabetes study (UKPDS): clinical and therapeutic implications for type 2 diabetes. Br J Clin Pharmacol [Internet]. 1999 Nov;48(5):643–8. Available from: https://pubmed.ncbi.nlm.nih.gov/10594464

9. CDC. National Diabetes Statistics Report 2020. Estimates of diabetes and its burden in the United States. 2020.

10. Gabbay KH. Aldose reductase inhibition in the treatment of diabetic neuropathy: where are we in 2004? Curr Diab Rep. 2004 Dec;4(6):405–8.

11. Kaiser N, Sasson S, Feener EP, Boukobza-Vardi N, Higashi S, Moller DE, et al. Differential regulation of glucose transport and transporters by glucose in vascular endothelial and smooth muscle cells. Diabetes. 1993 Jan;42(1):80–9.

12. Hammes H-P, Feng Y, Pfister F, Brownlee M. Diabetic retinopathy: targeting vasoregression. Diabetes. 2011 Jan;60(1):9–16.

13. ASHTON N. Injection of the retinal vascular system in the enucleated eye in diabetic retinopathy. Br J Ophthalmol [Internet]. 1950 Jan;34(1):38–41. Available from: https://pubmed.ncbi.nlm.nih.gov/15399194

14. Xu Q, Qaum T, Adamis AP. Sensitive Blood–Retinal Barrier Breakdown Quantitation Using Evans Blue. Invest Ophthalmol Vis Sci. 2001 Mar 1;42(3):789–94.

15. Cunha-Vaz J, Faria de Abreu JR, Campos AJ. Early breakdown of the blood-retinal barrier in diabetes. Br J Ophthalmol [Internet]. 1975 Nov;59(11):649–56. Available from: https://pubmed.ncbi.nlm.nih.gov/1203221

16. Antonetti D, Barber A, Khin S, Lieth E, Tarbell J, Gardner TW. Vascular permeability in experimental diabetes is associated with reduced endothelial occludin content: Vascular endothelial growth factor decreases occludin in retinal endothelial cells. Penn State Retina Research Group. Diabetes. 1998 Dec 1;47:1953–9.

17. Safi SZ, Qvist R, Kumar S, Batumalaie K, Ismail IS Bin. Molecular mechanisms of diabetic retinopathy, general preventive strategies, and novel therapeutic targets. Biomed Res Int.

2014;2014:801269.

18. Singh R, Barden A, Mori T, Beilin L. Advanced glycation end-products: a review. Diabetologia [Internet]. 2001;44(2):129–46. Available from: https://doi.org/10.1007/s001250051591

19. Brownlee Michael MD. ADVANCED PROTEIN GLYCOSYLATION IN DIABETES AND AGING. Annu Rev Med [Internet]. 1995 Feb 1;46(1):223–34. Available from: https://doi.org/10.1146/annurev.med.46.1.223

20. Huebschmann AG, Regensteiner JG, Vlassara H, Reusch JEB. Diabetes and Advanced Glycoxidation End Products. Diabetes Care [Internet]. 2006 Jun 1;29(6):1420 LP – 1432. Available from: http://care.diabetesjournals.org/content/29/6/1420.abstract

21. Lu C, He JC, Cai W, Liu H, Zhu L, Vlassara H. Advanced glycation endproduct (AGE) receptor 1 is a negative regulator of the inflammatory response to AGE in mesangial cells. Proc Natl Acad Sci U S A [Internet]. 2004 Aug 10;101(32):11767 LP – 11772. Available from: http://www.pnas.org/content/101/32/11767.abstract

22. He C, Koschinsky T, Buenting C, Vlassara H. Presence of Diabetic Complications in Type 1 Diabetic Patients Correlates with Low Expression of Mononuclear Cell AGE-Receptor-1 and Elevated Serum AGE. Mol Med [Internet]. 2001;7(3):159–68. Available from: https://doi.org/10.1007/BF03401949

23. Cumbie BC, Hermayer KL. Current concepts in targeted therapies for the pathophysiology of diabetic microvascular complications. Vasc Health Risk Manag [Internet]. 2007;3(6):823–32. Available from: https://pubmed.ncbi.nlm.nih.gov/18200803

24. Hammes HP, Martin S, Federlin K, Geisen K, Brownlee M. Aminoguanidine treatment inhibits the development of experimental diabetic retinopathy. Proc Natl Acad Sci U S A [Internet]. 1991 Dec 15;88(24):11555–8. Available from: https://pubmed.ncbi.nlm.nih.gov/1763069

25. Lee AY, Chung SK, Chung SS. Demonstration that polyol accumulation is responsible for diabetic cataract by the use of transgenic mice expressing the aldose reductase gene in the lens. Proc Natl Acad Sci [Internet]. 1995 Mar 28;92(7):2780 LP – 2784. Available from: http://www.pnas.org/content/92/7/2780.abstract

26. Gabbay KH. Hyperglycemia, polyol metabolism, and complications of diabetes mellitus. Annu Rev Med. 1975;26:521–36.

27. Fowler MJ. Microvascular and Macrovascular Complications of Diabetes. Clin Diabetes [Internet]. 2008 Apr 1;26(2):77 LP – 82. Available from: http://clinical.diabetesjournals.org/content/26/2/77.abstract

28. Fong DS, Aiello LP, Ferris FL, Klein R. Diabetic Retinopathy. Diabetes Care [Internet]. 2004 Oct 1;27(10):2540 LP – 2553. Available from: http://care.diabetesjournals.org/content/27/10/2540.abstract

29. Ferrara N, Davis-Smyth T. The Biology of Vascular Endothelial Growth Factor. Endocr Rev [Internet]. 1997 Feb 1;18(1):4–25. Available from: https://doi.org/10.1210/edrv.18.1.0287

30. Conn G, Bayne ML, Soderman DD, Kwok PW, Sullivan KA, Palisi TM, et al. Amino acid and cDNA sequences of a vascular endothelial cell mitogen that is homologous to platelet-derived growth factor. Proc Natl Acad Sci U S A [Internet]. 1990 Apr;87(7):2628–32. Available from: https://pubmed.ncbi.nlm.nih.gov/2320579

31. SHIMA, DT. Hypoxia induction of vascular endothelial growth factors in the retina : identification and characterization of vascular endothelial growth factor (VEGF) as the sole mitogen. Mol Med [Internet]. 1995 [cited 2020 Nov 22];2:64–71. Available from: http://ci.nii.ac.jp/naid/10017060096/en/

32. Brogi E, Wu T, Namiki A, Isner JM. Indirect angiogenic cytokines upregulate VEGF and bFGF gene expression in vascular smooth muscle cells, whereas hypoxia upregulates VEGF

expression only. Circulation [Internet]. 1994 Aug 1;90(2):649–52. Available from: https://doi.org/10.1161/01.CIR.90.2.649

33. Leung DW, Cachianes G, Kuang WJ, Goeddel D V, Ferrara N. Vascular endothelial growth factor is a secreted angiogenic mitogen. Science (80-) [Internet]. 1989 Dec 8;246(4935):1306 LP – 1309. Available from: http://science.sciencemag.org/content/246/4935/1306.abstract

34. Connolly DT, Olander J V, Heuvelman D, Nelson R, Monsell R, Siegel N, et al. Human vascular permeability factor. Isolation from U937 cells. J Biol Chem. 1989;264(33):20017–24.

35. Pepper MS, Ferrara N, Orci L, Montesano R. Potent synergism between vascular endothelial growth factor and basic fibroblast growth factor in the induction of angiogenesis in vitro. Biochem Biophys Res Commun [Internet]. 1992;189(2):824–31. Available from: http://www.sciencedirect.com/science/article/pii/0006291X92922775

36. Sone H, Kawakami Y, Okuda Y, Sekine Y, Honmura S, Matsuo K, et al. Ocular vascular endothelial growth factor levels in diabetic rats are elevated before observable retinal proliferative changes. Diabetologia [Internet]. 1997;40(6):726–30. Available from: https://doi.org/10.1007/s001250050740

37. Pe'er J, Folberg R, Itin A, Gnessin H, Hemo I, Keshet E. Upregulated expression of vascular endothelial growth factor in proliferative diabetic retinopathy. Br J Ophthalmol [Internet]. 1996 Mar 1;80(3):241 LP – 245. Available from: http://bjo.bmj.com/content/80/3/241.abstract

38. Boulton M, Foreman D, Williams G, McLeod D. VEGF localisation in diabetic retinopathy. Br J Ophthalmol [Internet]. 1998 May 1;82(5):561 LP – 568. Available from: http://bjo.bmj.com/content/82/5/561.abstract

39. Aiello LP, Avery RL, Arrigg PG, Keyt BA, Jampel HD, Shah ST, et al. Vascular Endothelial Growth Factor in Ocular Fluid of Patients with Diabetic Retinopathy and Other Retinal Disorders. N Engl J Med [Internet]. 1994 Dec 1;331(22):1480–7. Available from: https://doi.org/10.1056/NEJM199412013312203

40. Ellis EA, Guberski DL, Somogyi-Mann M, Grant MB. Increased H2O2, vascular endothelial growth factor and receptors in the retina of the BBZ/WOR diabetic rat. Free Radic Biol Med [Internet]. 2000;28(1):91–101. Available from: http://www.sciencedirect.com/science/article/pii/S0891584999002166

41. Sun J, Xu Y, Sun S, Sun Y, Wang X. Intermittent high glucose enhances cell proliferation and VEGF expression in retinal endothelial cells: the role of mitochondrial reactive oxygen species. Mol Cell Biochem [Internet]. 2010;343(1):27–35. Available from: https://doi.org/10.1007/s11010-010-0495-5

42. Gariano RF, Gardner TW. Retinal angiogenesis in development and disease. Nature [Internet]. 2005;438(7070):960–6. Available from: https://doi.org/10.1038/nature04482

43. Nishizuka Y. Intracellular signaling by hydrolysis of phospholipids and activation of protein kinase C. Science (80-) [Internet]. 1992 Oct 23;258(5082):607 LP – 614. Available from: http://science.sciencemag.org/content/258/5082/607.abstract

44. Xia P, Inoguchi T, Kern TS, Engerman RL, Oates PJ, King GL. Characterization of the Mechanism for the Chronic Activation of Diacylglycerol-Protein Kinase C Pathway in Diabetes and Hypergalactosemia. Diabetes [Internet]. 1994 Sep 1;43(9):1122 LP – 1129. Available from: http://diabetes.diabetesjournals.org/content/43/9/1122.abstract

45. Ishii H, Jirousek MR, Koya D, Takagi C, Xia P, Clermont A, et al. Amelioration of Vascular Dysfunctions in Diabetic Rats by an Oral PKC β Inhibitor. Science (80-) [Internet]. 1996 May 3;272(5262):728 LP – 731. Available from: http://science.sciencemag.org/content/272/5262/728.abstract

46. Koya D, King GL. Protein kinase C activation and the development of diabetic complications. Diabetes [Internet]. 1998 Jun 1;47(6):859 LP – 866. Available from:

http://diabetes.diabetesjournals.org/content/47/6/859.abstract

47. Adeshara K, Diwan A, Tupe R. Diabetes and Complications: Cellular Signaling Pathways, Current Understanding and Targeted Therapies. Curr Drug Targets. 2015 Dec 9;17.

48. Sone H, Deo BK, Kumagai AK. Enhancement of Glucose Transport by Vascular Endothelial Growth Factor in Retinal Endothelial Cells. Invest Ophthalmol Vis Sci. 2000 Jun 1;41(7):1876–84.

49. Ditzel J. Functional microangiopathy in diabetes mellitus. Diabetes. 1968;17(6):388–97.

50. Shore AC, Jaap AJ, Tooke JE. Capillary pressure in insulin dependent diabetic patients of long disease duration with and without microangiopathy. Diabet Med. 1992;9(Suppl 2):S11.

51. Parving H-H, Noer I, Deckert T, Evrin P-E, Nielsen SL, Lyngsøe J, et al. The effect of metabolic regulation on microvascular permeability to small and large molecules in short-term juvenile diabetics. Diabetologia. 1976;12(2):161–6.

52. Chawla A, Chawla R, Jaggi S. Microvasular and macrovascular complications in diabetes mellitus: Distinct or continuum? Indian J Endocrinol Metab [Internet]. 2016;20(4):546–51. Available from: https://pubmed.ncbi.nlm.nih.gov/27366724

53. Kobrin Klein BE. Overview of Epidemiologic Studies of Diabetic Retinopathy. Ophthalmic Epidemiol [Internet]. 2007 Jan 1;14(4):179–83. Available from: https://doi.org/10.1080/09286580701396720

54. Yau JWY, Rogers SL, Kawasaki R, Lamoureux EL, Kowalski JW, Bek T, et al. Global Prevalence and Major Risk Factors of Diabetic Retinopathy. Diabetes Care [Internet]. 2012 Mar 1;35(3):556 LP – 564. Available from: http://care.diabetesjournals.org/content/35/3/556.abstract

55. Zheng Y, He M, Congdon N. The worldwide epidemic of diabetic retinopathy. Indian J Ophthalmol [Internet]. 2012;60(5):428–31. Available from: https://pubmed.ncbi.nlm.nih.gov/22944754

56. M. WHP and WR. The Retinitis of Diabetes Mellitus: Preliminary Report. J Am Med Assoc. 1921;76(6):515–517.

57. Group E. Early photocoagulation for diabetic retinopathy: ETDRS report number 9. Ophthalmology. 1991;98(5):766–85.

58. Stitt AW, Curtis TM, Chen M, Medina RJ, McKay GJ, Jenkins A, et al. The progress in understanding and treatment of diabetic retinopathy. Prog Retin Eye Res [Internet]. 2016;51:156–86. Available from: http://www.sciencedirect.com/science/article/pii/S135094621500066X

59. Brownlee M. The Pathobiology of Diabetic Complications. Diabetes [Internet]. 2005 Jun 1;54(6):1615 LP – 1625. Available from: http://diabetes.diabetesjournals.org/content/54/6/1615.abstract

60. Nieuwdorp M, van Haeften TW, Gouverneur MCLG, Mooij HL, van Lieshout MHP, Levi M, et al. Loss of Endothelial Glycocalyx During Acute Hyperglycemia Coincides With Endothelial Dysfunction and Coagulation Activation In Vivo. Diabetes [Internet]. 2006 Feb 1;55(2):480 LP – 486. Available from: http://diabetes.diabetesjournals.org/content/55/2/480.abstract

61. Kristinsson JK, Gottfredsdóttir MS, Stefánsson E. Retinal vessel dilatation and elongation precedes diabetic macular oedema. Br J Ophthalmol [Internet]. 1997 Apr 1;81(4):274 LP – 278. Available from: http://bjo.bmj.com/content/81/4/274.abstract

62. Pemp B, Cherecheanu A, Garhofer G, Schmetterer L. Calculation of central retinal artery diameters from non-invasive ocular haemodynamic measurements in type 1 diabetes patients. Acta Ophthalmol. 2013;91(5):e348–52.

63. Naruse K, Nakamura J, Hamada Y, Nakayama M, Chaya S, Komori T, et al. Aldose Reductase Inhibition Prevents Glucose-induced Apoptosis in Cultured Bovine Retinal Microvascular Pericytes. Exp Eye Res [Internet]. 2000;71(3):309–15. Available from: http://www.sciencedirect.com/science/article/pii/S0014483500908820

64. Ejaz S, Chekarova I, Ejaz A, Sohail A, Lim CW. Importance of pericytes and mechanisms of pericyte loss during diabetic retinopathy. Diabetes, Obes Metab [Internet]. 2008 Jan 1;10(1):53–63. Available from: https://doi.org/10.1111/j.1463-1326.2007.00795.x

65. Orlidge A, D'Amore PA. Inhibition of capillary endothelial cell growth by pericytes and smooth muscle cells. J Cell Biol [Internet]. 1987 Sep;105(3):1455–62. Available from: https://pubmed.ncbi.nlm.nih.gov/3654761

66. Antonelli-Orlidge A, Saunders KB, Smith SR, D'Amore PA. An activated form of transforming growth factor beta is produced by cocultures of endothelial cells and pericytes. Proc Natl Acad Sci U S A [Internet]. 1989 Jun;86(12):4544–8. Available from: https://pubmed.ncbi.nlm.nih.gov/2734305

67. Porta EB and M. Pericyte Loss in Diabetic Retinopathy: Mechanisms and Consequences [Internet]. Vol. 20, Current Medicinal Chemistry. 2013. p. 3218–25. Available from: http://www.eurekaselect.com/node/113178/article

68. Huang H, He J, Johnson D, Wei Y, Liu Y, Wang S, et al. Deletion of Placental Growth Factor Prevents Diabetic Retinopathy and Is Associated With Akt Activation and HIF1α-VEGF Pathway Inhibition. Diabetes [Internet]. 2015 Jan 1;64(1):200 LP – 212. Available from: http://diabetes.diabetesjournals.org/content/64/1/200.abstract

69. Antonetti DA, Barber AJ, Hollinger LA, Wolpert EB, Gardner TW. Vascular Endothelial Growth Factor Induces Rapid Phosphorylation of Tight Junction Proteins Occludin and Zonula Occluden 1: A POTENTIAL MECHANISM FOR VASCULAR PERMEABILITY IN DIABETIC RETINOPATHY AND TUMORS . J Biol Chem [Internet]. 1999 Aug 13;274(33):23463–7. Available from: http://www.jbc.org/content/274/33/23463.abstract

70. Elman MJ, Aiello LP, Beck RW, Bressler NM, Bressler SB, Edwards AR, et al. Randomized Trial Evaluating Ranibizumab Plus Prompt or Deferred Laser or Triamcinolone Plus Prompt Laser for Diabetic Macular Edema. Ophthalmology [Internet]. 2010 Jun 1;117(6):1064-1077.e35. Available from: https://doi.org/10.1016/j.ophtha.2010.02.031

71. Heier JS, Korobelnik J-F, Brown DM, Schmidt-Erfurth U, Do D V, Midena E, et al. Intravitreal Aflibercept for Diabetic Macular Edema: 148-Week Results from the VISTA and VIVID Studies. Ophthalmology [Internet]. 2016 Nov 1;123(11):2376–85. Available from: https://doi.org/10.1016/j.ophtha.2016.07.032

72. Selvaraj K, Gowthamarajan K, Karri VVSR, Barauah UK, Ravisankar V, Jojo GM. Current treatment strategies and nanocarrier based approaches for the treatment and management of diabetic retinopathy. J Drug Target [Internet]. 2017 May 28;25(5):386–405. Available from: https://doi.org/10.1080/1061186X.2017.1280809

73. Duh EJ, Sun JK, Stitt AW. Diabetic retinopathy: current understanding, mechanisms, and treatment strategies. JCI insight [Internet]. 2017 Jul 20;2(14):e93751. Available from: https://pubmed.ncbi.nlm.nih.gov/28724805

74. Michaelson IC. The mode of development of the vascular system in the retina: With some observations on its significance for certain retinal diseases. Trans Ophthalmol Soc UK. 1948;68:137–80.

75. Senger DR, Perruzzi CA, Feder J, Dvorak HF. A highly conserved vascular permeability factor secreted by a variety of human and rodent tumor cell lines. Cancer Res. 1986;46(11):5629–32.

76. Jakeman LB, Winer J, Bennett GL, Altar CA, Ferrara N. Binding sites for vascular endothelial growth factor are localized on endothelial cells in adult rat tissues. J Clin Invest.

1992;89(1):244–53.

77. Adamis AP, Shima DT, Yeo K-T, Yeo TK, Brown LF, Berse B, et al. Synthesis and secretion of vascular permeability factor/vascular endothelial growth factor by human retinal pigment epithelial cells. Biochem Biophys Res Commun. 1993;193(2):631–8.

78. Pierce EA, Avery RL, Foley ED, Aiello LP, Smith LE. Vascular endothelial growth factor/vascular permeability factor expression in a mouse model of retinal neovascularization. Proc Natl Acad Sci. 1995;92(3):905–9.

79. Aiello LP, Pierce EA, Foley ED, Takagi H, Chen H, Riddle L, et al. Suppression of retinal neovascularization in vivo by inhibition of vascular endothelial growth factor (VEGF) using soluble VEGF-receptor chimeric proteins. Proc Natl Acad Sci. 1995;92(23):10457–61.

80. Scallan J, Huxley VH, Korthuis RJ. Capillary Fluid Exchange: Regulation, Functions, and Pathology. Colloq Ser Integr Syst Physiol From Mol to Funct [Internet]. 2010 Jan 1;2(1):1–94. Available from: https://doi.org/10.4199/C00006ED1V01Y201002ISP003

81. Burton AC. Relation of Structure to Function of the Tissues of the Wall of Blood Vessels. Physiol Rev [Internet]. 1954 Oct 1;34(4):619–42. Available from: https://doi.org/10.1152/physrev.1954.34.4.619

82. Rogers D, Lowe S. Ultrastructure of Blood Vessels - Arteries - Veins - TeachMeAnatomy [Internet]. 2017 [cited 2021 Jan 26]. Available from: https://teachmeanatomy.info/the-basics/ultrastructure/blood-vessels/

83. French JE. Atherosclerosis in relation to the structure and function of the arterial intima, with apecial regerence to the endothelium. Int Rev Exp Pathol. 1966;5:253–353.

84. Campbell GR, Campbell JH. Smooth muscle phenotypic changes in arterial wall homeostasis: Implications for the pathogenesis of atherosclerosis. Exp Mol Pathol [Internet]. 1985;42(2):139–62. Available from: http://www.sciencedirect.com/science/article/pii/0014480085900231

85. Campbell GR, Campbell JH, Manderson JA, Horrigan S, Rennick RE. Arterial smooth muscle. A multifunctional mesenchymal cell. Arch Pathol Lab Med. 1988;112(10):977–86.

86. Romero JC. Handbook of Physiology: A Critical, Comprehensive Presentation of Physiological Knowledge and Concepts. Section 2: The Cardiovascular System. Vol 4: Microcirculation. Mayo Clin Proc [Internet]. 1985 Jul 1;60(7):500–1. Available from: https://doi.org/10.1016/S0025-6196(12)60887-8

87. Lee KT, Lee KJ, Lee SK, Imai H, O'Neal RM. Poorly differentiated subendothelial cells in swine aortas. Exp Mol Pathol [Internet]. 1970;13(1):118–29. Available from: http://www.sciencedirect.com/science/article/pii/0014480070900894

88. Woolf N, Marty AT. Pathology of atherosclerosis. Crit Care Med. 1983;11(3):212.

89. Witzleb E. Functions of the Vascular System BT - Human Physiology. In: Schmidt RF, Thews G, editors. Berlin, Heidelberg: Springer Berlin Heidelberg; 1989. p. 480–542. Available from: https://doi.org/10.1007/978-3-642-73831-9_20

90. Wagner DD, Frenette PS. The vessel wall and its interactions. Blood [Internet]. 2008 Jun 1;111(11):5271–81. Available from: https://doi.org/10.1182/blood-2008-01-078204

91. Grotendorst GR, Seppä HE, Kleinman HK, Martin GR. Attachment of smooth muscle cells to collagen and their migration toward platelet-derived growth factor. Proc Natl Acad Sci U S A [Internet]. 1981 Jun;78(6):3669–72. Available from: https://pubmed.ncbi.nlm.nih.gov/6943570

92. Uzman A. Molecular biology of the cell (4th ed.): Alberts, B., Johnson, A., Lewis, J., Raff, M., Roberts, K., and Walter, P. Biochem Mol Biol Educ [Internet]. 2003 Jul 1;31(4):212–4. Available from: https://doi.org/10.1002/bmb.2003.494031049999

93. Jennings MA, Marchesi VT, Florey H. The Transport of Particles across the Walls of Small Blood Vessels. Proc R Soc London Ser B [Internet]. 1962 May 1;156:14–9. Available from: https://ui.adsabs.harvard.edu/abs/1962RSPSB.156...14J

94. Nerem RM, Cornhill JF. The Role of Fluid Mechanics in Atherogenesis. J Biomech Eng [Internet]. 1980 Aug 1;102(3):181–9. Available from: https://doi.org/10.1115/1.3149571

95. Rippe B, Haraldsson B. Transport of macromolecules across microvascular walls: the two-pore theory. Physiol Rev [Internet]. 1994 Jan 1;74(1):163–219. Available from: https://doi.org/10.1152/physrev.1994.74.1.163

96. Tarbell JM. Mass Transport in Arteries and the Localization of Atherosclerosis. Annu Rev Biomed Eng [Internet]. 2003 Aug 1;5(1):79–118. Available from: https://doi.org/10.1146/annurev.bioeng.5.040202.121529

97. Nollert MU, Diamond SL, McIntire L V. Hydrodynamic shear stress and mass transport modulation of endothelial cell metabolism. Biotechnol Bioeng [Internet]. 1991 Sep 1;38(6):588–602. Available from: https://doi.org/10.1002/bit.260380605

98. Ghim M, Alpresa P, Yang S-W, Braakman ST, Gray SG, Sherwin SJ, et al. Visualization of three pathways for macromolecule transport across cultured endothelium and their modification by flow. Am J Physiol Circ Physiol [Internet]. 2017 Jul 28;313(5):H959–73. Available from: https://doi.org/10.1152/ajpheart.00218.2017

99. Tarbell JM. Shear stress and the endothelial transport barrier. Cardiovasc Res [Internet]. 2010 Jul 15;87(2):320–30. Available from: https://doi.org/10.1093/cvr/cvq146

100. Salathe EP, An K-N. A mathematical analysis of fluid movement across capillary walls. Microvasc Res [Internet]. 1976;11(1):1–23. Available from: https://www.sciencedirect.com/science/article/pii/0026286276900728

101. Zeng Z, Jan K-M, Rumschitzki DS. A theory for water and macromolecular transport in the pulmonary artery wall with a detailed comparison to the aorta. Am J Physiol Circ Physiol [Internet]. 2011 Dec 23;302(8):H1683–99. Available from: https://doi.org/10.1152/ajpheart.00447.2011

102. Starling EH. On the absorption of fluids from the connective tissue spaces. Class Pap Crit Care. 1896;19:303.

103. Krogh A. The Anatomy and Physiology of Capillaries [Internet]. Yale University Press; 1922. (Mrs. Hepsa Ely Silliman memorial lectures). Available from: https://books.google.co.uk/books?id=QONqAAAAMAAJ

104. Landis EM. MICRO-INJECTION STUDIES OF CAPILLARY PERMEABILITY. Am J Physiol Content [Internet]. 1927 Oct 1;82(2):217–38. Available from: https://doi.org/10.1152/ajplegacy.1927.82.2.217

105. JR L. Capillary filtration-absorption balance reconsidered in light of dynamic extravascular factors. Exp Physiol [Internet]. 1991 Nov 1;76(6):825–57. Available from: https://doi.org/10.1113/expphysiol.1991.sp003549

106. Curry FE, Arkill KP, Michel CC. The Functions of Endothelial Glycocalyx and Their Effects on Patient Outcomes During the Perioperative Period. A Review of Current Methods to Evaluate Structure-Function Relations in the Glycocalyx in Both Basic Research and Clinical Settings BT - Periop. In: Farag E, Kurz A, editors. Cham: Springer International Publishing; 2020. p. 75–116. Available from: https://doi.org/10.1007/978-3-319-39141-0_3

107. Michel CC. CHAPTER 9 - Exchange of Fluid and Solutes Across Microvascular Walls. In: ALPERN RJ, HEBERT SCBT-S and GTK (Fourth E, editors. San Diego: Academic Press; 2008. p. 247–74. Available from: http://www.sciencedirect.com/science/article/pii/B9780120884889500127

108. Michel C. One Hundred Years of Starling's Hypothesis. Physiology [Internet]. 1996 Oct 1;11(5):229–37. Available from: https://doi.org/10.1152/physiologyonline.1996.11.5.229

109. Hu X, Weinbaum S. A New View of Starling's Hypothesis at the Microstructural Level. Microvasc Res [Internet]. 1999;58(3):281–304. Available from: http://www.sciencedirect.com/science/article/pii/S0026286299921775

110. Woodcock TE, Woodcock TM. Revised Starling equation and the glycocalyx model of transvascular fluid exchange: an improved paradigm for prescribing intravenous fluid therapy. BJA Br J Anaesth [Internet]. 2012 Mar 1;108(3):384–94. Available from: https://doi.org/10.1093/bja/aer515

111. Danielli JF. Capillary permeability and oedema in the perfused frog. J Physiol [Internet]. 1940 Mar 14;98(1):109–29. Available from: https://doi.org/10.1113/jphysiol.1940.sp003837

112. Reitsma S, Slaaf DW, Vink H, van Zandvoort MAMJ, oude Egbrink MGA. The endothelial glycocalyx: composition, functions, and visualization. Pflugers Arch [Internet]. 2007/01/26. 2007 Jun;454(3):345–59. Available from: https://pubmed.ncbi.nlm.nih.gov/17256154

113. CAREY DJ. Syndecans: multifunctional cell-surface co-receptors. Biochem J [Internet]. 1997 Oct 1;327(1):1–16. Available from: https://doi.org/10.1042/bj3270001

114. Fransson L-Å, Belting M, Cheng F, Jönsson M, Mani K, Sandgren S. Novel aspects of glypican glycobiology. Cell Mol Life Sci C [Internet]. 2004;61(9):1016–24. Available from: https://doi.org/10.1007/s00018-004-3445-0

115. Sugahara K, Mikami T, Uyama T, Mizuguchi S, Nomura K, Kitagawa H. Recent advances in the structural biology of chondroitin sulfate and dermatan sulfate. Curr Opin Struct Biol [Internet]. 2003;13(5):612–20. Available from: http://www.sciencedirect.com/science/article/pii/S0959440X03001441

116. Lee JY, Spicer AP. Hyaluronan: a multifunctional, megaDalton, stealth molecule. Curr Opin Cell Biol [Internet]. 2000;12(5):581–6. Available from: http://www.sciencedirect.com/science/article/pii/S0955067400001356

117. Huxley VH, Curry FE. Differential actions of albumin and plasma on capillary solute permeability. Am J Physiol Circ Physiol [Internet]. 1991 May 1;260(5):H1645–54. Available from: https://doi.org/10.1152/ajpheart.1991.260.5.H1645

118. Nieuwdorp M, Meuwese MC, Vink H, Hoekstra JBL, Kastelein JJP, Stroes ESG. The endothelial glycocalyx: a potential barrier between health and vascular disease. Curr Opin Lipidol [Internet]. 2005;16(5). Available from: https://journals.lww.com/co-lipidology/Fulltext/2005/10000/The_endothelial_glycocalyx__a_potential_barrier.3.aspx

119. David G, Bernfield MR. Collagen reduces glycosaminoglycan degradation by cultured mammary epithelial cells: possible mechanism for basal lamina formation. Proc Natl Acad Sci U S A [Internet]. 1979 Feb;76(2):786–90. Available from: https://pubmed.ncbi.nlm.nih.gov/284399

120. Kokenyesi R, Bernfield M. Core protein structure and sequence determine the site and presence of heparan sulfate and chondroitin sulfate on syndecan-1. J Biol Chem. 1994;269(16):12304–9.

121. Lopes CC, Dietrich CP, Nader HB. Specific structural features of syndecans and heparan sulfate chains are needed for cell signaling. Brazilian J Med Biol Res. 2006;39(2):157–67.

122. Ohlson M, Sörensson J, Haraldsson B. A gel-membrane model of glomerular charge and size selectivity in series. Am J Physiol Physiol [Internet]. 2001 Mar 1;280(3):F396–405. Available from: https://doi.org/10.1152/ajprenal.2001.280.3.F396

123. Rehm M, Zahler S, Lötsch M, Welsch U, Conzen P, Jacob M, et al. Endothelial Glycocalyx as an Additional Barrier Determining Extravasation of 6% Hydroxyethyl Starch or 5% Albumin

Solutions in the Coronary Vascular Bed. Anesthesiology [Internet]. 2004 May 1;100(5):1211–23. Available from: https://doi.org/10.1097/00000542-200405000-00025

124. Becker BF, Chappell D, Jacob M. Endothelial glycocalyx and coronary vascular permeability: the fringe benefit. Basic Res Cardiol [Internet]. 2010;105(6):687–701. Available from: https://doi.org/10.1007/s00395-010-0118-z

125. Haldenby KA, Chappell DC, Winlove CP, Parker KH, Firth JA. Focal and Regional Variations in the Composition of the Glycocalyx of Large Vessel Endothelium. J Vasc Res [Internet]. 1994;31(1):2–9. Available from: https://www.karger.com/DOI/10.1159/000159025

126. Yoon J-H, Lee E-S, Jeong Y. In vivo imaging of the cerebral endothelial glycocalyx in mice. J Vasc Res. 2017;54(2):59–67.

127. Luft JH. Fine structures of capillary and endocapillary layer as revealed by ruthenium red. Fed Proc [Internet]. 1966;25(6):1773–83. Available from: http://europepmc.org/abstract/MED/5927412

128. Hans V, R. DB. Identification of Distinct Luminal Domains for Macromolecules, Erythrocytes, and Leukocytes Within Mammalian Capillaries. Circ Res [Internet]. 1996 Sep 1;79(3):581–9. Available from: https://doi.org/10.1161/01.RES.79.3.581

129. Kolářová H, Ambrůzová B, Švihálková Šindlerová L, Klinke A, Kubala L. Modulation of Endothelial Glycocalyx Structure under Inflammatory Conditions. McCafferty D-M, editor. Mediators Inflamm [Internet]. 2014;2014:694312. Available from: https://doi.org/10.1155/2014/694312

130. Chappell D, Jacob M, Paul O, Rehm M, Welsch U, Stoeckelhuber M, et al. The glycocalyx of the human umbilical vein endothelial cell: an impressive structure ex vivo but not in culture. Circ Res. 2009;104(11):1313–7.

131. Potter DR, Damiano ER. The hydrodynamically relevant endothelial cell glycocalyx observed in vivo is absent in vitro. Circ Res. 2008;102(7):770–6.

132. Dewey Jr CF, Bussolari SR, Gimbrone Jr MA, Davies PF. The dynamic response of vascular endothelial cells to fluid shear stress. 1981;

133. Davies PF. Flow-mediated endothelial mechanotransduction. Physiol Rev. 1995;75(3):519–60.

134. Sieve I, Münster-Kühnel AK, Hilfiker-Kleiner D. Regulation and function of endothelial glycocalyx layer in vascular diseases. Vascul Pharmacol [Internet]. 2018;100:26–33. Available from: http://www.sciencedirect.com/science/article/pii/S1537189117301805

135. GOUVERNEUR M, VAN DEN BERG B, NIEUWDORP M, STROES E, VINK H. Vasculoprotective properties of the endothelial glycocalyx: effects of fluid shear stress. J Intern Med [Internet]. 2006 Apr 1;259(4):393–400. Available from: https://doi.org/10.1111/j.1365-2796.2006.01625.x

136. Evanko SP, Wight TN. Intracellular localization of hyaluronan in proliferating cells. J Histochem Cytochem. 1999;47(10):1331–41.

137. ARISAKA T, MITSUMATA M, KAWASUMI M, TOHJIMA T, HIROSE S, YOSHIDA Y. Effects of Shear Stress on Glycosaminoglycan Synthesis in Vascular Endothelial Cellsa. Ann N Y Acad Sci [Internet]. 1994 Jan 1;748(1):543–54. Available from: https://doi.org/10.1111/j.1749-6632.1994.tb17359.x

138. Broekhuizen LN, Mooij HL, Kastelein JJP, Stroes ESG, Vink H, Nieuwdorp M. Endothelial glycocalyx as potential diagnostic and therapeutic target in cardiovascular disease. Curr Opin Lipidol [Internet]. 2009;20(1). Available from: https://journals.lww.com/co-lipidology/Fulltext/2009/02000/Endothelial_glycocalyx_as_potential_diagnostic_and.11.aspx

139. Pries AR, Secomb TW, Gaehtgens P. The endothelial surface layer. Pflügers Arch.

2000;440(5):653–66.

140. Huxley VH, Williams DA. Role of a glycocalyx on coronary arteriole permeability to proteins: evidence from enzyme treatments. Am J Physiol Circ Physiol [Internet]. 2000 Apr 1;278(4):H1177–85. Available from: https://doi.org/10.1152/ajpheart.2000.278.4.H1177

141. Becker BF, Chappell D, Bruegger D, Annecke T, Jacob M. Therapeutic strategies targeting the endothelial glycocalyx: acute deficits, but great potential†. Cardiovasc Res [Internet]. 2010 Jul 15;87(2):300–10. Available from: https://doi.org/10.1093/cvr/cvq137

142. Perrin RM, Harper SJ, Bates DO. A Role for the Endothelial Glycocalyx in Regulating Microvascular Permeability in Diabetes Mellitus. Cell Biochem Biophys [Internet]. 2007;49(2):65–72. Available from: https://doi.org/10.1007/s12013-007-0041-6

143. Lieleg O, Baumgärtel RM, Bausch AR. Selective Filtering of Particles by the Extracellular Matrix: An Electrostatic Bandpass. Biophys J [Internet]. 2009 Sep 16;97(6):1569–77. Available from: https://doi.org/10.1016/j.bpj.2009.07.009

144. Vink H, Duling BR. Capillary endothelial surface layer selectively reduces plasma solute distribution volume. Am J Physiol Circ Physiol. 2000;278(1):H285–9.

145. Quinsey NS, Greedy AL, Bottomley SP, Whisstock JC, Pike RN. Antithrombin: in control of coagulation. Int J Biochem Cell Biol. 2004;36(3):386–9.

146. SHIMADA K, KOBAYASHI M, KIMURA S, NISHINAGA M, TAKEUCHI K, OZAWA T. Anticoagulant Heparin-like Glycosaminoglycans on Endothelial Cell Surface: 54th Annual Scientific Session of the Japanese Circulation Society. Jpn Circ J. 1991;55(10):1016–21.

147. Bruno L, Marco R, Cristina SM. Diabetic Retinopathy [Internet]. DL, INDIA: Jaypee Brothers Medical Publishers; 2015. Available from: http://ebookcentral.proquest.com/lib/leeds/detail.action?docID=4543597

148. Curry F-RE, Adamson RH. Vascular permeability modulation at the cell, microvessel, or whole organ level: towards closing gaps in our knowledge. Cardiovasc Res [Internet]. 2010 Jul 15;87(2):218–29. Available from: https://doi.org/10.1093/cvr/cvq115

149. Baldwin AL, Winlove CP. Effects of perfusate composition on binding of ruthenium red and gold colloid to glycocalyx of rabbit aortic endothelium. J Histochem Cytochem [Internet]. 1984 Mar 1;32(3):259–66. Available from: https://doi.org/10.1177/32.3.6198357

150. Clough G, Moffitt H. Immunoperoxidase labelling of albumin at the endothelial cell surface of frog mesenteric microvessels. Int J Microcirc Clin Exp. 1992;11(4):345–58.

151. Adamson RH. Permeability of frog mesenteric capillaries after partial pronase digestion of the endothelial glycocalyx. J Physiol [Internet]. 1990 Sep 1;428(1):1–13. Available from: https://doi.org/10.1113/jphysiol.1990.sp018197

152. Weinbaum S, Tarbell JM, Damiano ER. The Structure and Function of the Endothelial Glycocalyx Layer. Annu Rev Biomed Eng [Internet]. 2007 Jul 25;9(1):121–67. Available from: https://doi.org/10.1146/annurev.bioeng.9.060906.151959

153. Barker AL, Konopatskaya O, Neal CR, Macpherson J V, Whatmore JL, Winlove CP, et al. Observation and characterisation of the glycocalyx of viable human endothelial cells using confocal laser scanning microscopy. Phys Chem Chem Phys [Internet]. 2004;6(5):1006–11. Available from: http://dx.doi.org/10.1039/B312189E

154. Thi MM, Tarbell JM, Weinbaum S, Spray DC. The role of the glycocalyx in reorganization of the actin cytoskeleton under fluid shear stress: A “bumper-car” model. Proc Natl Acad Sci U S A [Internet]. 2004 Nov 23;101(47):16483 LP – 16488. Available from: http://www.pnas.org/content/101/47/16483.abstract

155. Stevens AP, Hlady V, Dull RO. Fluorescence correlation spectroscopy can probe albumin

dynamics inside lung endothelial glycocalyx. Am J Physiol Cell Mol Physiol [Internet]. 2007 Aug 1;293(2):L328–35. Available from: https://doi.org/10.1152/ajplung.00390.2006

156. Sims DE, Horne MM. Non-aqueous fixative preserves macromolecules on the endothelial cell surface: an in situ study. Eur J Morphol [Internet]. 1993;31(4):251–5. Available from: http://europepmc.org/abstract/MED/8172755

157. E. EE, P. MF, C. SD, M. TJ. Imaging the Endothelial Glycocalyx In Vitro by Rapid Freezing/Freeze Substitution Transmission Electron Microscopy. Arterioscler Thromb Vasc Biol [Internet]. 2011 Aug 1;31(8):1908–15. Available from: https://doi.org/10.1161/ATVBAHA.111.225268

158. Erlandsen SL, Kristich CJ, Dunny GM, Wells CL. High-resolution visualization of the microbial glycocalyx with low-voltage scanning electron microscopy: dependence on cationic dyes. J Histochem Cytochem [Internet]. 2004 Nov;52(11):1427–35. Available from: https://pubmed.ncbi.nlm.nih.gov/15505337

159. Rochow TG, Tucker PA. A Brief History of Microscopy BT - Introduction to Microscopy by Means of Light, Electrons, X Rays, or Acoustics. In: Rochow TG, Tucker PA, editors. Boston, MA: Springer US; 1994. p. 1–21. Available from: https://doi.org/10.1007/978-1-4899-1513-9_1

160. Merchant FA, Bartels KA, Bovik AC, Diller KR. 10.9 - Confocal Microscopy. In: BOVIK ALBT-H of I and VP (Second E, editor. Communications, Networking and Multimedia [Internet]. Burlington: Academic Press; 2005. p. 1291–XLI. Available from: https://www.sciencedirect.com/science/article/pii/B9780121197926501352

161. Vink H, Duling BR. Identification of distinct luminal domains for macromolecules, erythrocytes, and leukocytes within mammalian capillaries. Circ Res. 1996;79(3):581–9.

162. Dane MJC, van den Berg BM, Lee DH, Boels MGS, Tiemeier GL, Avramut MC, et al. A microscopic view on the renal endothelial glycocalyx. Am J Physiol Physiol [Internet]. 2015 Feb 11;308(9):F956–66. Available from: https://doi.org/10.1152/ajprenal.00532.2014

163. Kataoka H, Ushiyama A, Kawakami H, Akimoto Y, Matsubara S, Iijima T. Fluorescent imaging of endothelial glycocalyx layer with wheat germ agglutinin using intravital microscopy. Microsc Res Tech [Internet]. 2016 Jan 1;79(1):31–7. Available from: https://doi.org/10.1002/jemt.22602

164. Corstian A, Klijn E, Lagrand WK, Brugts JJ, Ince C, Spronk PE, et al. The microcirculation in health and critical disease. Prog Cardiovasc Dis. 2008;51(2):161–70.

165. Patterson G, Davidson M, Manley S, Lippincott-Schwartz J. Superresolution Imaging using Single-Molecule Localization. Annu Rev Phys Chem [Internet]. 2010 Mar 1;61(1):345–67. Available from: https://doi.org/10.1146/annurev.physchem.012809.103444

166. Rust MJ, Bates M, Zhuang X. Sub-diffraction-limit imaging by stochastic optical reconstruction microscopy (STORM). Nat Methods [Internet]. 2006;3(10):793–6. Available from: https://doi.org/10.1038/nmeth929

167. Jones SA, Shim S-H, He J, Zhuang X. Fast, three-dimensional super-resolution imaging of live cells. Nat Methods [Internet]. 2011/05/08. 2011 Jun;8(6):499–508. Available from: https://pubmed.ncbi.nlm.nih.gov/21552254

168. Sydor AM, Czymmek KJ, Puchner EM, Mennella V. Super-Resolution Microscopy: From Single Molecules to Supramolecular Assemblies. Trends Cell Biol [Internet]. 2015 Dec 1;25(12):730–48. Available from: https://doi.org/10.1016/j.tcb.2015.10.004

169. Broglie L de. XXXV. A tentative theory of light quanta. London, Edinburgh, Dublin Philos Mag J Sci [Internet]. 1924 Feb 1;47(278):446–58. Available from: https://doi.org/10.1080/14786442408634378

170. Rochow E. An Introduction to Microscopy by Means of Light, Electrons, X-Rays, or Ultrasound [Internet]. Springer US; 2012. Available from:

https://books.google.co.uk/books?id=g1jhBwAAQBAJ

171. Grundy PJ, Jones GA, Jones GA. Electron Microscopy in the Study of Materials [Internet]. Edward Arnold; 1976. (Structures and properties of solids). Available from: https://books.google.co.uk/books?id=-ZoeAQAAIAAJ

172. Walther T. Chapter 4 - Transmission Electron Microscopy of Nanostructures. In: Thomas S, Thomas R, Zachariah AK, Mishra RKBT-MM in NC, editors. Micro and Nano Technologies [Internet]. Elsevier; 2017. p. 105–34. Available from: http://www.sciencedirect.com/science/article/pii/B9780323461412000043

173. Knoll M, Ruska E. Das Elektronenmikroskop. Zeitschrift für Phys [Internet]. 1932;78(5):318–39. Available from: https://doi.org/10.1007/BF01342199

174. Hawkes PW. Advances in Electronics and Electron Physics [Internet]. Elsevier Science; 1991. (ISSN). Available from: https://books.google.co.uk/books?id=s6gMdNTTqG0C

175. Viswanathan P. Electron Microscopy [Internet]. MJP Publisher; 2019. Available from: https://books.google.co.uk/books?id=ceycDwAAQBAJ

176. Egerton R. Physical Principles of Electron Microscopy: An Introduction to TEM, SEM, and AEM [Internet]. Springer US; 2011. (Springer ebook collection / Chemistry and Materials Science 2005-2008). Available from: https://books.google.co.uk/books?id=t6TTgqp3O5MC

177. García de Abajo FJ. Optical excitations in electron microscopy. Rev Mod Phys [Internet]. 2010 Feb 3;82(1):209–75. Available from: https://link.aps.org/doi/10.1103/RevModPhys.82.209

178. Hunter EE, Silver M, Maloney P, Bendayan M, Evelyn HE. Practical Electron Microscopy: A Beginner's Illustrated Guide [Internet]. Cambridge University Press; 1993. Available from: https://books.google.co.uk/books?id=C-FuGuMiDoMC

179. Amelinckx S, van Dyck D, van Landuyt J, van Tendeloo G. Electron Microscopy: Principles and Fundamentals [Internet]. Wiley; 2008. Available from: https://books.google.co.uk/books?id=VgkBEidIlU8C

180. Aldrich HC, Todd WJ. Ultrastructure techniques for microorganisms. Springer Science & Business Media; 2012.

181. Pawley J, Erlandsen S. The case for low voltage high resolution scanning microscopy of biological samples. Scanning Microsc Suppl. 1989 Feb 1;3:163–78.

182. Matsusaka T. The fine structure of retinal capillaries in normal and increased permeability as revealed by ruthenium red staining. Albr von Graefes Arch für Klin und Exp Ophthalmol [Internet]. 1971;183(2):140–51. Available from: https://doi.org/10.1007/BF00407179

183. Janczyk P, Hansen S, Bahramsoltani M, Plendl J. The glycocalyx of human, bovine and murine microvascular endothelial cells cultured in vitro. J Electron Microsc (Tokyo) [Internet]. 2010 Aug 1;59(4):291–8. Available from: https://doi.org/10.1093/jmicro/dfq007

184. Luft JH. Ruthenium red and violet. I. Chemistry, purification, methods of use for electron microscopy and mechanism of action. Anat Rec [Internet]. 1971 Nov 1;171(3):347–68. Available from: https://doi.org/10.1002/ar.1091710302

185. Behnke O, Zelander T. Preservation of intercellular substances by the cationic dye alcian blue in preparative procedures for electron microscopy. J Ultrastruct Res [Internet]. 1970;31(5):424–38. Available from: http://www.sciencedirect.com/science/article/pii/S0022532070901590

186. Fassel TA, Edmiston CEBT-M in E. [15] Bacterial biofilms: Strategies for preparing glycocalyx for electron microscopy. In: Biofilms [Internet]. Academic Press; 1999. p. 194–203. Available from: http://www.sciencedirect.com/science/article/pii/S007668799910017X

187. ASHTON N. Injection of the retinal vascular system in the enucleated eye in diabetic retinopathy. Br J Ophthalmol. 1950 Jan;34(1):38–41.

188. Naccarato R, Maschio G, Sirigu F, Previato G, Rizzo A, Mioni G, et al. The muscle in diabetes mellitus. Virchows Arch B. 1969;4(1):283.

189. Kozak WM, Marker NA, Elmer KK. Effects of aldose reductase inhibition on the retina and health indices of streptozotocin-diabetic rats. Doc Ophthalmol. 1986;64(4):355–77.

190. Siperstein MD, Unger RH, Madison LL. Studies of muscle capillary basement membranes in normal subjects, diabetic, and prediabetic patients. J Clin Invest. 1968;47(9):1973–99.

191. Ljubimov A V, Burgeson RE, Butkowski RJ, Couchman JR, Zardi L, Ninomiya Y, et al. Basement membrane abnormalities in human eyes with diabetic retinopathy. J Histochem Cytochem. 1996;44(12):1469–79.

192. Tsilibary EC. Microvascular basement membranes in diabetes mellitus. J Pathol A J Pathol Soc Gt Britain Irel. 2003;200(4):537–46.

193. Walton HA, Byrne J, Robinson GB. Studies of the permeation properties of glomerular basement membrane: cross-linking renders glomerular basement membrane permeable to protein. Biochim Biophys Acta (BBA)-Molecular Basis Dis. 1992;1138(3):173–83.

194. Boyd-White J, Williams JC. Effect of cross-linking on matrix permeability: a model for AGE-modified basement membranes. Diabetes. 1996;45(3):348–53.

195. Roy S, Sato T, Paryani G, Kao R. Downregulation of fibronectin overexpression reduces basement membrane thickening and vascular lesions in retinas of galactose-fed rats. Diabetes. 2003;52(5):1229–34.

196. Roy S, Ha J, Trudeau K, Beglova E. Vascular Basement Membrane Thickening in Diabetic Retinopathy. Curr Eye Res [Internet]. 2010 Dec 1;35(12):1045–56. Available from: https://doi.org/10.3109/02713683.2010.514659

197. Yang X, Scott HA, Monickaraj F, Xu J, Ardekani S, Nitta CF, et al. Basement membrane stiffening promotes retinal endothelial activation associated with diabetes. FASEB J [Internet]. 2016 Feb 1;30(2):601–11. Available from: https://doi.org/10.1096/fj.15-277962

198. Foster RR, Armstrong L, Baker S, Wong DWL, Wylie EC, Ramnath R, et al. Glycosaminoglycan regulation by VEGFA and VEGFC of the glomerular microvascular endothelial cell glycocalyx in vitro. Am J Pathol [Internet]. 2013/06/12. 2013 Aug;183(2):604–16. Available from: https://pubmed.ncbi.nlm.nih.gov/23770346

199. Hoeben ANN, Landuyt B, Highley MS, Wildiers H, Van Oosterom AT, De Bruijn EA. Vascular endothelial growth factor and angiogenesis. Pharmacol Rev. 2004;56(4):549–80.

200. Penn JS, Madan A, Caldwell RB, Bartoli M, Caldwell RW, Hartnett ME. Vascular endothelial growth factor in eye disease. Prog Retin Eye Res. 2008;27(4):331–71.

201. Houck KA, Leung DW, Rowland AM, Winer J, Ferrara NJ. Dual regulation of vascular endothelial growth factor bioavailability by genetic and proteolytic mechanisms. J Biol Chem. 1992;267(36):26031–7.

202. Nowak DG, Woolard J, Amin EM, Konopatskaya O, Saleem MA, Churchill AJ, et al. Expression of pro-and anti-angiogenic isoforms of VEGF is differentially regulated by splicing and growth factors. J Cell Sci. 2008;121(20):3487–95.

203. Artac RA, McFee RM, Longfellow Smith RA, Baltes-Breitwisch MM, Clopton DT, Cupp AS. Neutralization of vascular endothelial growth factor antiangiogenic isoforms is more effective than treatment with proangiogenic isoforms in stimulating vascular development and follicle progression in the perinatal rat ovary. Biol Reprod. 2009;81(5):978–88.

204. Simons M, Gordon E, Claesson-Welsh L. Mechanisms and regulation of endothelial VEGF receptor signalling. Nat Rev Mol cell Biol. 2016;17(10):611–25.

205. Li X, Padhan N, Sjöström EO, Roche FP, Testini C, Honkura N, et al. VEGFR2 pY949 signalling regulates adherens junction integrity and metastatic spread. Nat Commun. 2016;7(1):1–16.

206. Oltean S, Qiu Y, Ferguson JK, Stevens M, Neal C, Russell A, et al. Vascular Endothelial Growth Factor-A165b Is Protective and Restores Endothelial Glycocalyx in Diabetic Nephropathy. J Am Soc Nephrol [Internet]. 2014/12/26. 2015 Aug;26(8):1889–904. Available from: https://pubmed.ncbi.nlm.nih.gov/25542969

207. Sanford JR, Ellis JD, Cazalla D, Cáceres JF. Reversible phosphorylation differentially affects nuclear and cytoplasmic functions of splicing factor 2/alternative splicing factor. Proc Natl Acad Sci. 2005;102(42):15042–7.

208. Nowak DG, Amin EM, Rennel ES, Hoareau-Aveilla C, Gammons M, Damodoran G, et al. Regulation of vascular endothelial growth factor (VEGF) splicing from pro-angiogenic to anti-angiogenic isoforms: a novel therapeutic strategy for angiogenesis. J Biol Chem. 2010;285(8):5532–40.

209. Oltean S, Gammons M, Hulse R, Hamdollah-Zadeh M, Mavrou A, Donaldson L, et al. SRPK1 inhibition in vivo: modulation of VEGF splicing and potential treatment for multiple diseases. Biochem Soc Trans. 2012;40(4):831–5.

210. Ergorul C, Ray A, Huang W, Darland D, Luo ZK, Grosskreutz CL. Levels of vascular endothelial growth factor-A165b (VEGF-A165b) are elevated in experimental glaucoma. Mol Vis. 2008;14:1517.

211. GeneCards. EXT1 [Internet]. 2021. Available from: https://www.genecards.org/cgi-bin/carddisp.pl?gene=EXT1#diseases

212. Busse M, Feta A, Presto J, Wilén M, Grønning M, Kjellén L, et al. Contribution of EXT1, EXT2, and EXTL3 to Heparan Sulfate Chain Elongation *. J Biol Chem [Internet]. 2007 Nov 9;282(45):32802–10. Available from: https://doi.org/10.1074/jbc.M703560200

213. Lüdecke H-J, Ahn J, Lin X, Hill A, Wagner MJ, Schomburg L, et al. Genomic Organization and Promoter Structure of the Human EXT1 Gene. Genomics [Internet]. 1997;40(2):351–4. Available from: https://www.sciencedirect.com/science/article/pii/S0888754396945772

214. Ishimaru D, Gotoh M, Takayama S, Kosaki R, Matsumoto Y, Narimatsu H, et al. Large-scale mutational analysis in the EXT1 and EXT2 genes for Japanese patients with multiple osteochondromas. BMC Genet [Internet]. 2016 Mar 9;17:52. Available from: https://pubmed.ncbi.nlm.nih.gov/26961984

215. Guo X, Lin M, Shi T, Yan W, Chen W. Targeted Next-Generation Sequencing Newly Identifies Mutations in *Exostosin-1* and *Exostosin-2* Genes of Patients with Multiple Osteochondromas. Tohoku J Exp Med. 2017;242(3):173–81.

216. Goni O. No TitleThe elusive functions of EXT1 and EXT2. Cent Int Heal Dep Biomed Fac Med Univ Bergen, Norw [Internet]. 2021; Available from: https://bora.uib.no/bora-xmlui/bitstream/handle/11250/2760494/The-elusive-functions-of-EXT1-and-EXT2-converted.pdf?sequence=1

217. Mooij HL, Cabrales P, Bernelot Moens SJ, Xu D, Udayappan SD, Tsai AG, et al. Loss of function in heparan sulfate elongation genes EXT1 and EXT 2 results in improved nitric oxide bioavailability and endothelial function. J Am Heart Assoc [Internet]. 2014 Dec 2;3(6):e001274–e001274. Available from: https://pubmed.ncbi.nlm.nih.gov/25468659

218. Pahakis MY, Kosky JR, Dull RO, Tarbell JM. The role of endothelial glycocalyx components in mechanotransduction of fluid shear stress. Biochem Biophys Res Commun [Internet]. 2007/02/02. 2007 Mar 30;355(1):228–33. Available from:

https://pubmed.ncbi.nlm.nih.gov/17291452

219. TARBELL JM, PAHAKIS MY. Mechanotransduction and the glycocalyx. J Intern Med [Internet]. 2006 Apr 1;259(4):339–50. Available from: https://doi.org/10.1111/j.1365-2796.2006.01620.x

220. van den Born J, Gunnarsson K, Bakker MAH, Kjellén L, Kusche-Gullberg M, Maccarana M, et al. Presence of N-Unsubstituted Glucosamine Units in Native Heparan Sulfate Revealed by a Monoclonal Antibody (∗). J Biol Chem [Internet]. 1995 Dec 29;270(52):31303–9. Available from: https://doi.org/10.1074/jbc.270.52.31303

221. Forsberg E, Kjellén L. Heparan sulfate: lessons from knockout mice. J Clin Invest [Internet]. 2001 Jul;108(2):175–80. Available from: https://pubmed.ncbi.nlm.nih.gov/11457868

222. Lind T, Tufaro F, McCormick C, Lindahl U, Lidholt K. The Putative Tumor Suppressors EXT1 and EXT2 Are Glycosyltransferases Required for the Biosynthesis of Heparan Sulfate *. J Biol Chem [Internet]. 1998 Oct 9;273(41):26265–8. Available from: https://doi.org/10.1074/jbc.273.41.26265

223. Sugahara K, Kitagawa H. Heparin and Heparan Sulfate Biosynthesis. IUBMB Life [Internet]. 2002 Oct 1;54(4):163–75. Available from: https://doi.org/10.1080/15216540214928

224. Kjellen L. Glucosaminyl N-deacetylase/N-sulphotransferases in heparan sulphate biosynthesis and biology. Biochem Soc Trans. 2003;31(2):340–2.

225. Zak BM, Crawford BE, Esko JD. Hereditary multiple exostoses and heparan sulfate polymerization. Biochim Biophys Acta - Gen Subj [Internet]. 2002;1573(3):346–55. Available from: https://www.sciencedirect.com/science/article/pii/S0304416502004026

226. Caravà E, Moretto P, Caon I, Parnigoni A, Passi A, Karousou E, et al. HA and HS Changes in Endothelial Inflammatory Activation. Vol. 11, Biomolecules . 2021.

227. Kjellén L, Lindahl U. Specificity of glycosaminoglycan–protein interactions. Curr Opin Struct Biol [Internet]. 2018;50:101–8. Available from: https://www.sciencedirect.com/science/article/pii/S0959440X17301495

228. Chiodelli P, Mitola S, Ravelli C, Oreste P, Rusnati M, Presta M. Heparan Sulfate Proteoglycans Mediate the Angiogenic Activity of the Vascular Endothelial Growth Factor Receptor-2 Agonist Gremlin. Arterioscler Thromb Vasc Biol [Internet]. 2011 Dec 1;31(12):e116–27. Available from: https://doi.org/10.1161/ATVBAHA.111.235184

229. Araki K, Araki M, Yamamura K. Targeted integration of DNA using mutant lox sites in embryonic stem cells. Nucleic Acids Res [Internet]. 1997 Feb 15;25(4):868–72. Available from: https://pubmed.ncbi.nlm.nih.gov/9016639

230. Missirlis PI, Smailus DE, Holt RA. A high-throughput screen identifying sequence and promiscuity characteristics of the loxP spacer region in Cre-mediated recombination. BMC Genomics [Internet]. 2006 Apr 4;7:73. Available from: https://pubmed.ncbi.nlm.nih.gov/16595017

231. Kuhlman SJ, Huang ZJ. High-resolution labeling and functional manipulation of specific neuron types in mouse brain by Cre-activated viral gene expression. PLoS One [Internet]. 2008 Apr 16;3(4):e2005–e2005. Available from: https://pubmed.ncbi.nlm.nih.gov/18414675

232. Tronche F, Casanova E, Turiault M, Sahly I, Kellendonk C. When reverse genetics meets physiology: the use of site-specific recombinases in mice. FEBS Lett [Internet]. 2002 Oct 2;529(1):116–21. Available from: https://doi.org/10.1016/S0014-5793(02)03266-0

233. Vestweber D. VE-Cadherin. Arterioscler Thromb Vasc Biol [Internet]. 2008 Feb 1;28(2):223–32. Available from: https://doi.org/10.1161/ATVBAHA.107.158014

234. Villa KL, Berry KP, Subramanian J, Cha JW, Oh WC, Kwon H-B, et al. Inhibitory Synapses Are

Repeatedly Assembled and Removed at Persistent Sites In Vivo. Neuron [Internet]. 2016/02/04. 2016 Feb 17;89(4):756–69. Available from: https://pubmed.ncbi.nlm.nih.gov/26853302

235. Henry CBS, Duling BR. Permeation of the luminal capillary glycocalyx is determined by hyaluronan. Am J Physiol Circ Physiol [Internet]. 1999 Aug 1;277(2):H508–14. Available from: https://doi.org/10.1152/ajpheart.1999.277.2.H508

236. Nieuwdorp M, Meuwese MC, Mooij HL, Ince C, Broekhuizen LN, Kastelein JJP, et al. Measuring endothelial glycocalyx dimensions in humans: a potential novel tool to monitor vascular vulnerability. J Appl Physiol [Internet]. 2008 Mar 1;104(3):845–52. Available from: https://doi.org/10.1152/japplphysiol.00440.2007

237. Iba T, Levy JH. Derangement of the endothelial glycocalyx in sepsis. J Thromb Haemost [Internet]. 2019 Feb 1;17(2):283–94. Available from: https://doi.org/10.1111/jth.14371

238. Schindelin J, Arganda-Carreras I, Frise E, Kaynig V, Longair M, Pietzsch T, et al. Fiji: an open-source platform for biological-image analysis. Nat Methods. 2012;9(7):676–82.

239. Saadane A, Lessieur EM, Du Y, Liu H, Kern TS. Successful induction of diabetes in mice demonstrates no gender difference in development of early diabetic retinopathy. PLoS One [Internet]. 2020 Sep 17;15(9):e0238727–e0238727. Available from: https://pubmed.ncbi.nlm.nih.gov/32941450

240. Graham ML, Janecek JL, Kittredge JA, Hering BJ, Schuurman H-J. The streptozotocin-induced diabetic nude mouse model: differences between animals from different sources. Comp Med [Internet]. 2011 Aug;61(4):356–60. Available from: https://pubmed.ncbi.nlm.nih.gov/22330251

241. Lenzen S. The mechanisms of alloxan- and streptozotocin-induced diabetes. Diabetologia [Internet]. 2008;51(2):216–26. Available from: https://doi.org/10.1007/s00125-007-0886-7

242. Grossman EJ, Lee DD, Tao J, Wilson RA, Park S-Y, Bell GI, et al. Glycemic control promotes pancreatic beta-cell regeneration in streptozotocin-induced diabetic mice. PLoS One [Internet]. 2010 Jan 18;5(1):e8749–e8749. Available from: https://pubmed.ncbi.nlm.nih.gov/20090914

243. King AJF. The use of animal models in diabetes research. Br J Pharmacol [Internet]. 2012 Jun;166(3):877–94. Available from: https://pubmed.ncbi.nlm.nih.gov/22352879

244. Masaru I, Fumitoshi I, S. PA, Marc T-L, Yu Y. Mammalian Brain Morphogenesis and Midline Axon Guidance Require Heparan Sulfate. Science (80-) [Internet]. 2003 Nov 7;302(5647):1044–6. Available from: https://doi.org/10.1126/science.1090497

245. Matsumoto Y, Irie F, Inatani M, Tessier-Lavigne M, Yamaguchi Y. Netrin-1/DCC Signaling in Commissural Axon Guidance Requires Cell-Autonomous Expression of Heparan Sulfate. J Neurosci [Internet]. 2007 Apr 18;27(16):4342 LP – 4350. Available from: http://www.jneurosci.org/content/27/16/4342.abstract

246. Lin X, Wei G, Shi Z, Dryer L, Esko JD, Wells DE, et al. Disruption of Gastrulation and Heparan Sulfate Biosynthesis in EXT1-Deficient Mice. Dev Biol [Internet]. 2000;224(2):299–311. Available from: https://www.sciencedirect.com/science/article/pii/S0012160600997987

247. Allen CL, Malhi NK, Whatmore JD, Bates DO, Arkill KP. Non-invasive measurement of retinal permeability in a diabetic rat model. Microcirculation. 2020;

248. Arkill KP, NEAL CR, MANTELL JM, MICHEL CC, QVORTRUP K, ROSTGAARD J, et al. 3D Reconstruction of the Glycocalyx Structure in Mammalian Capillaries using Electron Tomography. Microcirculation [Internet]. 2012 May 1;19(4):343–51. Available from: https://doi.org/10.1111/j.1549-8719.2012.00168.x

249. Targosz-Korecka M, Jaglarz M, Malek-Zietek KE, Gregorius A, Zakrzewska A, Sitek B, et al. AFM-based detection of glycocalyx degradation and endothelial stiffening in the db/db mouse

model of diabetes. Sci Rep [Internet]. 2017;7(1):15951. Available from: https://doi.org/10.1038/s41598-017-16179-7

250. van den Berg BM, Vink H, Spaan JAE. The Endothelial Glycocalyx Protects Against Myocardial Edema. Circ Res [Internet]. 2003 Apr 4;92(6):592–4. Available from: https://doi.org/10.1161/01.RES.0000065917.53950.75

251. Levick JR, Michel CC. Microvascular fluid exchange and the revised Starling principle. Cardiovasc Res [Internet]. 2010 Jul 15;87(2):198–210. Available from: https://doi.org/10.1093/cvr/cvq062

252. Adamson RH, Lenz JF, Zhang X, Adamson GN, Weinbaum S, Curry FE. Oncotic pressures opposing filtration across non-fenestrated rat microvessels. J Physiol. 2004;

253. Betteridge KB, Arkill KP, Neal CR, Harper SJ, Foster RR, Satchell SC, et al. Sialic acids regulate microvessel permeability, revealed by novel in vivo studies of endothelial glycocalyx structure and function. J Physiol [Internet]. 2017 Aug 1;595(15):5015–35. Available from: https://doi.org/10.1113/JP274167

254. Thomsen MS, Birkelund S, Burkhart A, Stensballe A, Moos T. Synthesis and deposition of basement membrane proteins by primary brain capillary endothelial cells in a murine model of the blood–brain barrier. J Neurochem [Internet]. 2017 Mar 1;140(5):741–54. Available from: https://doi.org/10.1111/jnc.13747

255. Yamaguchi Y, Inatani M, Matsumoto Y, Ogawa J, Irie F. Roles of Heparan Sulfate in Mammalian Brain Development: Current Views Based on the Findings from Ext1 Conditional Knockout Studies. In: Zhang LBT-P in MB and TS, editor. Glycosaminoglycans in Development, Health and Disease [Internet]. Academic Press; 2010. p. 133–52. Available from: https://www.sciencedirect.com/science/article/pii/S187711731093007X

256. Hook AL, Hogwood J, Gray E, Mulloy B, Merry CLR. High sensitivity analysis of nanogram quantities of glycosaminoglycans using ToF-SIMS. Commun Chem [Internet]. 2021;4(1):67. Available from: https://doi.org/10.1038/s42004-021-00506-1